Simulation of the Flow in Dolomitic Aquifers Using the Thermo-Nuclear ^{14}C Isotope Injected into the Atmosphere as a Tracer

Report to the
Water Research Commission

by

D.B. Bredenkamp
Private Groundwater Consultant

and

H Janse van Rensburg
Aquisim Consulting

WRC Report No. KV 251/10
ISBN 978-1-4312-0026-9

August 2010

Obtainable from

Water Research Commission
Private Bag X03
GEZINA, 0031

The publication of this report emanates from a project entitled *Simulation of the Flow in Dolomitic Aquifers Using the Thermo-Nuclear ^{14}C Isotope Injected into the Atmosphere as a Tracer* (WRC Project K8/895/1).

Executive summary

Introduction

This project is an extension of a previous study investigating the use of natural ^{14}C and tritium as part of the fall-out from nuclear tests. Although good simulations of the observed ^{14}C in the springs have been obtained using an analytical Excel model, a full 3D simulation was necessary to verify the results obtained by the Excel model and enhance the confidence in using the ^{14}C as a natural tool in the assessment of the storage capacity of these aquifers. At the same time the use of a bimodal recharge process in the Excel model, was put under scrutiny to compare the results, accepting the input of ^{14}C to be characteristic of a particular dolomitic aquifer, as is reflected by the bicarbonate concentration of the water emanating from the spring. The 3D model has been applied to the Molopo and Buffelshoek dolomite compartments in the NW province, representing typical dolomite aquifers for which ^{14}C measurements has been carried out over a period of almost 40 years.

The main aim was to obtain an estimate of the storage capacity of these aquifers employing a 3D Finite element model (using FEFLOW). This was an extension of a successful modelling investigation conducted for the dolomitic compartments to the northwest of Zeerust using a 2D FEFLOW model (PMA, Consortium, 2002). A storativity parameter value of S = 0.075 was derived for the Molopo Compartment and 0.035 for the Buffelshoek Compartment. The storativity proved to be independent of the configuration of S with depth and therefore could as well conform to a decline with depth, as was derived from the core recovery of boreholes (Enslin and Kriel, 1967) and from an interpretation of the hydrographs of several monitoring boreholes in the region.

The mixing and travel times of water in the aquifer under natural recharge conditions have been simulated by means of non-real injections of tracers at different depths and distances from the spring outlet. This revealed why the mixing conformed to a 2D mixing model that was used in the Excel model. The turn-over of water in the aquifer has been inferred from the travel times simulated from the point injections of the artificial tracers, as well as from the volume of water in storage calculated from the S value, in relation to the average annual recharge of the aquifer. This produced an average turnover time of 40 to 50 years for the Molopo Compartment and in the range of 20 for the smaller Buffelshoek Compartment. The results obtained from the analytical Excel model provided surprisingly good comparisons to the 3D mixing model.

The 3D finite element model proved to be the superior model and has provided an excellent validation of the reliability of the simple analytical Excel model. Together they have firmly established the reliable quantitative assessment of the resource potential of these aquifers (or

compartments).

Objectives of the project

The main objectives of the project can be summarised as:

1) To compare the results of the analytical simulation of the reappearance of the ^{14}C released as a pulse into the dolomitic aquifers via recharge, with those derived from a 3D numerical simulation model. This was applied to both a larger and smaller flow system namely the Molopo and Buffelshoek Compartments respectively both of which drains the Eccles dolomitic formation.
2) To assess the impact and sensitivity of different variable inputs of ^{14}C by the natural recharge from rainfall, i.e. deriving the characteristic ^{14}C concentration of the infiltrating water either from a bimodal or single recharge input.
3) To determine the effect on the simulated ^{14}C response by extending the rainfall record to predict the decline of the ^{14}C pulse back to its pre-bomb levels. At the same time the most recent ^{14}C measurements were checked against the simulated values obtained for both the analytical model and the 3D simulation models.
4) Ascertain the role of the permeability (K) and storativity (S) of the aquifer, which could not be derived from the analytical model.
5) Derive the turn-over time of water in the aquifer according to the 3D model in relation to the recharge or average flow of the spring; and to compare the results with that of the analytical model.
6) Determine from the 3D model the propagation and re-appearance of pollution at a dolomitic spring. (This illustrates the admixture of different artificial injections of pollution).

The conceptual mixing and flow model

The conceptual model of a two-layered mixing system that was derived from the Excel model has been validated by means of a 3D FEM simulation of the flow and mass transport. The aquifer was subdivided into 8 layers to a depth of 70 meters. The first finite element mesh comprised of 125 000 finite elements, for the mixing in the system. This showed that the water from the different layers attain the same mixed concentration within a period of 30 to 40 months. Over about the next 100 years the concentration gradually increases to that corresponding to the input concentration. The short period to achieve complete mixing compares well to the 36 months which is calculated using the Excel model, representing the shallow water that is recharged within a range of 4 km from the spring outlet. The deeper component of the flow in the Excel model is recharged at a distance from 5 to 20 km from the spring. This has been incorporated as several multiples of the average ^{14}C input over a period of about 400 months prior to the 36 months, which represent contributions of recharge up to about 100 years, which was comparable to the results obtained from the FEM.

It was illustrated during the study that the input ^{14}C in relation to that of the atmosphere could be regarded as a characteristic of a specific aquifer that is determined by the recharge and it

corresponds to the bicarbonate concentration of the groundwater. A higher ^{14}C input value is affected if the recharge occurs from water infiltrating through the soil or limestone layer overlying the aquifer, in comparison to lower ^{14}C content if the recharge bypasses the soil overburden. In both cases the bicarbonate concentration of the groundwater indicates which the dominant process is. In this way the ^{14}C input factor relative to that of the atmosphere could be derived. The pre-bomb concentration of the groundwater proved to be of particular significance for a reliable determination of the S value of the aquifer system. If the value is too low the S value would be too small and vice versa.

The temporal variability of the rainfall proved not to have a great impact in view of the fact that the response of the springs, which is controlled by the hydraulic head of the aquifer, is determined by the average rainfall over a period of 24 to 36 months. This causes the ^{14}C input from a month of high rainfall to be smoothed by the time this water reaches the spring outflow.

The recharge of the aquifers corresponded to an exponential rainfall relationship, whilst the long-term average recharge had to conform to that derived from the Chloride Mass Balance method (CMB), which from the previous study formed the only independent estimate. The variability of the ^{14}C input from individual months of high rainfall conforms to an exponential recharge response. This could effectively be incorporated by an exponential, a quadratic or binomial rainfall-recharge relationships. The effective monthly input was derived by averaging the values over several months, e.g. in the case of the Excel model over 36 months (Bredenkamp et al., 2007).

Assumptions

a. Anisotropy and Heterogeneity

The aquifer was configured to conform to the known natural condition of an anisotropic dolomitic aquifer insofar that for the dolomite the transmissivity and S-value declines with depth. Therefore the S and T values was declining with depth being assigned over the entire aquifer as 8 layers which have been the same except for the high transmissive zone which had to be incorporated to yield of the springflow and the best water level response at the available monitoring boreholes. This configuration has been tested using the same anisotropy but with runs with highly transmissive zone at depth and at the middle of the layers to see what the effect that would be on the reappearance of the ^{14}C tracer.

In all the cases the best (same) simulation has been attained as long as the average S value of the system was 7.5%. This could not be incorporated in the empirical simulation in the previous project – and has been incorporated in the length of the relative mixing periods. An uncertain aspect is the delineation of the aquifer boundaries in the case of Molopo compartment which has not been done with a particle tracer outline of flow directed to the spring (as has been done for Buffelshoek eye).

Therefore, if part of the recharge is derived from the Lyttelton which has a smaller S value, the 7.5% derived would be slightly smaller – in proportion to the likely additional area of recharge and its S value(similar to Buffelshoek), an area which could not be more that 10%. That would yield an S for the Molopo system to be about 6.8%.

b. Radio-carbon interaction with the aquifer matrix

This has not been incorporated and was checked with Prof Vogel who has said that experiments carried out in Heidelberg indicated that exchange occurs only significantly if the temperature of the water (experimental system) is increased to around 50 degrees Celsius. The further argument is that if there had been exchange a status of equilibrium would be reached when reverse exchange would take place. The fact that the travel times of the injected artificial tracers which had been assumed to be non exchangeable with the aquifer material has yielded, was the same as that of the ^{14}C provides proof that the ^{14}C does not significantly exchange with the dolomite matrix.

In the case of tritium there is a delay if the aquifer is overlain by a thick overburden of soil/ unconsolidated non dolomitic layer. This has been demonstrated in Bredenkamp et al. (2007). The delay there is by exchange, i.e. the hydrogen atoms in the soil moisture – similar to the method using the bomb tritium in the unsaturated overburden to determine the rate of displacement of the tritium input pulse (refer to the application in the Rietondale aquifer.

In the case of ^{14}C the input occurs at the root zone of the plants which bypasses most of the unsaturated zone and therefore enters the aquifer sooner than the tritium pulse.

c. Calibration of the 8-layer model

The calibration of the 8 layer model was attained for the different assigned transmissivity and S configurations – in all cases according to the measured ^{14}C values reappearing at the spring outflow in relation to the input from the rainfall.

The recharge to the aquifer proved to conform to an exponential relationship, which is similar to the quadratic binomial recharge relationship used in Bredenkamp et al. (2007).

Summary of the main results

The results obtained from the 3D finite element model proved to be reconcilable with that of the Excel model. The value of the average transmissivity (T) and aquifer storativity (S) could only be derived from the 3D model, but it proved to be independent of the configuration of S with depth. Aquifer storage S values were assigned according to other methods, which have shown that the S-values decline exponentially with depth. Correspondingly the transmissivity and S values were adjusted to conform to a similar decline with depth as both parameters vary according to the karstification of the dolomite. An average S-value of 0.075 has been obtained from the 3D model for the Molopo Compartment and a value of 0.035 for

Buffelshoek Compartment.

The turnover of water in the aquifer was inferred from the travel times of injections of artificial tracers, as well as from the volume of water in storage. The latter was calculated from the S-value in relation to the size of the aquifer, which produced an average turnover time of 40 to 50 years. This is comparable to that obtained from the Excel model, which in the previous study has yielded a turnover time of 22 years (Bredenkamp et al., 2007) The latter value appeared to have been calculated incorrectly. Adjusting the initial ^{14}C scaling-factor from 0.77 to 0.72 and assuming all the recharge to occur as rapid infiltrating water, a turnover time of 40 years was obtained.

The outcome of the project has significantly contributed to an improved understanding and assessment of the recharge and mixing of water that takes place in an aquifer, even within a complex and heterogeneous system such as the Eccles dolomite. The 3D numerical finite element modelling provided validation of the results obtained by the empirical Excel model. Although the applications of the empirical Excel model to some of the springs would have to be improved, the results from the Excel model will be acceptable for the interim but all the major dolomite aquifers needs to be simulated by 3D modelling.

Recommendation

It is essential for 3D finite element models to be compiled for all the larger dolomitic aquifers, such as Grootfontein Compartment near Mmabatho, Lichtenburg Compartment, Schoonspruit Compartment and Malmani Compartment in the Upper-Molopo area in view of their importance as sustainable water resource supply systems, as well as their vulnerability to pollution. The same applies to the smaller springs in the Zeerust area, which could be combined into one model. This approach would incorporate the leakage between aquifers, which has not yet been addressed previously in terms of mixing. This would also be a logical extension to the 2D modelling by which the piezometry and the discharge of the springs have been calibrated successfully.

Likewise the dolomitic compartments feeding the following springs should be modelled by 3D finite element simulations:

- Maloney eye, Gerhard Minnebron , Turffontein and eyes in the West Rand mining area,

- Pretoria Grootfontein and the Upper and Lower Fountain springs of Pretoria,

- The Delmas and East Rand dolomite,

- The eyes in the Kuruman dolomite and the aquifer supplying Sishen,

This is the best way to address the constraints of the groundwater supplies and prioritizing their investigation in South Africa.

The ^{14}C measurements should be continued to confirm the declining trend of ^{14}C, but sampling should be repeated only at intervals of about 10 years for the next twenty years. It is of utmost importance that the ^{14}C analysis should be performed according to accepted standards, which does not seem to be the case with several of the most recent samples.

Acknowledgements

The Water Research Commission for approval of the project and the funding of the present and previous project.

Department of Water Affairs and Forestry for the provision of data of the dolomitic springs and for the continued ^{14}C and chemical measurements.

J C Vogel having initiated the ^{14}C measurements and for his keen interest and discussions throughout the different phases of the interpretations; and for the quality control of the ^{14}C measurements while Director of QUADRO at the CSIR

Table of Contents

List of Figures

List of Tables

1 INTRODUCTION

This project was a logical continuation of the favourable results that have been obtained by means of an analytical model in simulating the re-appearance of the ^{14}C and tritium pulses injected into the atmosphere (Bredenkamp et al., 2007). This mass-flux of ^{14}C entered the dolomitic groundwater reservoirs as part of the groundwater recharge which re-appears in the spring outflow. The main drive behind the project has been that the ^{14}C pulse in the rainfall labels the recharge to the dolomitic aquifers and provided a unique natural injection of tracer through the processes of groundwater recharge and flow through the aquifer. The ^{14}C content of the spring flow thus provided a unique opportunity to reveal the processes of infiltration and admixing occurring in these aquifers, until the tracer pulse re-appears at the spring outflow. *A major breakthrough was made with the postulation (Bredenkamp and Van Wyk (2004) that the ^{14}C acted as a tracer, whereby the observed low concentrations of ^{14}C emanating at the springs do not indicate old water, but can be attributed to*:

1. The infiltration processes in a dolomitic compartment, yielding different ^{14}C values, which all represent recent recharge and from;

2. The mixing of the groundwater of different historical transient times, to reach the spring.

The characteristic ^{14}C value of the recharge is affected by a different uptake of ^{14}C in the dissolution of carbonate from the bedrock dolomite to form bicarbonate. The dissolution of bicarbonate occurs as a result of different recharge processes, whereby the ^{14}C of recently recharge water could range from 55% to 85% modern Carbon.

Through a postulated bi-modal dissolution of the carbonate it was possible to relate the ^{14}C of the recharge to the bicarbonate concentration of the groundwater, which is high if the ^{14}C content is high and vice versa, whilst in both cases the bicarbonate is still in a saturated-equilibrium with the available CO_2. This has lead to a postulation that the bicarbonate also provides an indication of the dominant recharge process. Thus in the case of more direct infiltration it would yield low bicarbonate, or higher bicarbonate if the infiltration occurs through an alluvium soil cover overlying the aquifer (Bredenkamp and Van Wyk, 2004).

It was therefore concluded that the measured ^{14}C (and tritium) values observed in the spring represent a mixture of recently recharged water and that it is derived from an effective two-layered aquifer. The one component is derived from recharge occurring over the preceding 24 to 36 months; and the second from a much longer historical period in the range of about 350 to 400 months preceding historical month 37. An empirical Excel model was developed by which the ^{14}C, as well as tritium, provided an acceptable conceptual flow-mixing model to simulate the breakthrough of these natural injected tracers in the spring outflow (Bredenkamp and Van Wyk, 2004 and Bredenkamp et al., 2007).

In spite of the sound conceptual hydrological basis and the insight that has been gained in characterizing the various aquifers and the meaningful results that have been obtained, the model results was not received favourably by some of the critics, because it involved the manipulation of too many parameters with no incorporation of the hydrodynamic flow and dimensions of the aquifer. The model has nevertheless provided a new insight into the processes of recharge and mixing occurring in these aquifers and provided an explanation of why the water is of recent origin, irrespective of the ^{14}C content being high or low. The analytical model also yielded acceptable quantitative estimates of the turn-over time of water in these aquifers, from which the volume of water stored in the aquifer in relation to the recharge, could be derived.

It was therefore of critical importance to verify the analytical model by means of a full 3D numerical flow model, which in itself was a logical extension of a provisional 2D-simulation model compiled by the PMA Consortium (2002) for a large part of the Upper-Molopo dolomite of which the area is indicated in Figure 1. *Although this 2D model could successfully simulate the flow-response of the springs, the storage capacity or turn-over time of the dolomitic groundwater aquifers could not be obtained.*

2 OBJECTIVES OF THE STUDY

The main objectives of the study were to:

1. Compare the results of the analytical simulation of the re-appearance of the ^{14}C pulse that has been introduced into the dolomitic aquifers via recharge, with those derived from a 3D numerical simulation model. This was applied to the large Molopo eye and the small Buffelshoek eye dolomitic compartment.

2. Assess the impact and sensitivity of different variations of the variable input of ^{14}C by the recharge, i.e. deriving the characteristic ^{14}C concentration of the infiltrating water either from a bi-modal or single characteristic recharge input.

3. Determine the effect on the simulated ^{14}C response by extending the rainfall record to predict the likely decline of the ^{14}C pulse to its pre-bomb levels. At the same time the most recent ^{14}C measurements were to be checked against the simulated values obtained for both the analytical model and the 3D simulation models.

4. Ascertain the role of the kinematic porosity of the aquifer (in this instance well related to the specific yield (S value) of the aquifer), which could not be derived from the analytical model.

5. Derive the turn-over time of water in the aquifer according to the 3D numerical simulation model in relation to the recharge or average flow of the spring; and to compare the results with that of the analytical model.

6. Determine from the 3D numerical model the propagation and re-appearance of pollution at a dolomitic spring. (The present report will illustrate the admixture by way of different artificial injections of pollution).

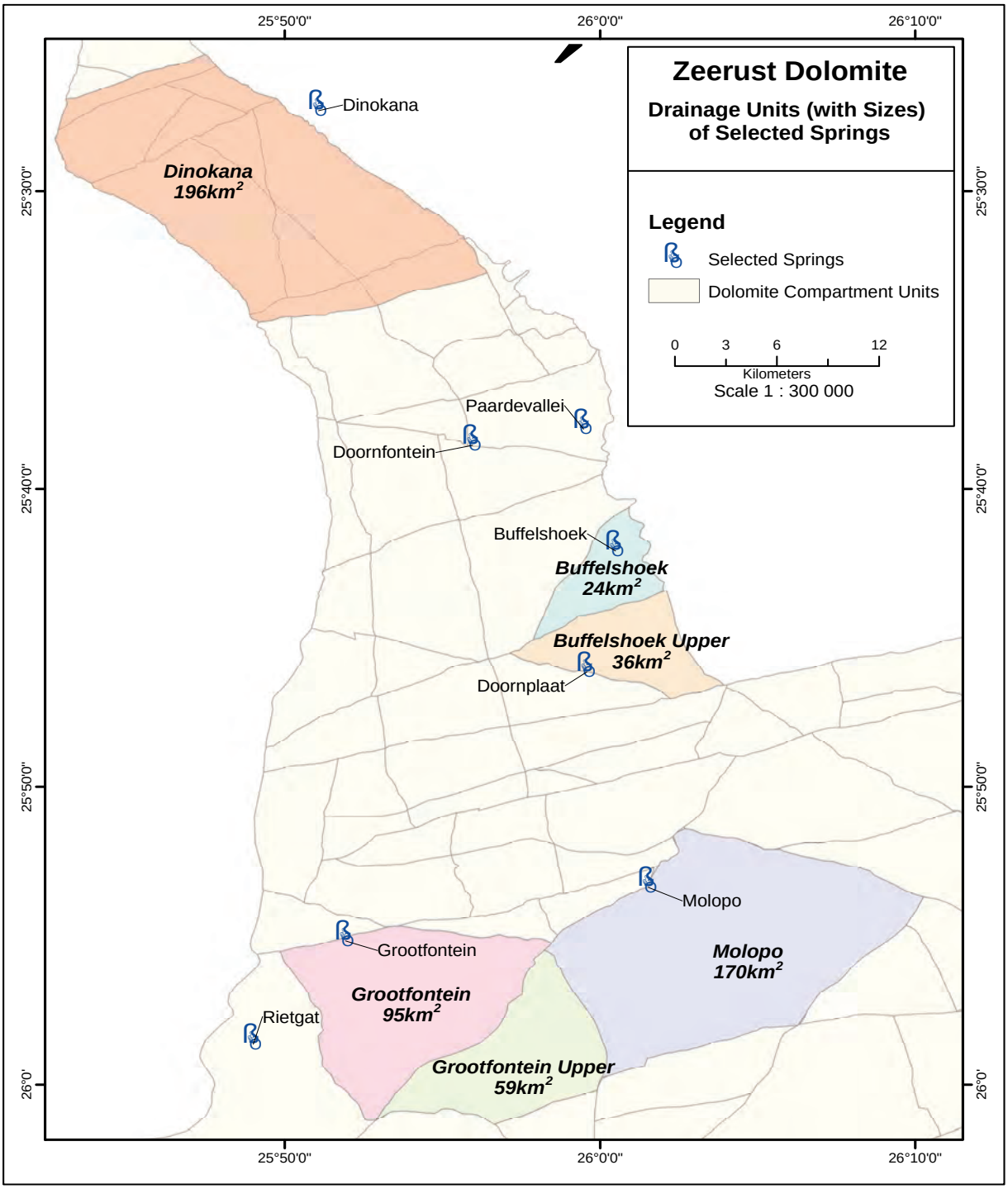

Figure 1 – Location of springs across the study area.

3 Recharge of the dolomitic aquifers

3.1 Background

Similar estimates of recharge that had successfully been used for the empirical Excel simulations (Bredenkamp et al., 2005) were used as input to the 3D numerical model developed for the present study.

The recharge derived by PMA (2002) has been checked against the simulation of the flow of Buffelshoek and Molopo eyes and it was found that the flow responses closely matched the observed flows even if a different combination of rainfall stations of the area is used. This indicates that the measured data from the rainfall stations represents the rainfall distribution and events across the study area well.

The ^{14}C of the groundwater has a characteristic value for each aquifer and is generally lower in the chert-rich Eccles and Monte Christo Formations (compared to chert-poor formations such as the Oaktree/Lyttleton Formations); representing a more direct and higher average recharge and specific yield, for large perennial springs such as Molopo eye and Dinokana eyes (see Figure 1). The same applies to springs oozing from smaller compartments, such as Buffelshoek, Doornplaat and Vergenoeg that also receives their recharge from this formation. The Grootfontein and Doornfontein eyes however are recharged predominantly from the Monte Christo dolomite. Although also chert-rich, it is less susceptible to direct recharge probably because it is covered by soil and limestone deposits. According to the previous analytical modelling, the Grootfontein and Doornfontein aquifers appear to experience a delay in the emergence of the ^{14}C pulse at the spring, which has been attributed to the limestone covering the Monte Christo and Oaktree dolomite in this region. (Although not relevant to the present study, the tritium responses showed a delay in comparison to the ^{14}C results, which is attributed to exchange of tritium with hydrogen atoms contained in the unsaturated calcretes/soil overlying the dolomite (Bredenkamp et al., 2007).

3.2 Incorporation of recharge into the flow model.

In the present 3D numerical model evaluation the input of ^{14}C was introduced as a characteristic of a specific aquifer, since the focus was to simulate the 3D propagation and the time response of the breakthrough of ^{14}C in the spring outflow, rather than to resolve the recharge processes.

3.2.1 Simulation of the reappearance of the nuclear-bomb ^{14}C in the rainfall in the spring outflow for Buffelshoek eye (located as in Figure 1).

The Buffelshoek spring has played an important role in determining the recharge in relation to rainfall because of:

- The availability of a good rainfall record of and a good coverage of chemical analysis from the spring.
- A comparative long record of the groundwater levels of the nearby Wondergat, which fluctuate in a similar response to the flow of the springs in the area.
- Minimal impact of abstraction on the flow of the spring.

3.2.2 Tracer input

The same analytical Excel program that has previously being used for the ^{14}C simulations has been applied in the present study, whilst the 3D numerical flow and mass transport model was also applied to simulate the ^{14}C breakthrough at the springs that have been modelled. The recharge used in the 3D simulation model has been treated in a similar way. The variable monthly recharge has been multiplied with the ^{14}C content of the rainfall to derive the monthly input-load of ^{14}C (i.e. seepage flux [m/d] x ^{14}C). The ^{14}C content of the spring water was determined by mixing of the monthly ^{14}C input from recharge over a shorter period preceding a specific month, with the average ^{14}C input of a longer period prior to the first. In most cases a multiple >1 of ^{14}C over the longer period had to be incorporated to obtain the best simulation. (According to the 3D numerical model it appeared that the incorporation of the multiple factor corresponded to the dilution affected by the water stored in the aquifer (refer to Section 5).

The ^{14}C content of the water of month i (C_i) derived from the Excel model, which essentially is a two-box model, is given by eq.1 below:

$$C_i = \frac{1}{p+1}\left([\frac{gaw}{u} \sum_{i-u+1}^{i} A_i (Rf_i > t_1)] \frac{1}{Rf_i} + \frac{p}{(j-k)} \sum_{i-k+1}^{i-1} C_{i-1} \right) \quad \text{……..…….eq.1}$$

Where A_i is the ^{14}C value of atmospheric CO_2 in month i.

Rf_i = the rainfall of month i

w = the weighting factor by which the recharge coefficient a varies according to the

average rainfall over the preceding 36 month being higher or lower than the long-term average rainfall (over a period of about 300 to 400 months).

g = the fraction of the input ^{14}C A_i, which determines the characteristic ^{14}C of the

recharge of a specific aquifer;

p = the multiple of deep water that mixes with the concentration of the shallow-water contribution of the spring.

The summation period (j-k) is the number of months prior to j over which the concentration of the deep water is averaged (usually several hundred months) and is summated to month i-1 (the latter are concentration values already calculated); j is mostly 36 because of it being the rainfall period that on average best corresponds to the flow of the springs. The average rainfall over this period therefore determines the hydraulic gradient, which controls the outflow of the springs. The parameter p indicates that the deep flow component extends over a period much longer than j-k. Multiples of p>1 of the deep flow had to be incorporated in view of the postulated conceptual mixing model being limited by insufficient historical ^{14}C input due to a short rainfall record. The effect on the simulation by an extension of the rainfall record has been examined by inserting additional rainfall data in the beginning of the rainfall series. Similarly monthly rainfall data has been added to the record to simulate the decline of the injected ^{14}C tracer in the long term. NB! **The analytical model therefore essentially represents a two-layer mixing model.**

3.2.3 Rainfall input

The rainfall data of Slurry (508/649) and Ottoshoop (508/8258) has been used as the key stations to simulate the reappearance of ^{14}C of Buffelshoek eye with the analytical model (see Figure 1). The water level fluctuations of the Wondergat correspond very well to the flow of the spring and therefore to the recharge. The rainfall of Slurry has been pre-dated to 1910 and the full rainfall record up to 2009 was used to compare the simulated ^{14}C with the measured values. To predict the future decline of the ^{14}C pulse, the full monthly rainfall series from 1910 to 2009 has been added onto the existing record.

3.2.4 Determination of the recharge coefficient using the Chloride mass balance method

The simulated flow of Buffelshoek has been used in conjunction with the delineated recharge area of the spring (Figure 2) to derive the average chloride concentration of the rainfall, which is the key to the reliable determination of the average recharge, according to the chloride mass balance method (CMB) as is presented below.

$$a = \frac{Cl_{Rf}}{Cl_{gw}} \qquad \text{…….. eq. 2}$$

Where a = the recharge coefficient

The method is particularly reliable for dolomitic aquifers because the rainfall is the only source of chloride with no contribution from the geological formations.

Cl_{Rf} = the average chloride concentration of the rainfall, which is the unknown to be solved.

Cl_{gw} = the chloride of the spring water.

The chloride of the groundwater Cl_{gw} (i) has been measured intermittently for Buffelshoek spring over a period of several years but Cl_{Rf} ideally has to be obtained from rainfall samples collected over many years. Cl_{Rf} could however be derived from eq.2 by plotting the simulated Cl_{gw}(i) values (derived from a rainfall-recharge relationship) in comparison to the measured values; whilst at the same time changing the recharge area until the best match between the simulated and measured Cl values has been obtained..

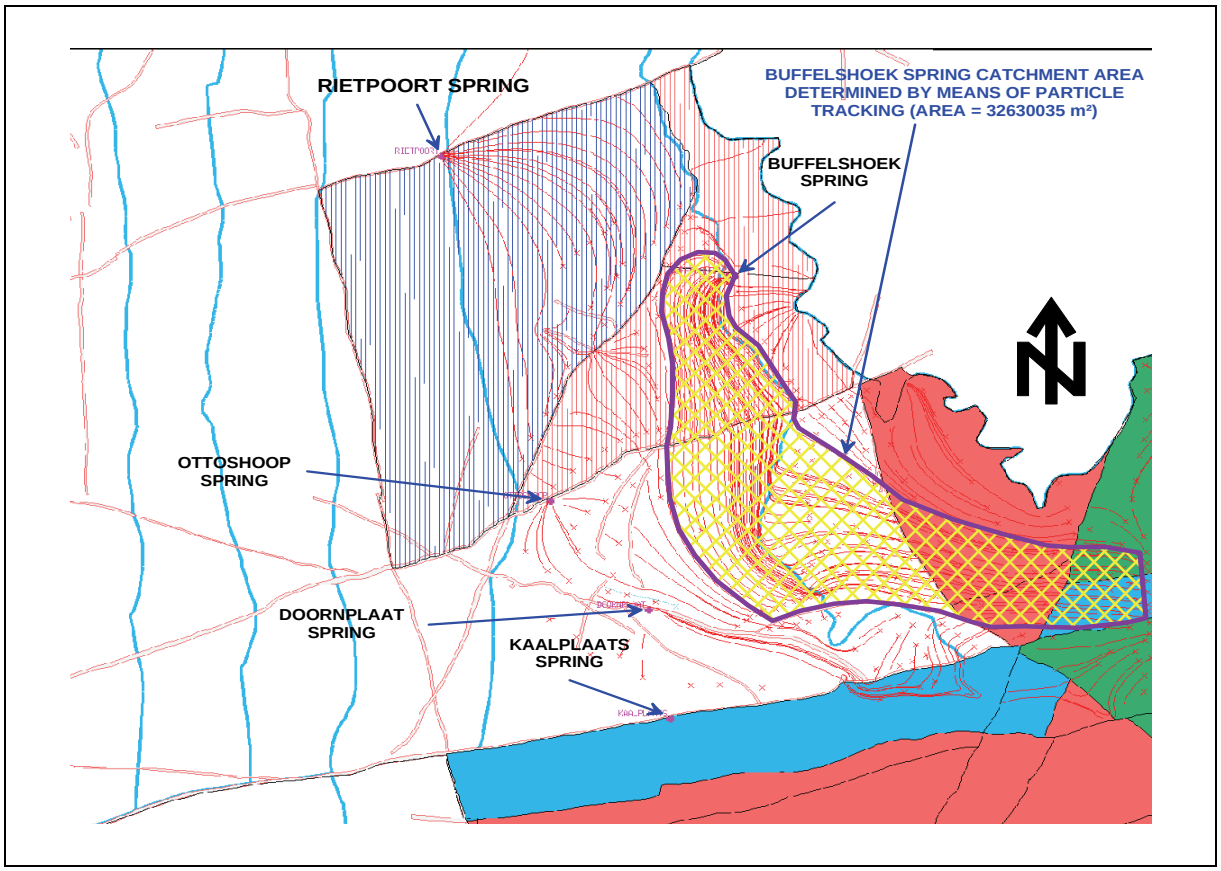

Figure 2 – Flow lines derived from the Regional 2D Aquifer Model (PMA Consortium, 2002).

Figure 2 shows the flow lines derived for some dolomitic compartments in the Upper-Molopo (Northwest Region) to the outflow of the springs. As is indicated the actual area contributing to the flow of Buffelshoek eye is more complex than that delineated by the geological boundaries shown in Figure 1. According to a particle trace of flow the recharge area was delineated to be 32.6 km^2.

The recharge value obtained for Buffelshoek eye is regarded to be well representative of the entire study area presently investigated. The flow records of the different springs that have been used in the 2D-dynamical modelling by the PMA Consortium (2002) and the ^{14}C simulations have been adjusted to yield similar average flows to those derived from the Cl method (See Table 1).

From the Cl concentration of the rainfall, the recharge areas of the Molopo eye and the other springs indicated in Figure 1 could be determined. These areas corresponded well with the compartments delineated in the 2D dynamical model. The rainfall data of Slurry, Ottoshoop

Table 1 – Simulation of ^{14}C at Buffelshoek Eye using the Excel Spreadsheet Model.

Minimum error	32.93
Lower threshold (mm)	12.50
Higher threshold (mm)	55.60
Recharge factor (L)	0.11
Recharge factor (H)	0.05
^{14}C factor (L)	0.80
^{14}C factor (H)	0.76
Multiple factor	3.01
Lag months period 1 mth	36.0
Lag period 2 mth	348.0
Rainfall weighting	36
Further lag Sim ^{14}C mth	1
HCO3 of spring water (mg/l)	228.90
Measured HCO3 (mg/l)	228.00
Area spring (sq km)	28.0
Cl of spring	5.07
Cl ratio (CMB recharge)	0.11
^{14}C sim recharge	0.11

and Lichtenburg were used to derive the flow of the Molopo spring. As the variability of all the springs corresponds to the average rainfall over a preceding period of 36 or 48 months, the rainfall pertaining to the specific spring, is not a critical factor because of the high correlation of the regional monthly rainfall within a radius of 50 km. This is confirmed by the good correspondence between the water levels of the Wondergat and the flows of all the springs situated within a radius of 50 km (Bredenkamp, 2000 and Stephens and Bredenkamp, 2005).

The outflow of the springs obtained with the 3D numerical model and their respective areas were used to obtain the ^{14}C responses. However the ^{14}C input contributed by leakage of groundwater from the higher-lying dolomitic compartments was not included in the 3D numerical model. The latter has been accommodated in the extensive 2D flow model previously compiled by the PMA Consortium (2002), which has successfully simulated the flow response of the springs as well as the regional groundwater levels over the 1972-2006. Further testing in the present project has revealed that the impact of the inflow from higher lying compartments is not large and could be omitted in the 3D model. In the case of Molopo and Buffelshoek springs which have been selected to apply the 3D numerical model, the contribution of recharge from adjacent compartments has been proven to be negligible.

4 APPLICATIONS

4.1 ^{14}C simulations with Excel model

In view of the uncertainty associated in having a rainfall series that is too short, the rainfall record previously used has been extended, by inserting an additional 10 years of monthly rainfall at the start of the record. The sensitivity of the model outcome using one or two threshold rainfalls for recharge to occur was also tested. This was necessary to determine if the ^{14}C results are improved using a single or bimodal recharge model.

The sensitivity of the simulations to the following changes of the analytical model was assessed.

1. Instead of using a bimodal recharge process (Bredenkamp et al., 2007) to account for the variable ^{14}C content of the groundwater, the ^{14}C of the recharging groundwater was *regarded to be a characteristic of the aquifer* that is to be obtained from the model. This later proved to be incorrect and in this respect the bicarbonate content of the groundwater provided the link in deriving the characteristic value. This also reduced the number of parameters of the model. The average recharge of the different springs was calculated from the chloride concentration of the spring, whilst the average bicarbonate of the springs is still a viable alternative method to confirm the recharge coefficient of the dolomitic aquifers. (Bredenkamp et al., 2007).

2. Assessing the sensitivity of the outcome of the analytical method was necessary because of an insufficient rainfall record preceding the existing record, to ensure a more reliable incorporation of the deep-flow component of recharge in the simulation of the ^{14}C. For this reason the rainfall record has been extended by inserting 10 years of monthly rainfall prior to that previously used.

3. Verifying the reliability of the latest ^{14}C measurements against the predicted values using an extended rainfall record to simulate the ^{14}C response for many years in the future. The full existing rainfall record was added onto the present series as it represented a similar monthly and long-term variability of rainfall.

4. An exponential rainfall-recharge relationship was employed. This also compared to a binomial or quadratic function that had been used in the Excel model. This allowed comparison of the outcome of the spring flow simulations with those derived by the PMA Consortium (2002) applying an exponential recharge response to the rainfall.

4.2 Application of Excel model to different springs

4.2.1 Impact of rainfall records on the Excel simulations.

The calculated ^{14}C input of the recharge is derived according to a formula similar to that used by the PMA Consortium (2002), which corresponds to an exponential rainfall recharge relationship as is shown in Figure 3. This figure also shows the best regression between the exponential recharge relationship in comparison to that used by Bredenkamp et al. (2007).

Figure 3 clearly shows that the recharge derived from the variable monthly flow of the spring, corresponds well with the moving average rainfall over a period of the 36 months preceding a specific month. The main difference between the two recharge models is that a higher recharge is derived from the exponential relationship for high monthly rainfalls. The recharge is then averaged over several months. Although a monthly rainfall threshold had to be exceeded for recharge to occur, it was found that even applying no threshold would yield comparable estimates of the variable recharge. In this way the number of variables has been reduced. The moving *average rainfall over the preceding 36 months was incorporated in a quadratic relationship to calculate the monthly recharge. The recharge coefficient is* weighted by the ratio of the 36 month average rainfall to the long-term average rainfall of the area (see eq.2. It was because of the good correlation between the flow of a spring and the 36 month moving average rainfall that it has been used in the analytical mixing model, to simulate the ^{14}C content of the spring outflow (Bredenkamp et al., 2005 and 2007).

The recharge that was applied in the extended Excel model is shown below (See Figure 3 and Figure 4).

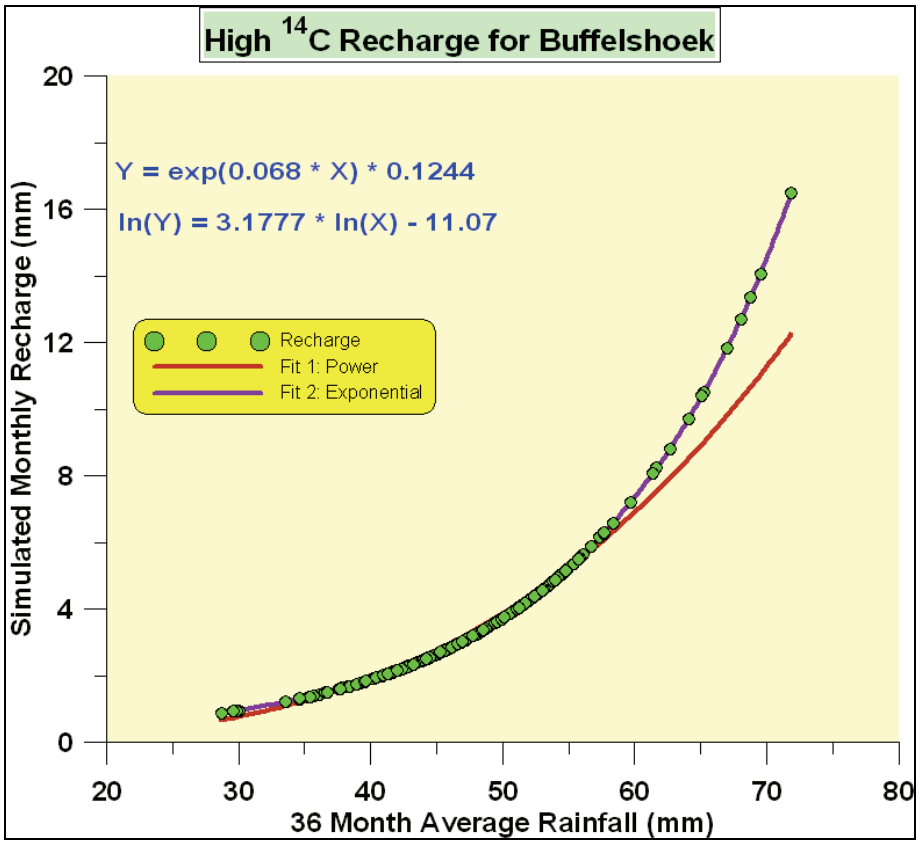

Figure 3 – Recharge derived from monthly rainfall in excess of a single high threshold rainfall in relation to the moving average monthly rainfall over the preceding 36 months for Buffelshoek Eye.

Figure 3 depicts the recharge derived from monthly rainfall in excess of a single high threshold rainfall in relation to the moving average monthly rainfall over the preceding 36 months for Buffelshoek Eye. The recharge corresponded well to a binomial, a power and an exponential relationship. It yielded recharge in relation to a low threshold rainfall and ensuring that an average recharge compatible to the chloride method (CMB) is obtained.

Similarly Figure 4 depicts the recharge response by incorporating both a low and high threshold value in relation to the 36 month moving average rainfall that was used in the ^{14}C simulations of Bredenkamp et al. (2007).

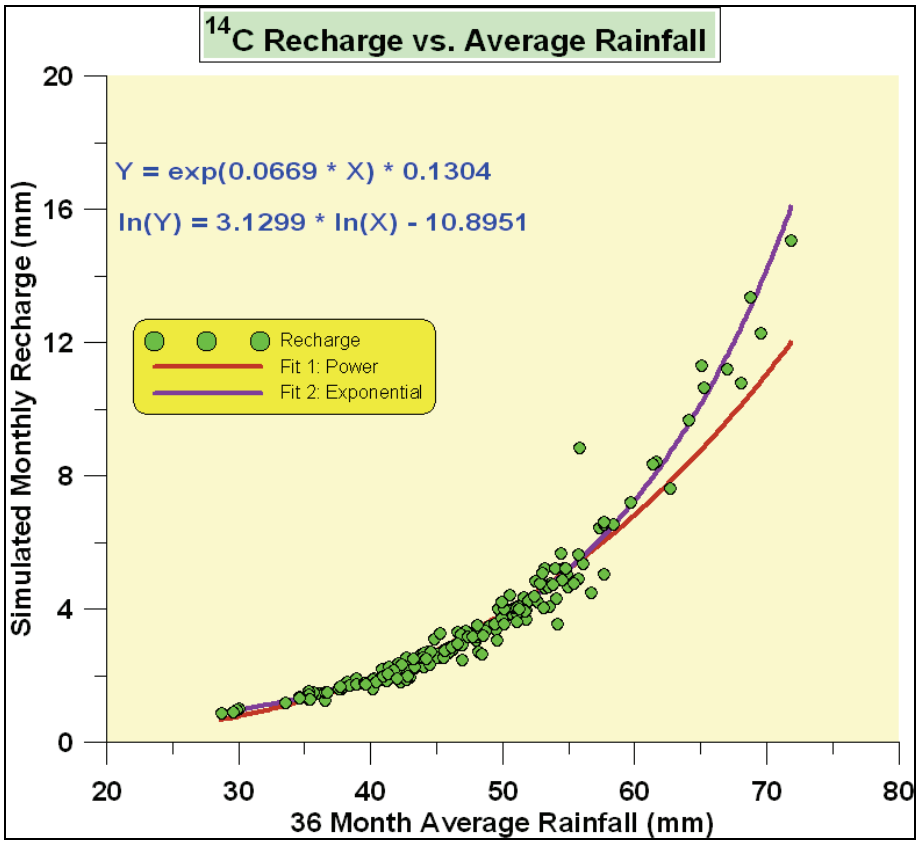

Figure 4 – Recharge response by incorporating both a low and high threshold value.

It was clear that the recharge, although derived from different rainfall recharge relationships, still corresponds to an exponential response to rainfall in excess of a threshold rainfall. Irrespective of what recharge-relationship is used, it must still yield the same average recharge as that produced by the CMB method (see Eq. 2).

4.2.2 Results obtained from Analytical Excel model

The simulations of the ^{14}C response of Molopo, Buffelshoek, Doornplaat eye and Dinokana eyes, using the simple analytical Excel model, were repeated to assess the effect of incorporating a normal and fast recharge component, or either, but which still yield corresponding bicarbonate concentrations of the spring water. A typical result of the analytical model simulations of Buffelshoek is shown in Figure 5 and examples of other springs are shown in Appendix B (also refer to Bredenkamp et al., 2007). The ^{14}C simulation was derived for Buffelshoek eye assuming that rainfall in excess of a low and high threshold rainfall would affect recharge; the average recharge conforms to the CMB ratio namely 11.05% (The average ^{14}C factor used was 0.775).

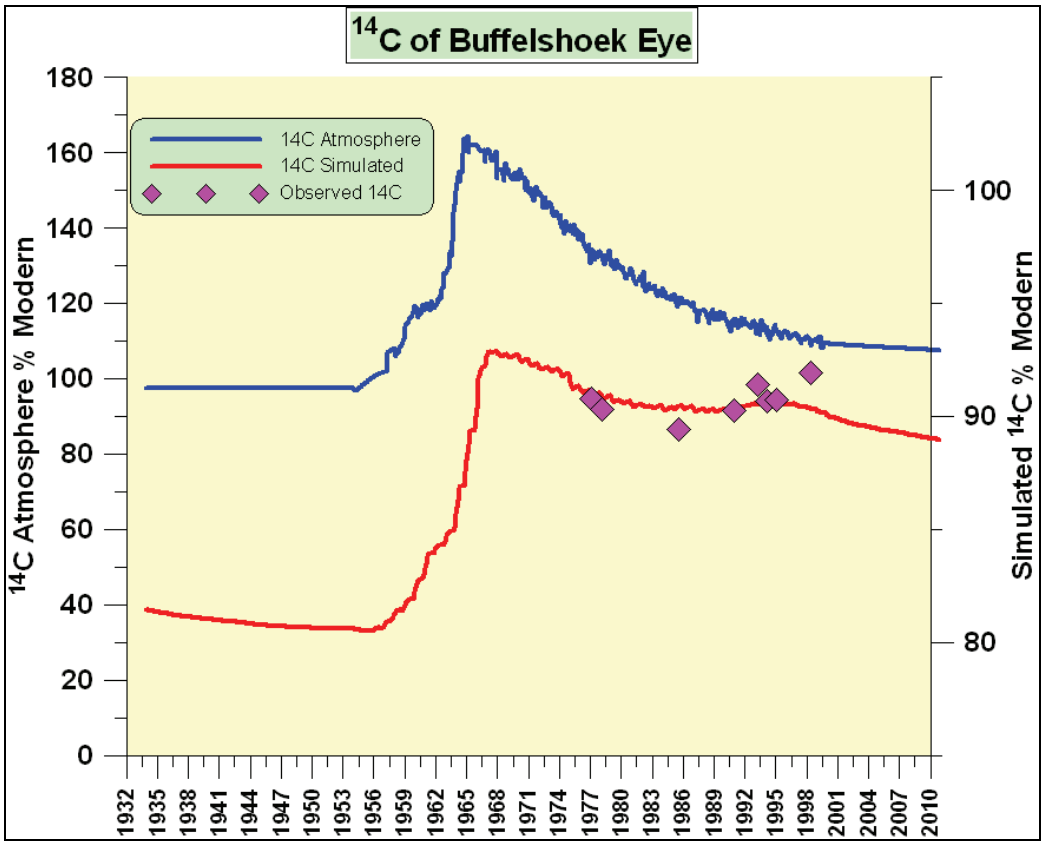

Figure 5 – Excel Simulated vs. Observed ^{14}C for Buffelshoek Eye in relation to ^{14}C Atmosphere assuming parameter values as depicted in Table 1.

4.2.3 Simulation of the long-term response of the ^{14}C in verifying the most recent ^{14}C measurements.

4.2.3.1 Buffelshoek eye – comparison of ^{14}C simulated with the original macro-analytical Excel model

The outcome of the simulation with the macro-based model is shown in Figure 6 having extended the rainfall to 2009, whilst Figure 7 presents the result extending the rainfall record to year 2082.

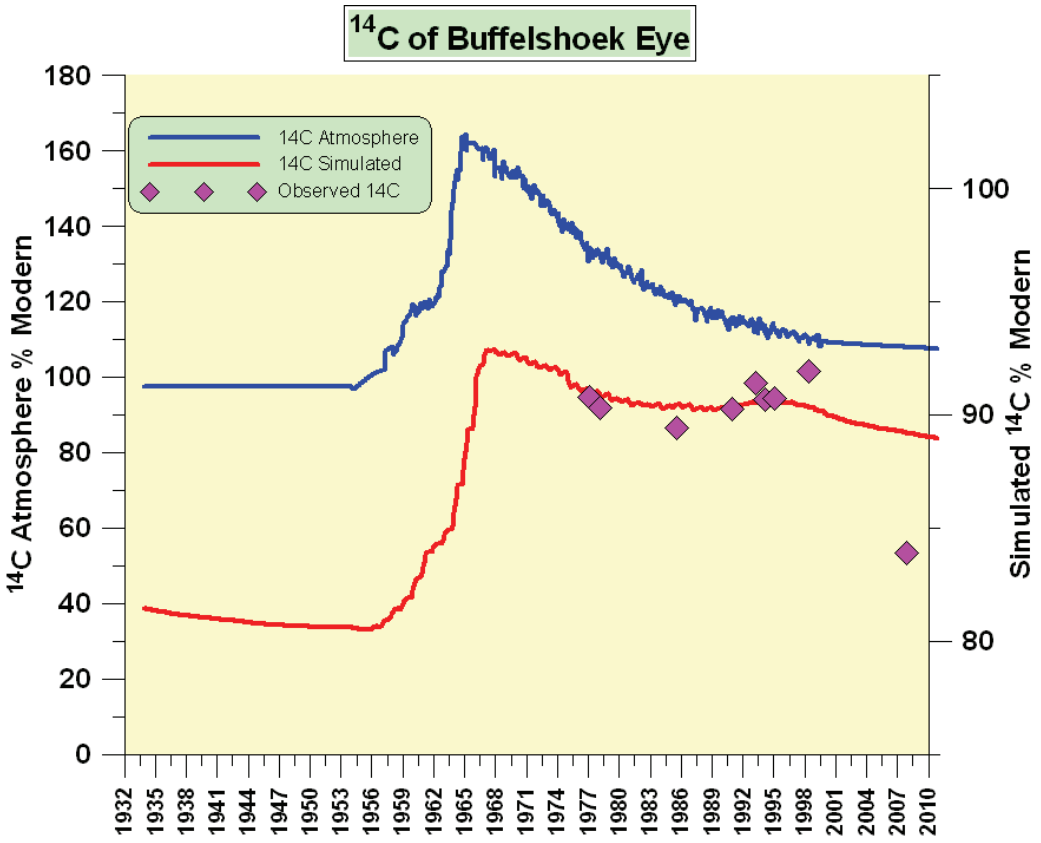

Figure 6 – Excel Simulated vs. Observed ^{14}C for Buffelshoek Eye in relation to ^{14}C Atmosphere assuming parameter values as depicted in Table 1. The last ^{14}C measurement of Buffelshoek eye deviates significantly from the simulated curve indicating that the value is not reliable.

Table 2 – Results of ^{14}C simulations for different recharge formulas.

Buffelshoek eye	Exponential	Exponential	Bimodal Recharge	Buffelshoek eye long added rainfall
Error min	4.80	2.79		
Lower threshold	12.5	12.5	9.8	9.8
Higher threshold	60.3	59.6	62.1	62.1
Recharge factor (L)		0.1241	0.072	0.072
Recharge factor (H)	0.34		0.037	0.037
^{14}C factor (L)	0.817	0.817		
^{14}C factor (H)			0.83	0.83
Final multiple factor	2.51	3.22	2.9	2.9
Lag months period 1	36	36	36	36
Lag period 2	367	367	345	345
Long term rainfall				
Start year	1922	1922	10 yr Rainfall	Added 10 yrs rainfall
Start month	1	1	in front	in front and 80 yrs at end
Months for Lt average	944	944		
Rainfall weighting	36	36	36	36
Further lag Sim ^{14}C	23	32	22	25
Measured HCO3	228.8	228.8	228.8	228.8
Area spring (sq km)	45	32	32	32
Cl rech =	0.1105	0.1105	0.1105	0.1105
Model rech =	0.1105	0.1105	0.1105	0.1105

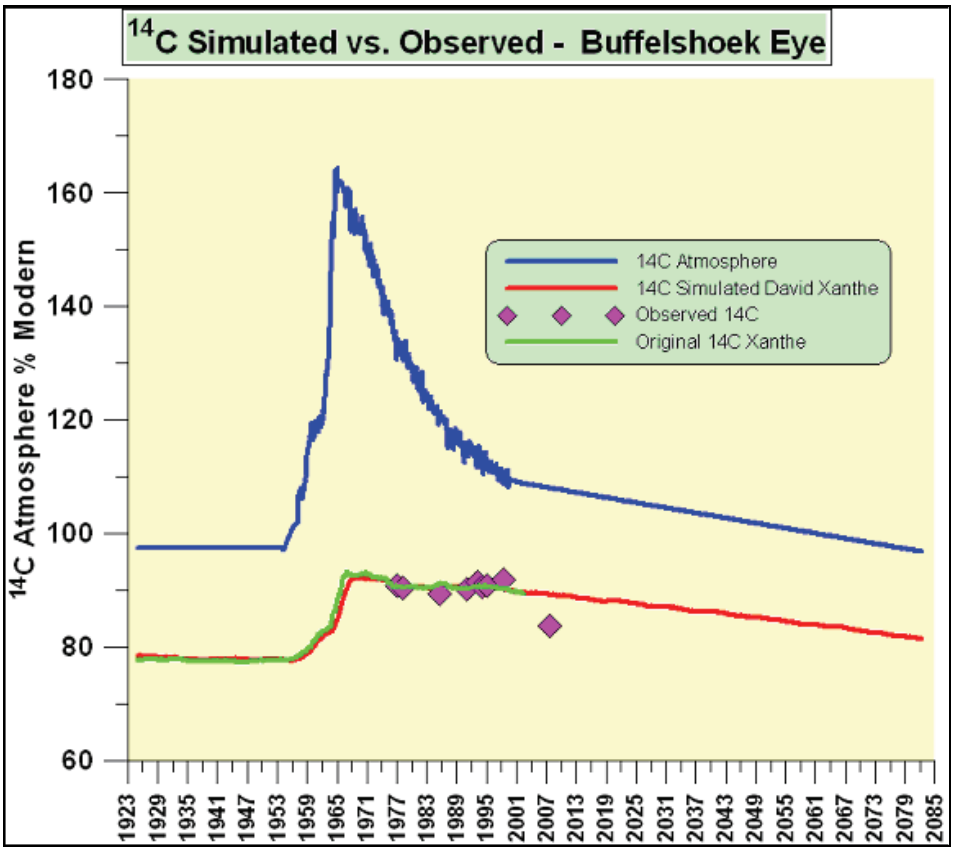

Figure 7 – Excel Simulated vs. Observed ^{14}C for Buffelshoek Eye in relation to ^{14}C Atmosphere assuming parameter values as depicted in Table 1 (Simulation extended to 2082).

The last ^{14}C measurement for Buffelshoek eye of Nov 2007, again clearly deviates from the previous simulation. Figure 7 indicates that only by 2088 the ^{14}C values of the spring would almost be back to the pre-bomb levels.

The incorporation of the multiple factor is that it effectively accommodates the long-term mixing component despite an insufficient historical rainfall record (see Section 4.4)

4.3 ^{14}C measurements of some springs in relation to the spring flow.

The most recent ^{14}C measurement of Buffelshoek (Nov 2007) shows a significant deviation from the simulated value, that was derived from the previously best analytical simulation (see Figure 6 and Figure 7). This indicates that the ^{14}C measurement or the processing; or sampling of the water, or both, have been unreliable. As is later on shown, this ^{14}C value, although still being too low, fitted closer to the revised long-term response when the initial pre-bomb ^{14}C content of the spring was adjusted according to the bicarbonate concentration of the spring water.

According to Figure 8 there appears to be a correlation between the discharge rates of the springs and the measured ^{14}C. This provides further confirmation that the most recent measured ^{14}C value of Buffelshoek eye is unreliable. Figure 8 confirms why the incorporation of the short mixing period of 36 months in the analytical model is acceptable. It not only controls the flow rate of the springs but also contributes to the component of recent recharge occurring in close proximity to the spring. (Figure 8 and Figure 9)

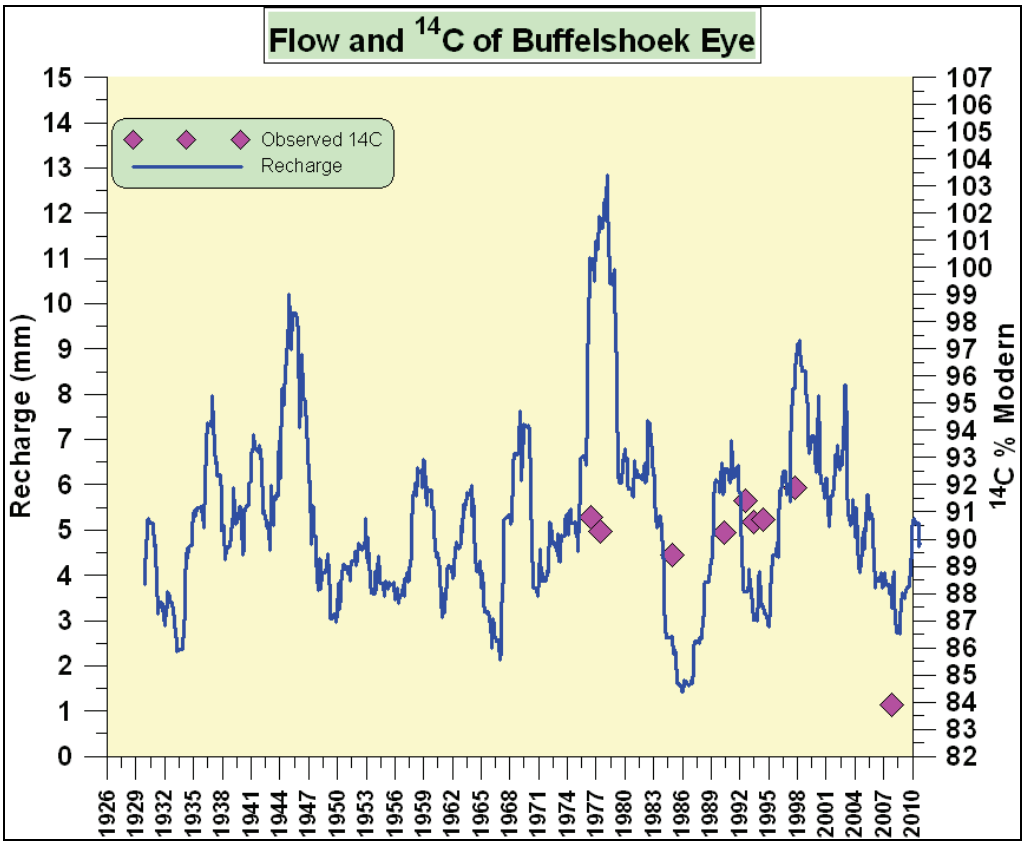

Figure 8 – Correlation between the discharge rates of the springs and the measured ^{14}C.

The most recent ^{14}C measurement of Buffelshoek eye (of 2007) in relation to the recharge indicates it to be an outlier in comparison to the other measurements.

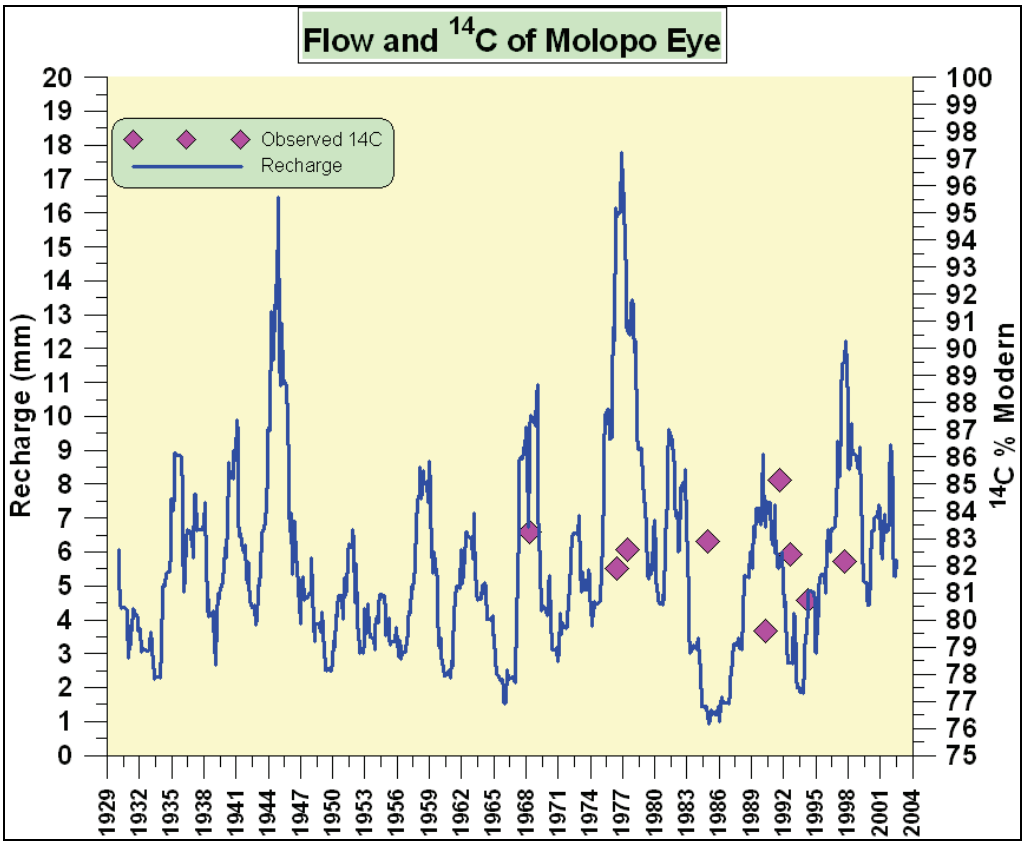

Figure 9 – ^{14}C measurement of Molopo eye (up to 2007) in relation to the recharge.

According to the simulated ^{14}C response (Figure 9) the ^{14}C values show a definite correspondence to the recharge and therefore to the flow of the spring.

4.4 The impact of the adjustment of the mixing period in the analytical model illustrated for Buffelshoek eye – simulated with the Excel model

Figure 10 indicates that the simulated ^{14}C response critically depends on the averaging period of the ^{14}C of the deeper flow component. In this case the deep flow was also averaged over 36 months (similar to the shallow flow), in comparison to an averaging period of about 345 months, which produced the good simulation represented by the graph in green. The simulated ^{14}C pulse for the shorter averaging period is much poorer than that derived from the longer averaging period using the same multiple of 2.9 (see Table 2). This clearly shows that the aquifer reduces to a two layered mixing model. The one represents more recent flow, whilst the second is a mix of 2.9 times the average flow over about 320 months prior to the 36 month period. The multiple factor is an effective way of incorporating an even longer mixing period that is limited by too short a rainfall series.

It is evident that any rainfall-recharge relationship conforming to an exponential response would reliably simulate the recharge and flow of the springs. The analytical ^{14}C models also yielded consistent results using different rainfall series from the same region or if the rainfall series is extended. The high correlations of the rainfall of all stations within a radius of about 50 km, explains the similar regional response of recharge or of the ^{14}C simulations, if part of the rainfall from a nearby station is used to substitute missing rainfall data.

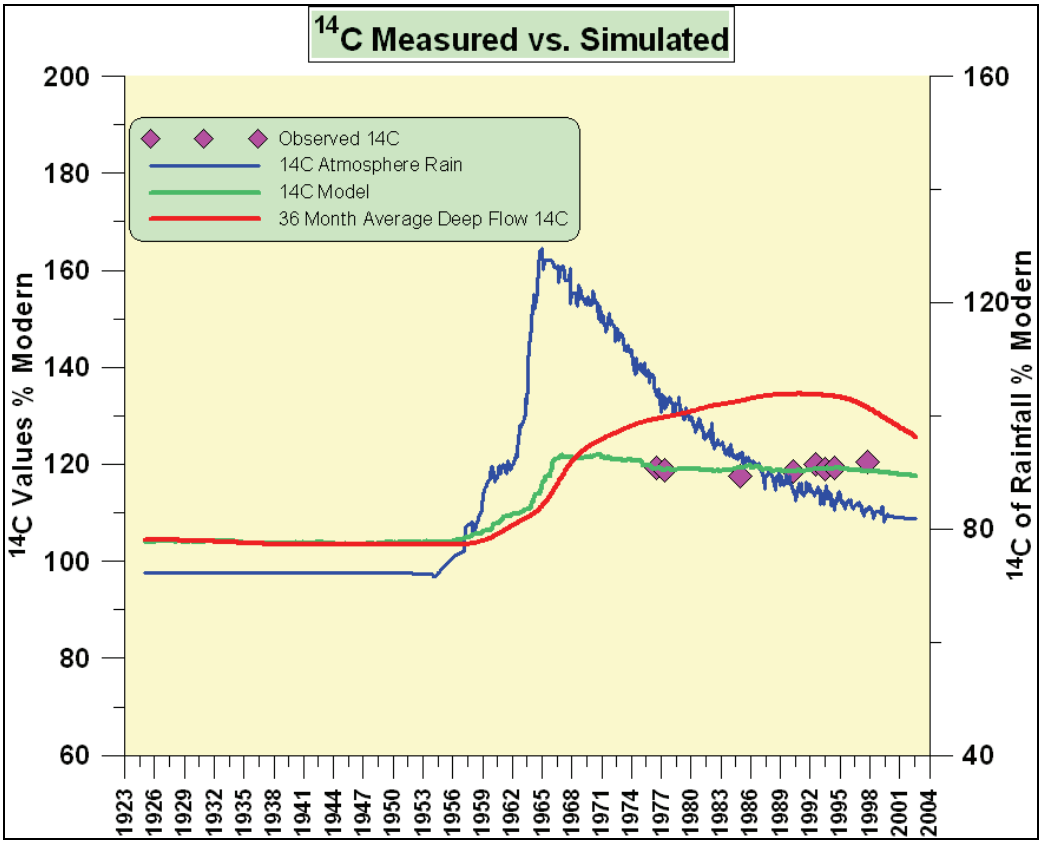

Figure 10 – ^{14}C Simulated vs. Observed

From Figure 10 it is evident that the red graph represents the ^{14}C outcome if the deep flow is averaged over 36 months and not over 320 months, which is represented by the graph in blue. The same multiple 2.9 times the deep flow has been applied (see Table 2).

More examples are shown in Appendix 2 of how the most recent ^{14}C measurements obtained in 2007 compare to the simulated ones of other springs.

5 SIMULATIONS BY MEANS OF THE 3D FEFLOW MODEL

5.1 Molopo eye compartment

In view of the magnitude of the 2D dynamic model, which had previously been developed by the PMA Consortium (2002), it was too ambitious for the entire dolomitic area to be included in the present 3D model study (Figure 1), Hence only the large Molopo compartment and that of the smaller Buffelshoek eye, have been incorporated as suitable case studies in comparison to the Excel simulations. Both springs emanate from the chert-rich Eccles dolomite and have reliable measurements of ^{14}C. In addition, the discharge of these springs could be simulated by a well-calibrated rainfall/recharge relationship.

Figure 11 depicts the recharge area of Molopo eye according to the delineating boundary dykes. Position 1 indicates the location of the eye. Point 2 is a point midway in the aquifer and point 3 was selected on the eastern boundary of the recharge area. Point 2 is about 8.6 km and point 3 about 20 km from the spring outflow.

5.1.1 Finite element model of Molopo eye

The 3D model of the Molopo eye compartment has been compiled with the FEFLOW program. The aquifer model comprised of a mesh of surface as well as depth elements. The first model accommodated a coarser finite element mesh comprising of 125160 finite elements (see Figure 12). Number of nodes = 72 324. Mesh Area = 130 km^2 which covers the Eccles Formation.

A finer mesh of 599 000 elements was used to simulate the propagation and dispersion of a tracer injected at points 2 and 3, as well as obtaining the breakthrough of the tracer at point 1 (see Figure 26 and Figure 31).

The purpose of the selected three points is to illustrate:

1. The changes in concentrations occurring from the input of an artificial tracer

2. The propagation and breakthrough of the tracer at the spring outlet; and of an artificial injected tracer at points 2 and 3.

The calibration of the model has ensured that the spring flow (Figure 13) and piezometric levels of the model corresponded to the measured values (Figure 14 and Figure 15). The calibrated transmissivity distribution is depicted in Figure 16. Figure 16 shows the

transmissivity of a high permeability zone (in brown) which proved essential in achieving the best overall simulation of the flow of the spring and of the water level responses at the observation boreholes. The transmissivity of the bounding dykes are shown in blue, with the thicker lines indicating the outer boundaries. The thin blue lines represent some dykes that fall within the drainage area of the spring; they act as partial restrictions of the flow according to their permeability. The mixing was simulated for each of the three points shown in Figure 11.

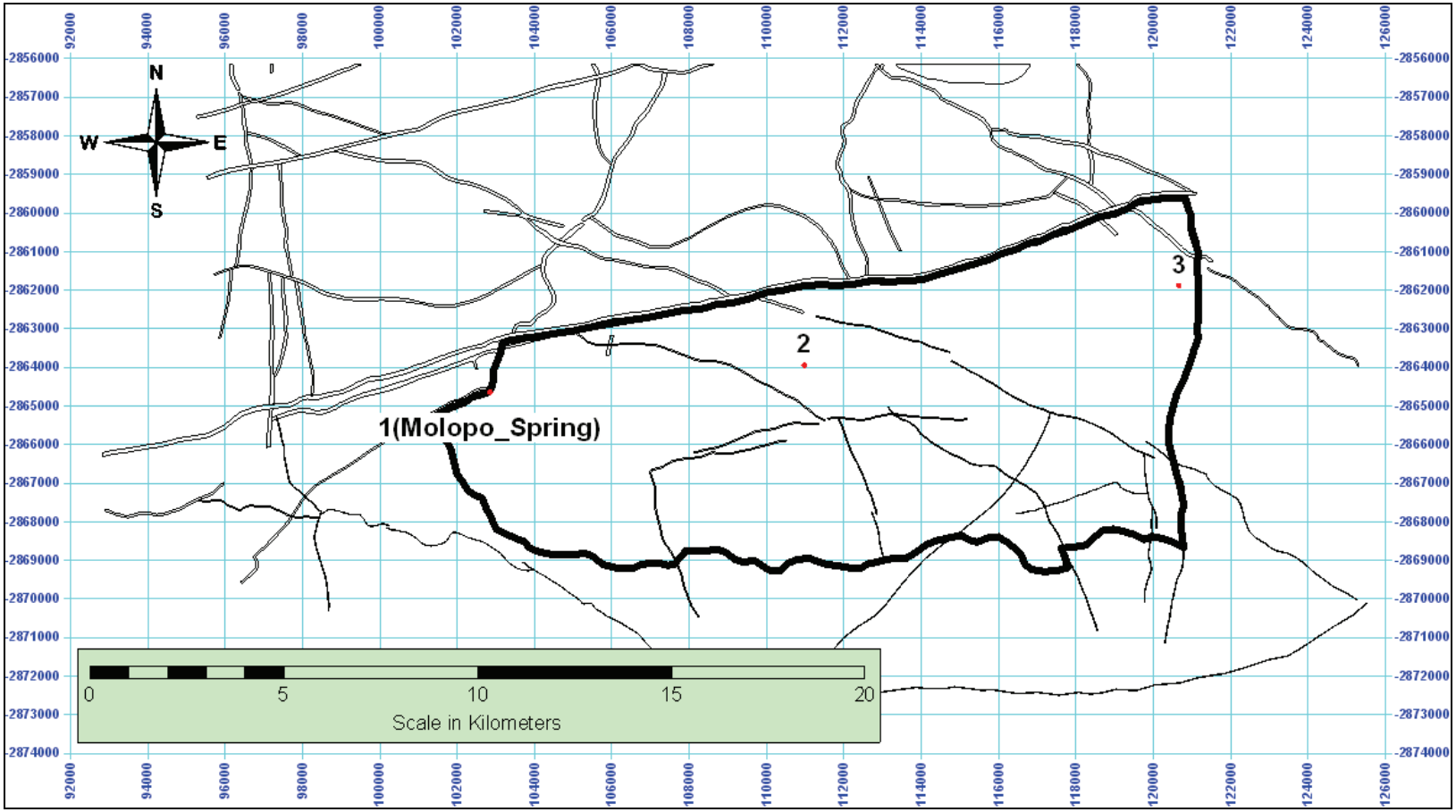

Figure 11 – Recharge area of Molopo eye according to the delineating boundary dykes.

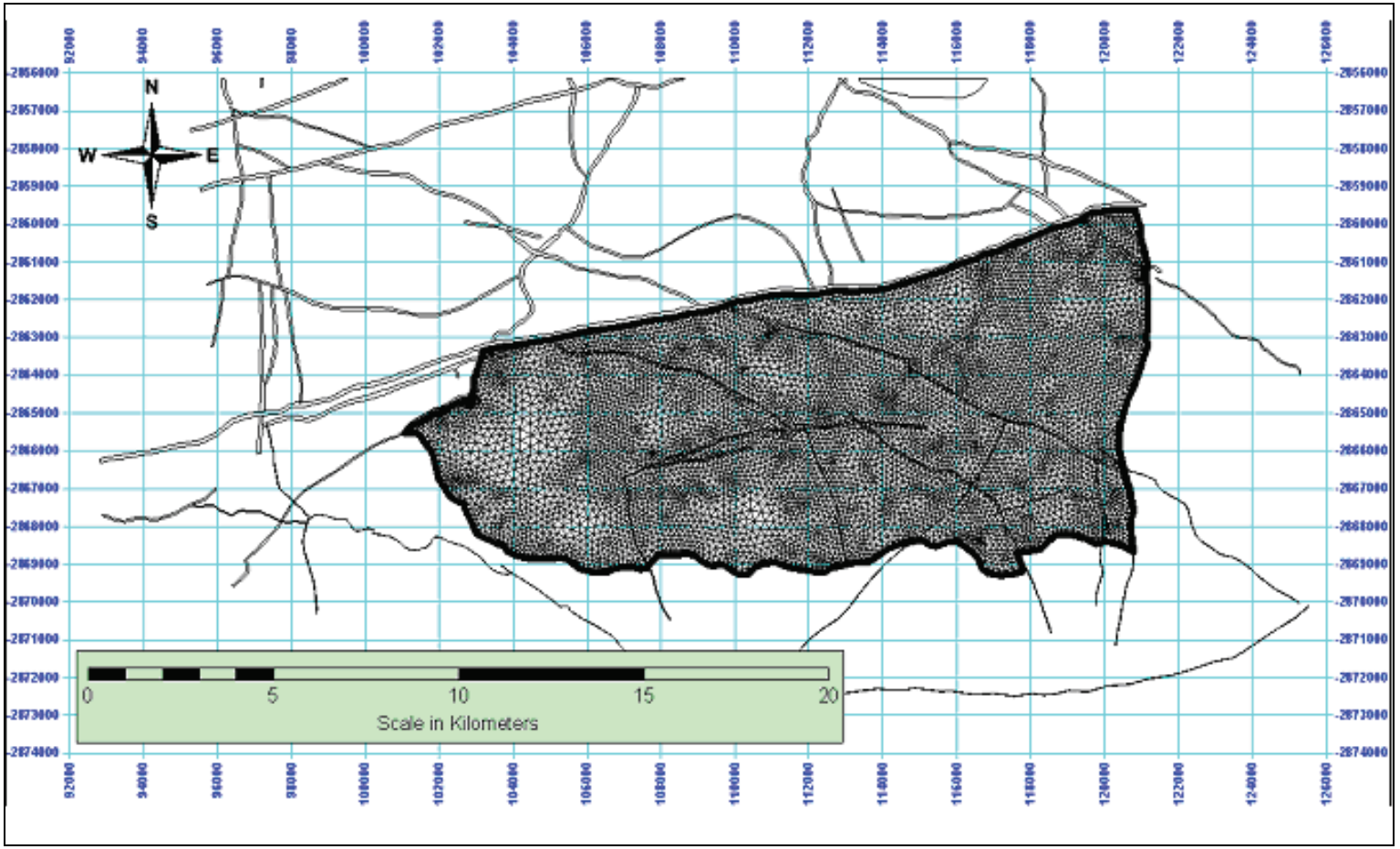

Figure 12 – First Finite element mesh of 125160 elements used for the simulation of ^{14}C.

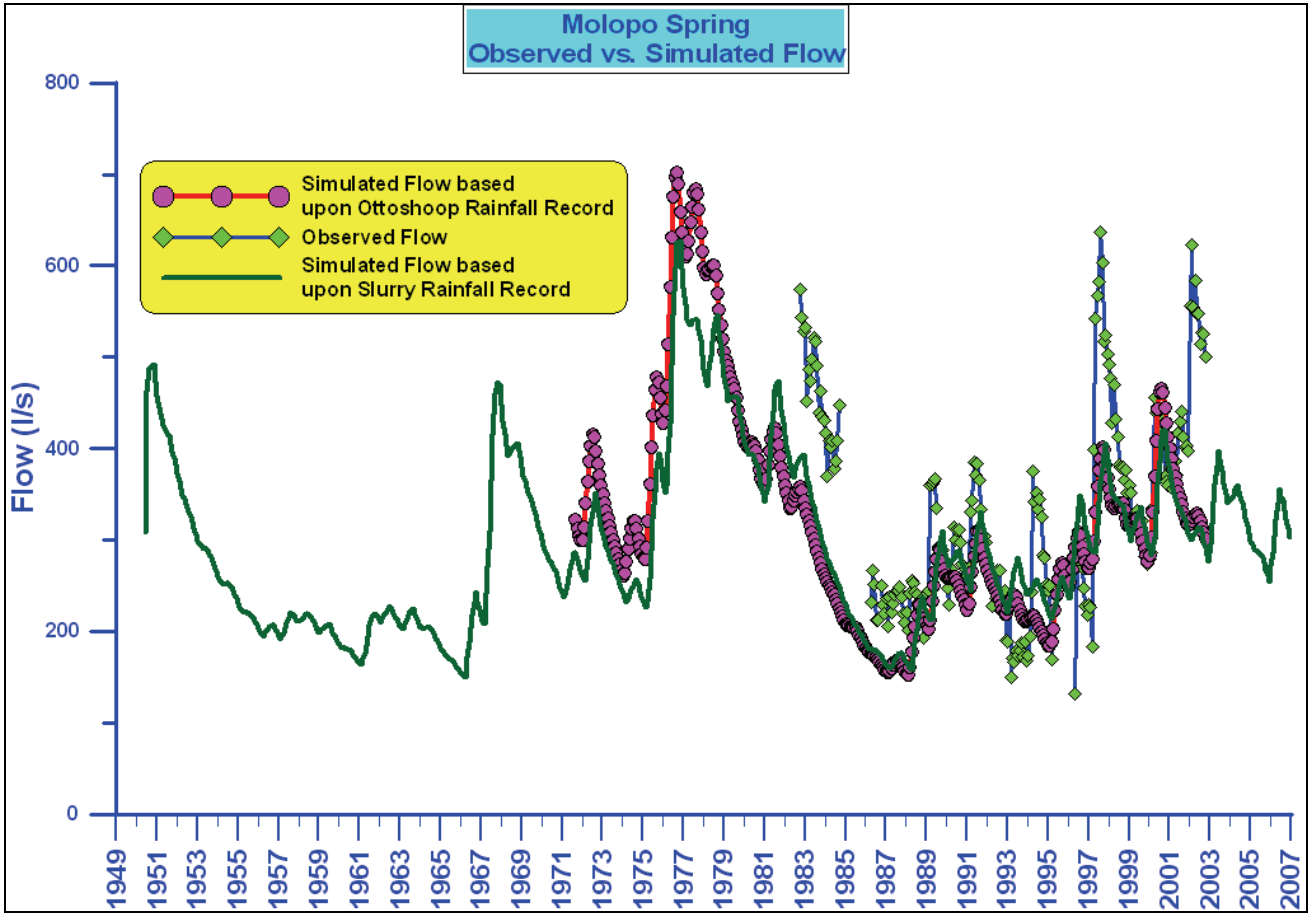

Figure 13 – Simulated vs. Observed Flow for the Molopo Spring.

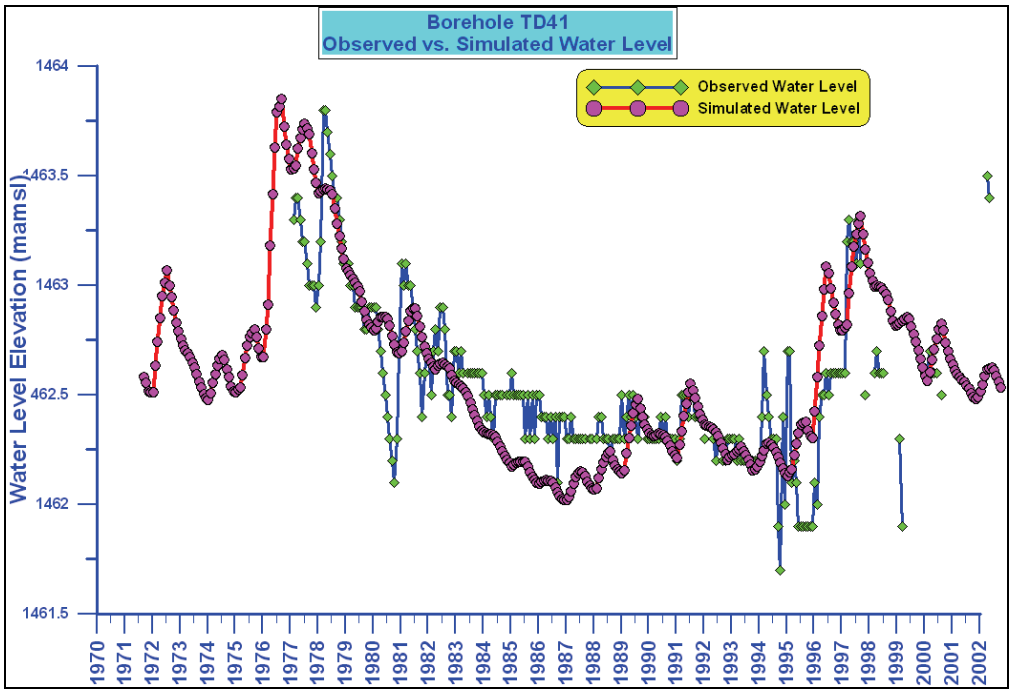

Figure 14 – Simulated vs. Observed Flow for borehole TD 41.

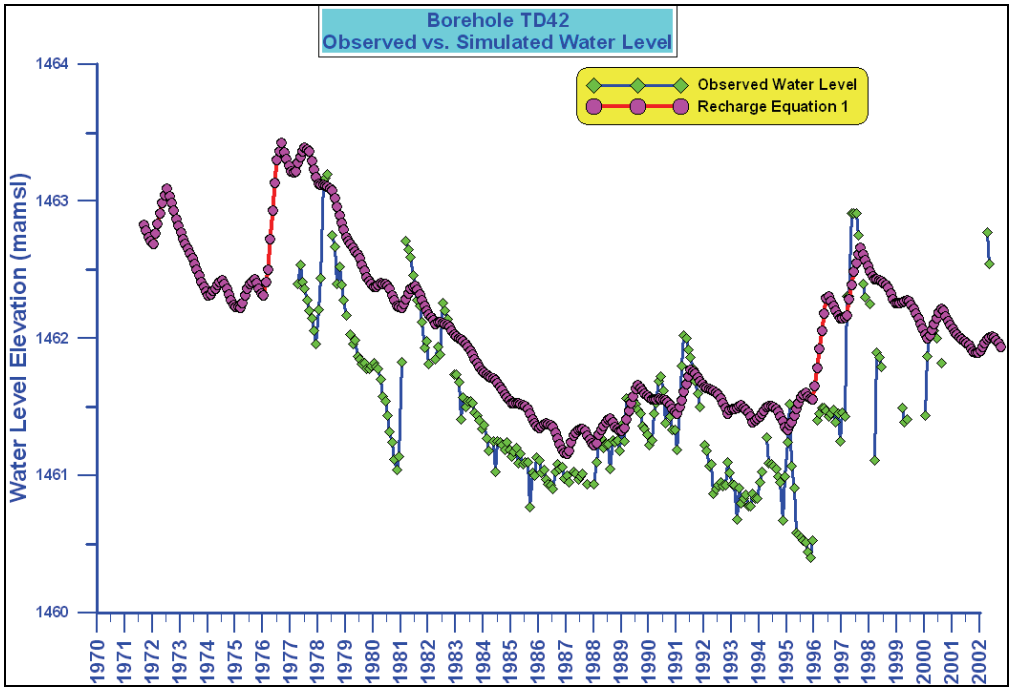

Figure 15 – Simulated vs. Observed Flow for borehole TD 42.

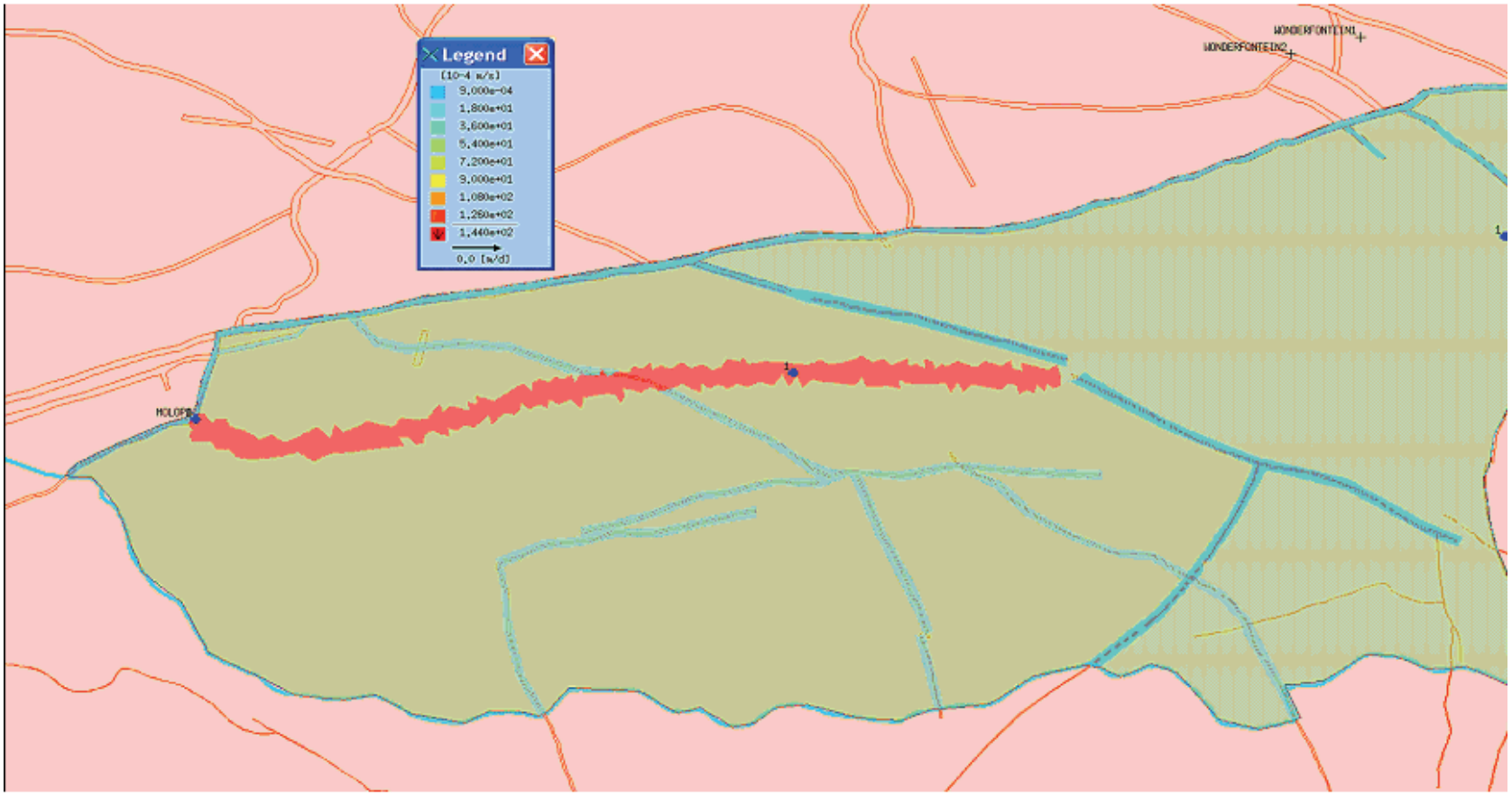

Figure 16 – Transmissivity distribution for calibrated aquifer conditions (from PMA Consortium, 2002).

5.1.2 3D modelling input

Layers were inserted to a depth of 80 meters and to reveal the breakthrough and dilution of the tracer occurring at the three selected points. The respective graphs picture the mixing that occurs for sustained average recharge and provided verification of the short and long averaging periods that have been used in the analytical model.

The first 3D modelling scenario was aimed at obtaining the best simulation of the measured ^{14}C values with natural recharge (derived from the monthly rainfall series) and permeability K and porosity (S) of the aquifer. The T values corresponded to that which had been derived for the best 2D dynamical model depicted in Figure 16. In the 3D model the T values of the different layers were adjusted by a factor varying proportional to the respective S values, whilst the average T still corresponded to the values that have produced the best 2D simulation.

Table 3 – The transmissivity (T) values applied to the different layers of the aquifer (T = K*D where K is the permeability and D the thickness of the layer).

	Scenario 1	Scenario 2
LAYER	T Factor	T Factor
1	1.8	0.2
2	1.6	0.2
3	1.4	2
4	1.2	2
5	0.8	1.5
6	0.6	1
7	0.4	0.7
8	0.2	0.4
Average	1	1

The porosity-values assigned to the different layers used in the model are shown in Table 4.

Table 4 – Different configurations of the porosity (S) for the various layers of aquifer.

Scenario	Porosity	Porosity	Porosity	Porosity	Porosity	Porosity	Porosity	Porosity
	Layer 1	Layer 2	Layer 3	Layer 4	Layer 5	Layer 6	Layer 7	Layer 8
	%	%	%	%	%	%	%	%
Base case	3	3	3	3	3	3	3	3
1	1.5	1.5	6	6	3	3	3	3
2	1.5	1.5	1.5	12	12	12	3	3
3	0.75	0.75	1.5	15	15	15	6	6

The porosity (S-value) have initially not conformed to that which was derived from the interpretation of core recovery of diamond drilled boreholes in the Far West Rand/Carletonville dolomite by Enslin and Kriel (1967). The outcome from a re-simulation has shown no difference to other varying configurations of S with depth, as long as the average S-value is 0.075.

5.1.3 Simulations results

5.1.3.1 Artificial tracer input

In the 3D model of the aquifer an artificial tracer input with a concentration of 70 was assigned to the first 5 layers; and for the 3 deeper layers a concentration of zero. The latter was an arbitrary value for demonstration purposes. The modelling was started with the aquifer in a dynamical equilibrium just before the injection of the experimental tracer concentrations. The following two graphs show the concentration changes effected in the different layers for selected intervals after the start.

5.1.3.2 Tracer reappearance at point 1, i.e. the position of the eye

Figure 17 indicates that the concentrations of the 5 upper layers declined over a period between 30 to 40 days, and then started increasing until gradually merging over 300 days to temporarily attain the same concentrations as the other layers. The 3 deeper layers reacted similarly but their concentrations increased from the start until the concentrations of all the layers attained the same mixed value, after a period of about 300 days. From this point onwards the combined mixed concentration still maintained a gradual increase and over the next 100 years the starting concentrations would still not have been reached. The tracer concentrations of layers 7 and 8 reacted similar to that of layer 6; showing increasing concentrations from the start and coalescing within 30 to 40 days with that of the upper

layers. It is clear that the initial mixed concentration (of about 40) is obtained within a relative short period of about 300 days, which correspond with the short mixing period of 36 months that was used in the analytical Excel model. The subsequent period up to about 100 years corresponds to the long Excel period multiplied by the factor in the analytical model.

5.1.3.3 Tracer mixing at point 2, i.e. mid-point within Compartment

The temporal mixing that takes place in the middle of the aquifer (represented by point 2) is shown in Figure 18.

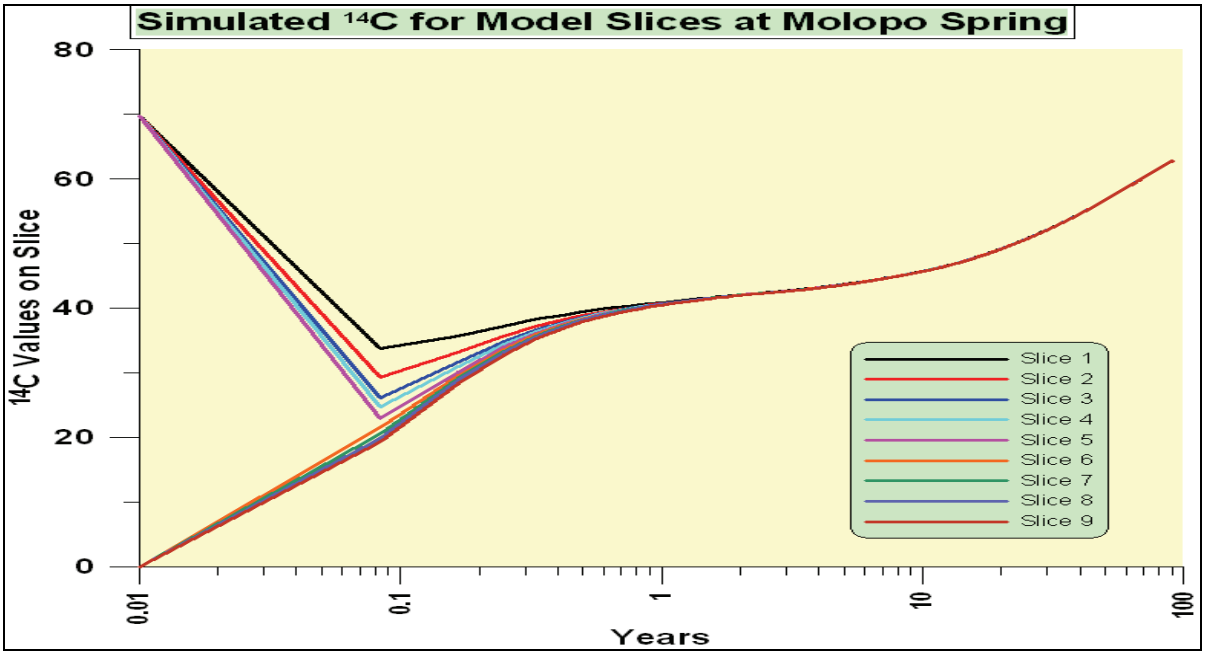

Figure 17 – Plot of the time-varying response of the tracer concentrations for the 8 modelling layers (9 slices) at the point representative of outlet of the Molopo spring in the 3D model.

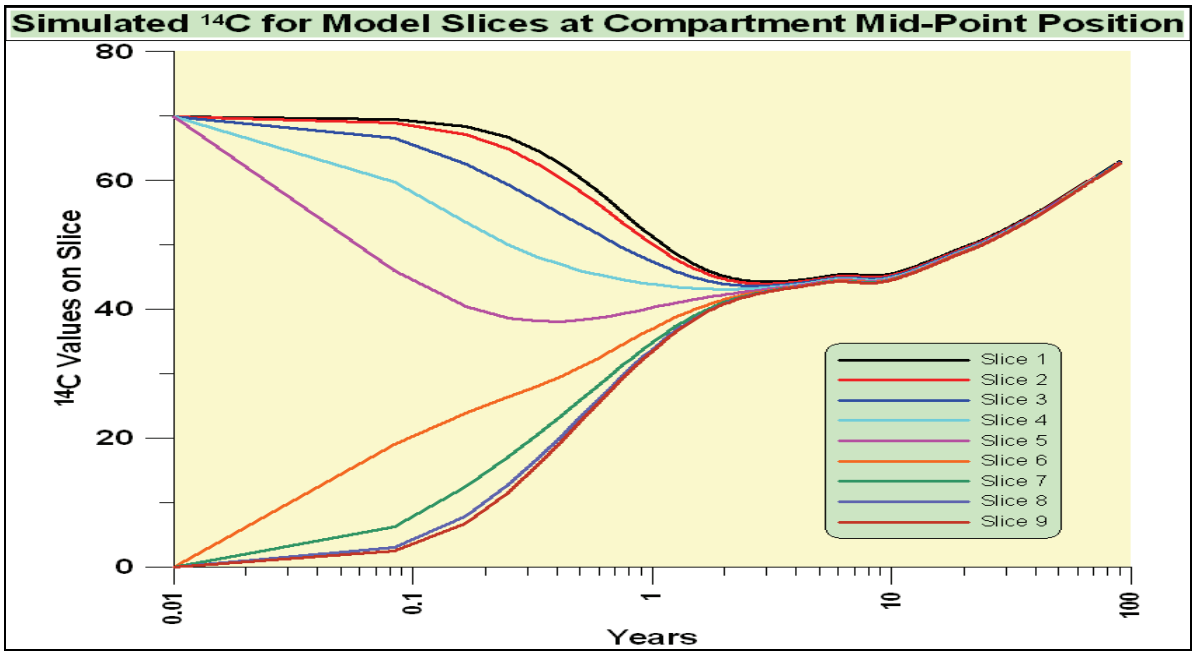

Figure 18 – Plot of the time-varying response of the tracer concentrations for the 8 modelling layers (9 slices) at a mid-point (point 2 on Figure 11) in the 3D model.

This indicates a more drawn-out mixing pattern, which is essentially the same as that of point 1, but taking about 4 years to reach a uniform mix of about 44 (see Figure 18).

5.1.3.4 Tracer mixing at point 3, i.e. end-point within the Compartment

The mixing effected in the different layers for point 3 (Figure 11) are shown in Figure 19, which indicates that a much larger period would be required to reach a uniform mixed concentration. After 100 years the tracer concentration in all the layers would still not have attained an equilibrium value at point 3. This can be explained by the small lateral flow and only vertical flow that could effect a uniform mixed concentration.

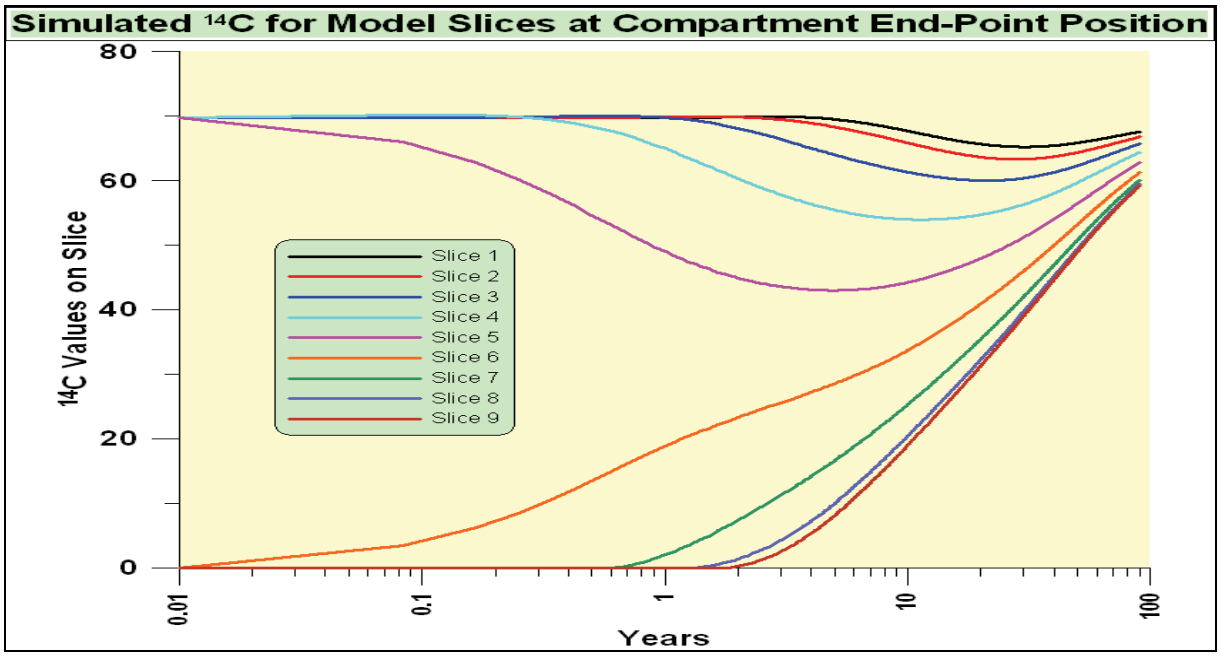

Figure 19 – Plot of the time-varying response of the tracer concentrations for the 8 modelling layers (9 slices) at a mid-point (point 3 on Figure 11) in the 3D model.

5.1.3.5 Simulation of the natural ^{14}C pulse

The correspondence obtained between the simulated and measured ^{14}C values for the different configurations of the 3D FEM model of the Molopo eye aquifer, is shown in the next figure. This has been achieved using the same input ^{14}C pulse as that of the Excel model injected via the recharge. The recharge controlling the input has been calculated from the rainfall relationship that yielded the best simulation of the spring flow derived from the available rainfall record.

The input ^{14}C value of rainfall for the Molopo spring prior to the advent of the bomb ^{14}C was assumed to be 70%, which was lower than the value of 77% that was initially derived according to the Excel model. The latter value has been obtained having assumed that the recharge is affected by the bimodal infiltration process. In the present study the recharge was assumed to be contributed only by recharge bypassing the soil zone, which occurs from rainfall exceeding a threshold of about 30 mm per month. The recharge coefficient was changed until the long-term average recharge corresponded to that derived from the chloride method (CMB method). At the same time the simulated bicarbonate concentration of the spring was calculated using the method applied by Bredenkamp et al. (2007). Accordingly the bicarbonate could vary between 0.5, i.e. for recharge infiltrating fast, and 0.9 for recharge passing through the root zone. From this the average bicarbonate of Molopo eye corresponded to an initial ^{14}C input factor of 0.73 of that of the atmosphere. This was close to

the factor of 0.7 which had been assumed purely on the grounds that the Eccles dolomite has a high recharge. The use of a factor 0.7 instead of 0.73 in the simulation would require a small increase of the storativity that was obtained from the original 3D model.

Figure 20 clearly illustrates that there is a consistent improvement of the simulation outcome, from the base-case representing a constant porosity (S-value) of 3% for all layers of the aquifer, to scenario 3 for which the average S-values of intermediate layers increase, as is indicated in Table 3. The best match has been obtained if the average S-value for all layers was 7.5% (see Figure 20). This value was independent of the configuration of the values of S assigned to the different layers and can therefore also conform to an exponential declining S with depth. The latter is a more acceptable configuration according to Enslin and Kriel (1967) and it also conforms to an exponential decline of S with depth derived by Bredenkamp (cf Bredenkamp et al., 2004). This relationship has been obtained from the interpretation of different hydrographs in the Upper-Molopo dolomite, from a combination of the moving average and cumulative rainfall departure methods (see Figure 21). An average S-value of 0.027 and an effective aquifer thickness of 80 m have been obtained for the regional dolomite from the relationship shown in Figure 21. This S-value is much lower than the value of 0.075, which was derived from the aquifer of Molopo eye from the 3D simulation of the ^{14}C. This is explicable as Figure 21 has been compiled from the interpretation of hydrographs of boreholes covering the larger part of the Upper-Molopo dolomite, whereas the Molopo Eye is predominantly recharged from the Eccles aquifer, which is known to have the highest S-value of all the dolomite formations (Stephens and Bredenkamp 2005).

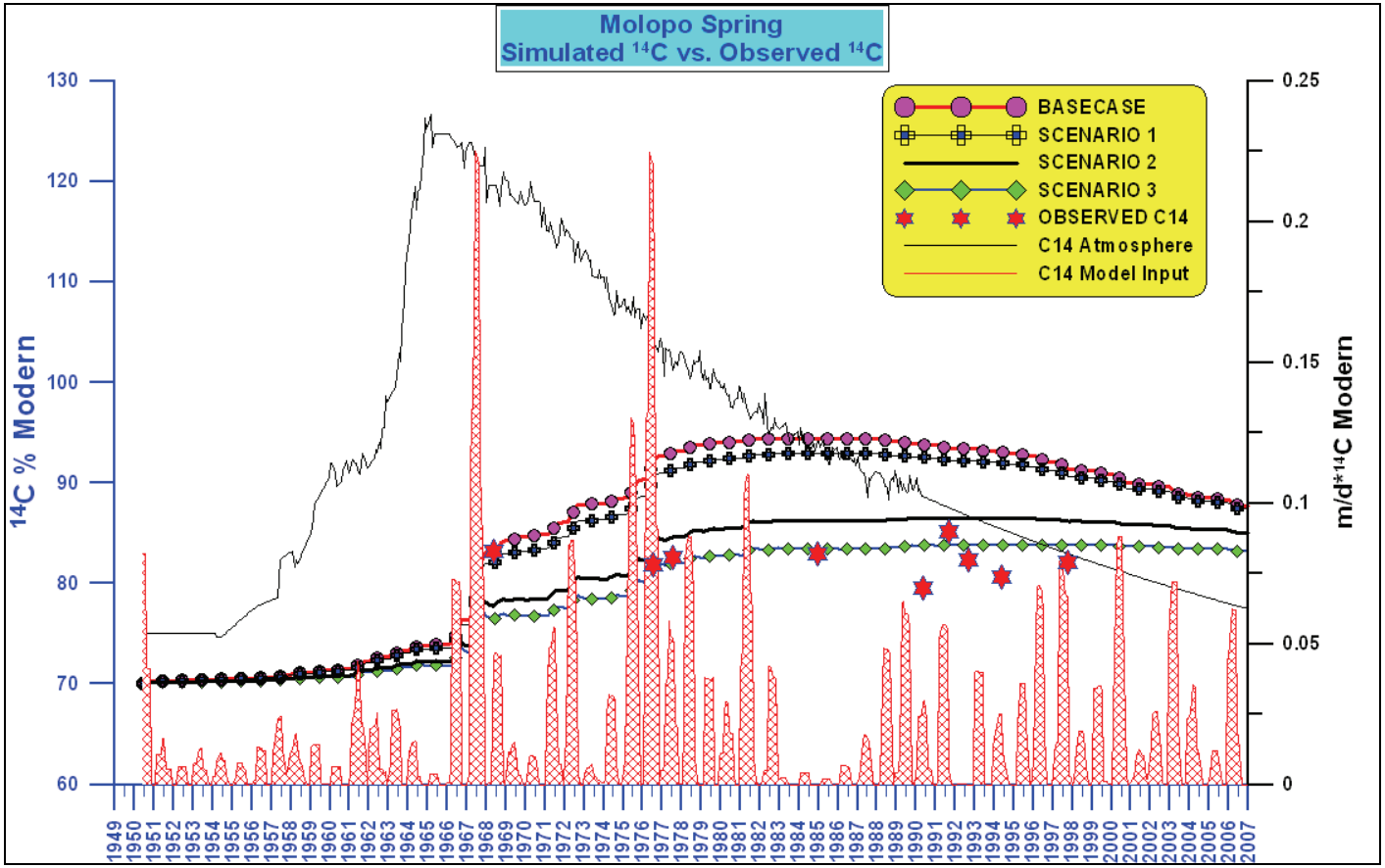

Figure 20 – Simulated ^{14}C values of the Molopo spring water according to different scenarios, using the variable input of ^{14}C introduced by the recharge. The mixing is controlled by the hydrodynamic flow until the recharged water eventually emanates at the spring.

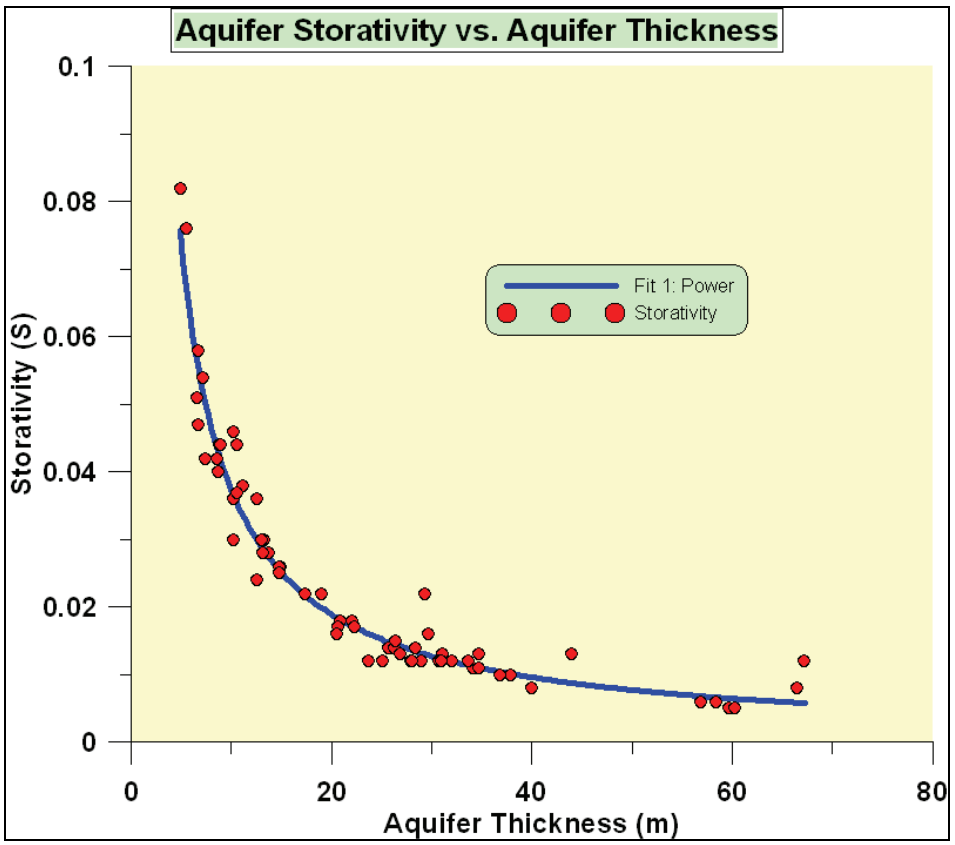

Figure 21 – Aquifer storativity vs. aquifer thickness. Decline of S with depth in dolomitic aquifers in the Upper-Molopo area indicating an effective aquifer thickness of 80 metres used in the 3D model. (Bredenkamp et al., 2005).

The FEM model was run again using the configuration of S-values with depth shown in Table 5. The simulations with average S values of 0.075 for scenarios 3, 6 and 7 produced identical best simulations. This clearly indicated that the outcome to the simulation is independent of the configuration of S as long as the average porosity is 7.5% (Figure 22).

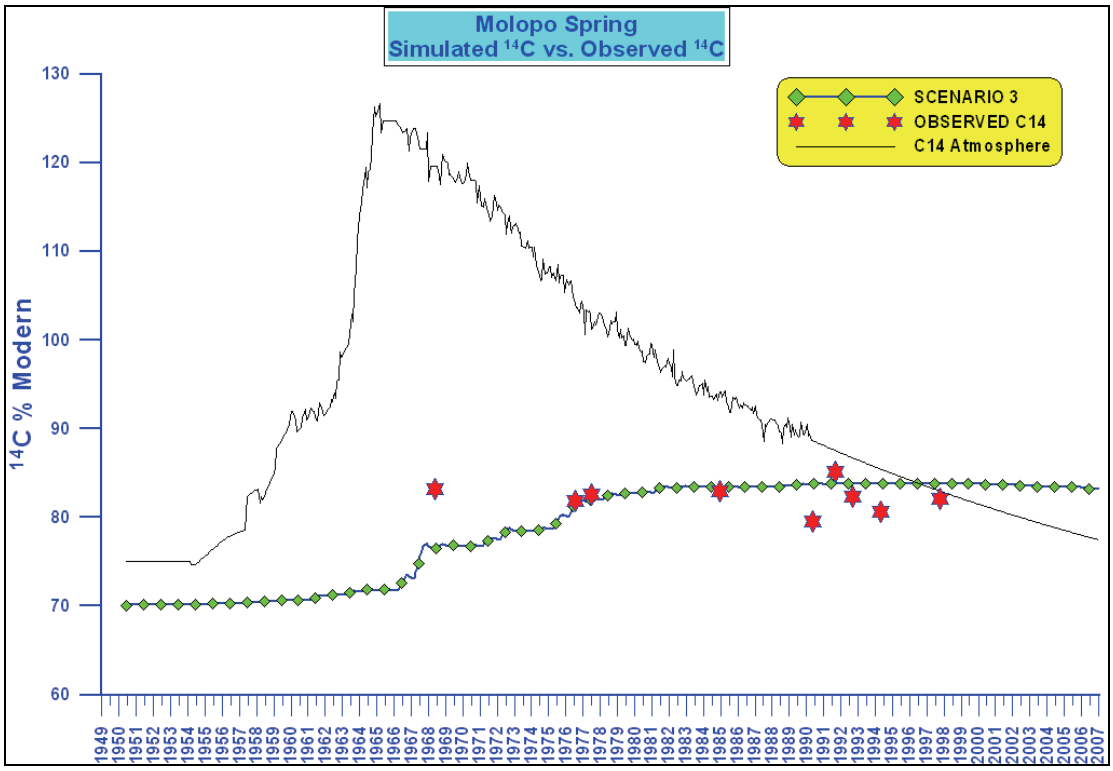

Figure 22 – Correspondence of the best match obtained (S = 0.075) with the 3D FEM simulation model in comparison to the measured ^{14}C values of Molopo eye.

Table 5 – The different configurations of the S values assigned in the FEM model.

Scenario	Layer 1	Layer 2	Layer 3	Layer 4	Layer 5	Layer 6	Layer 7	Layer 8	Average
	Porosity (%)								
Basecase	3	3	3	3	3	3	3	3	3
1	1.5	1.5	6	6	3	3	3	3	3.38
2	1.5	1.5	1.5	12	12	12	3	3	5.75
3	0.75	0.75	1.5	15	15	15	6	6	**7.5**
4	0.375	0.375	0.75	15	15	15	6	6	7.31
5	9	6	3	1	9	6	3	1	4.7
6	12	9	6	3	12	9	6	3	**7.5**
7	7.5	7.5	7.5	7.5	7.5	7.5	7.5	7.5	**7.5**
8*	1.5	1.5	1.5	12	12	12	3	3	5.75

5.1.3.6 Simulation of the long-term ^{14}C response of Molopo Spring

The long-term response of ^{14}C at the spring was simulated using the configuration of S and T that have produced the best simulation (see Table 5 and Figure 22). However the rainfall record was extended by inserting a duplicate of the present rainfall series onto the observed rainfall series. The variation of the spring flow that was derived from the exponential rainfall-recharge relationship used by the PMA Consortium (2002) is shown in Figure 23.

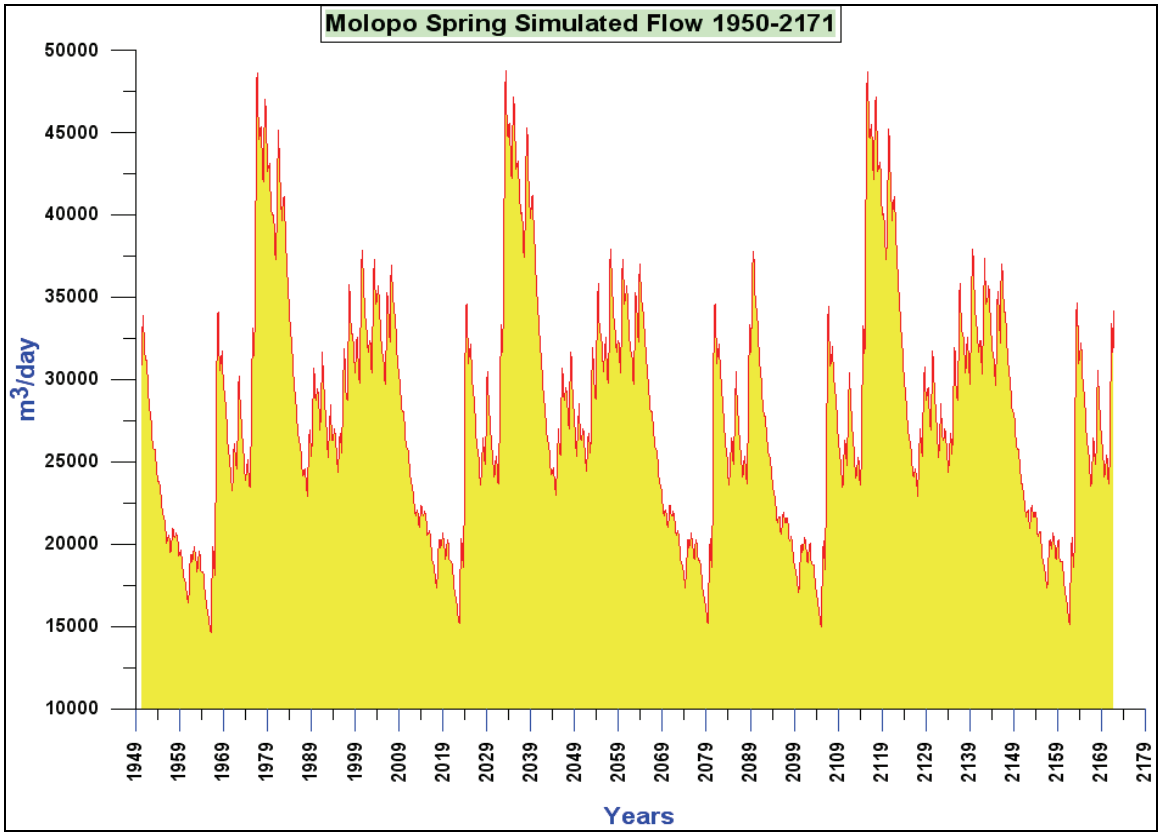

Figure 23 – The simulated highly variable recharge that controls the ^{14}C input load of the 3D flow model, to simulate the ^{14}C breakthrough (i.e. ^{14}C * m/d - recharge) shown in Figure 20.

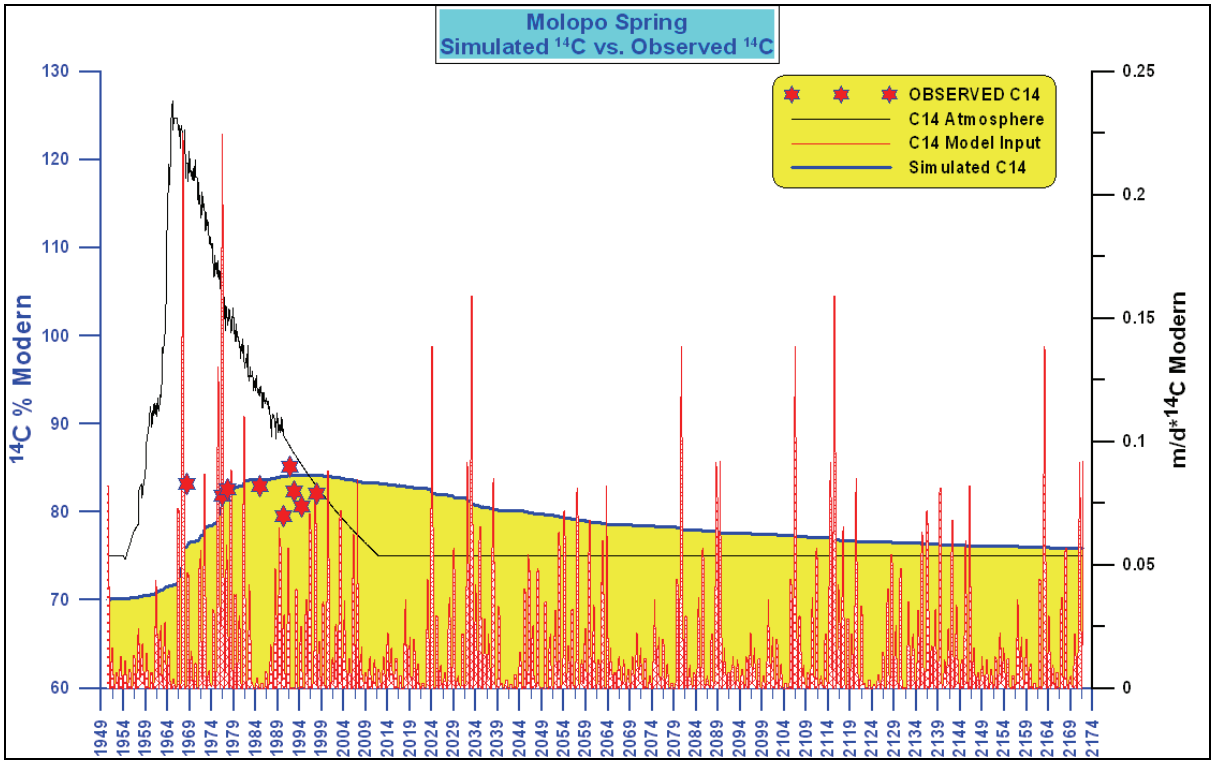

Figure 24 – Graph of the measured ^{14}Cvalues in relation to the simulated long-term ^{14}C response of Molopo eye according to the 3D simulation model using the extended rainfall series up to year 2174.

In spite of the spread of the observed ^{14}C values in comparison to the smooth simulated ones, the correspondence is still good considering the inherent uncertainty associated with the measured values. It is evident that the highest peak of the ^{14}C was reached around year 1995, i.e. a ^{14}C value of 84% mod. From 1994 the concentration will maintain a gradual decline until the year 2174 but the pre-bomb concentrations of ^{14}C of the atmosphere would still not have been reached by then.

The comparison between the long-term ^{14}C response derived from the Excel model and that of the 3D model is shown in Figure 25. In both cases the ^{14}C measurement of 2007 shows up as an outlier and therefore appears to be an unreliable value. Overall the long-term decline of both models is similar, although their fit to the measured points are slightly different. According to both models the initial pre-bomb ^{14}C levels would only be attained around the year 2130, which stresses the long-term vulnerability of these aquifers to pollution.

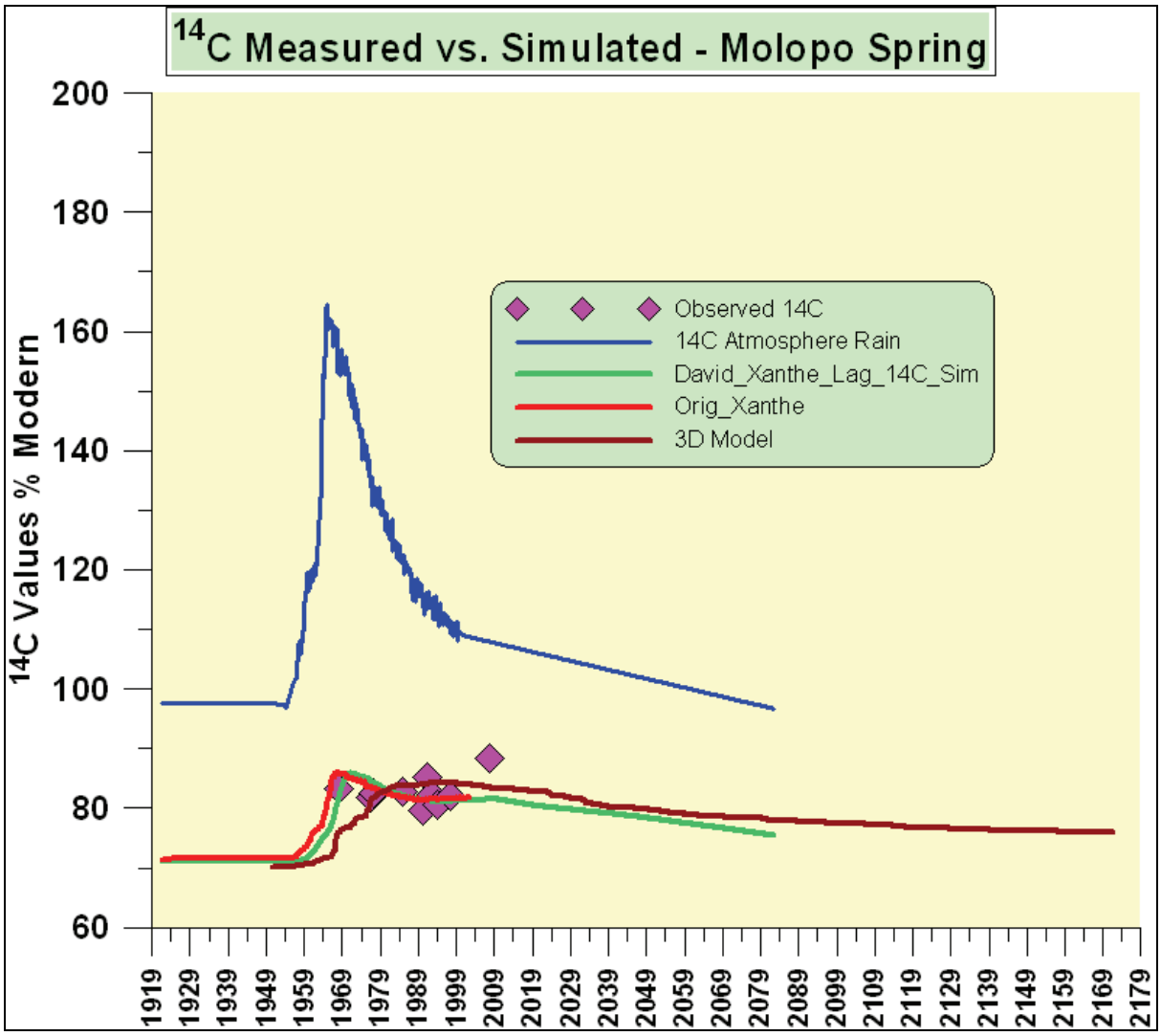

Figure 25 – Comparison between the long-term simulations with the Excel model and the 3D flow model. The measured ^{14}C value of 2007 is clearly off the trend and is regarded to be unreliable.

5.1.3.7 Deriving the travel time in relation to the distance from the spring

One of the main objectives of the study was to assess the propagation of an ideal tracer, simulating pollution through the aquifer under the same natural flow conditions as was derived with the 3D model. A fictitious tracer with a concentration of 100 000 was injected as a sustained input at points 2 and 3 in the 3D model, which respectively are 8 and 18.5 km from the spring outlet. The breakthrough of these tracers at the spring outflow point, using the extended rainfall record that has been applied to simulate the ^{14}C response is shown in Figure 26.

.

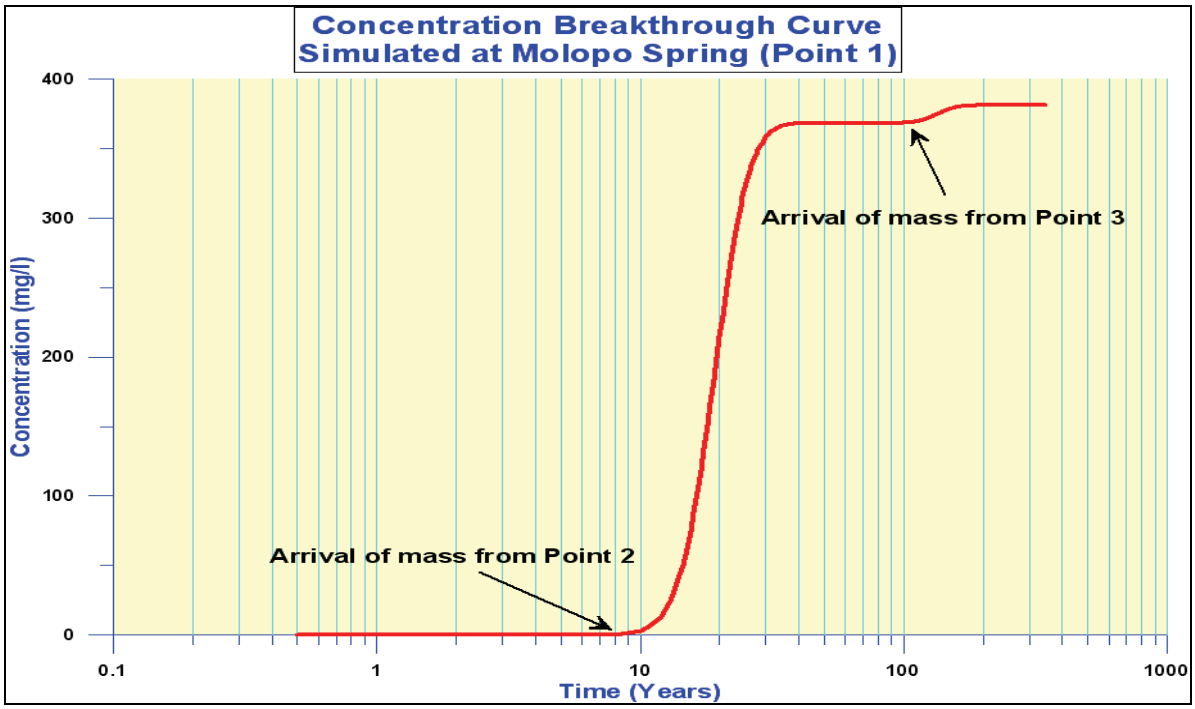

Figure 26 – The response of tracer injections at point 2 and 3 in the 3D simulation model, to derive the travel time of pollution in the aquifer. The points 2 and 3 are respectively 8 and 18.5 km from the spring outlet.

As is shown in Figure 26, the tracer injected at point 2 would start reappearing after 10 years; and would peak after 40 years. The injected tracer at point 3 would start appearing after 120 years and would have reached its maximum about 180 years after the start of the tracer injection. A plot of these arrival times against the distances from the spring is shown in Figure 27, which conforms to an exponential increase in the travel time versus the distance.

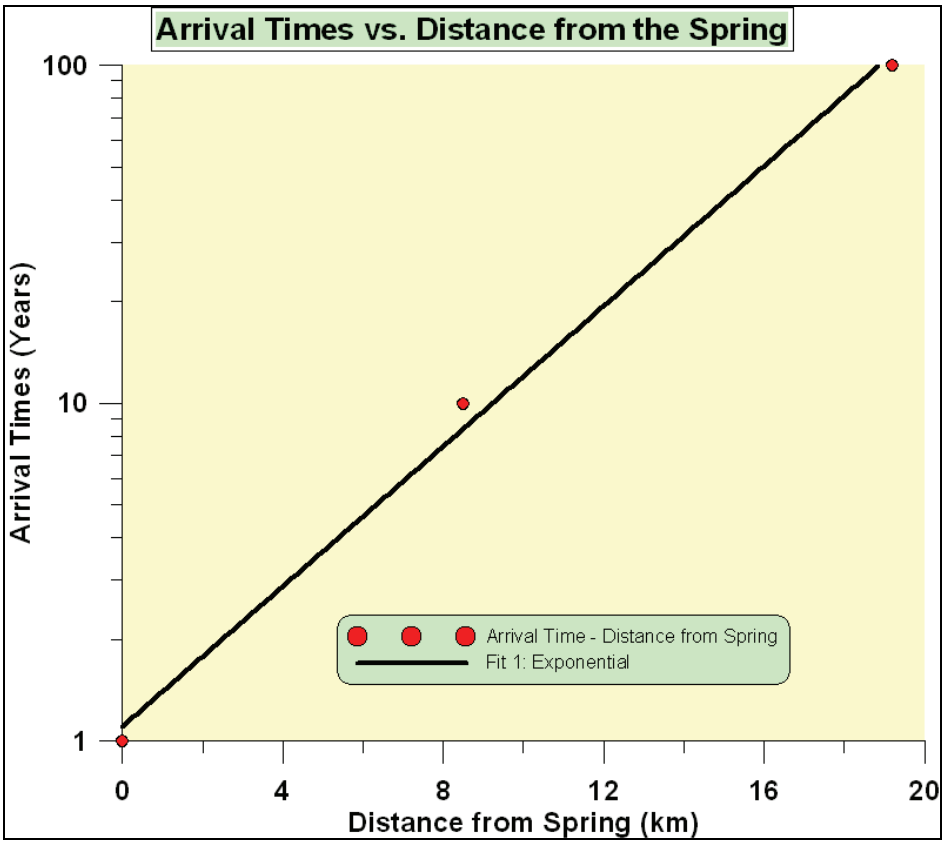

Figure 27 – Relationship between the arrival times and injection distances of a tracer in the recharge compartment of Molopo eye, according to the simulation of the flow by means of a 3D finite element model.

Figure 28 shows the propagation of the tracer plumes at points 2 and 3 after 5 years and Figure 29 that after 10 years. The latter shows that after 10 years the first tracer from point 2 would have reached the spring, whilst the plume from point 3 would have advanced very little. The plumes clearly indicate not much lateral dispersion of the tracers and they also display the slow propagation of the tracers from the point 3 over this period.

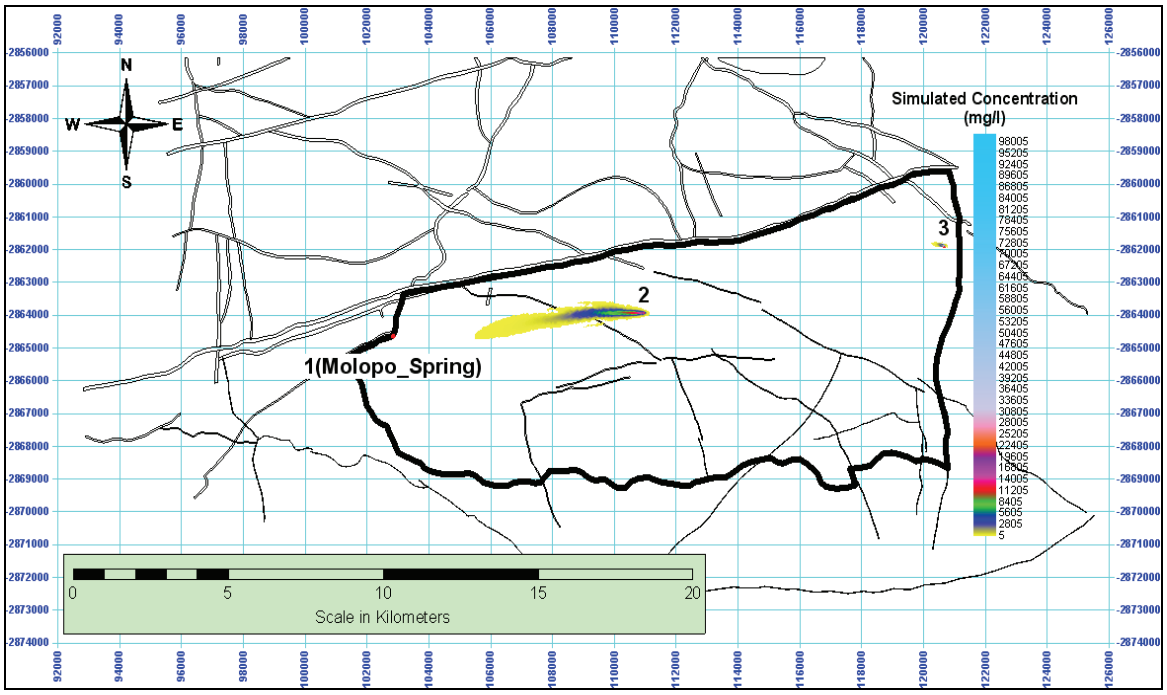

Figure 28 – The propagation of tracers injected at point 2 and 3 in the model of the Molopo aquifer after a period of 5 years.

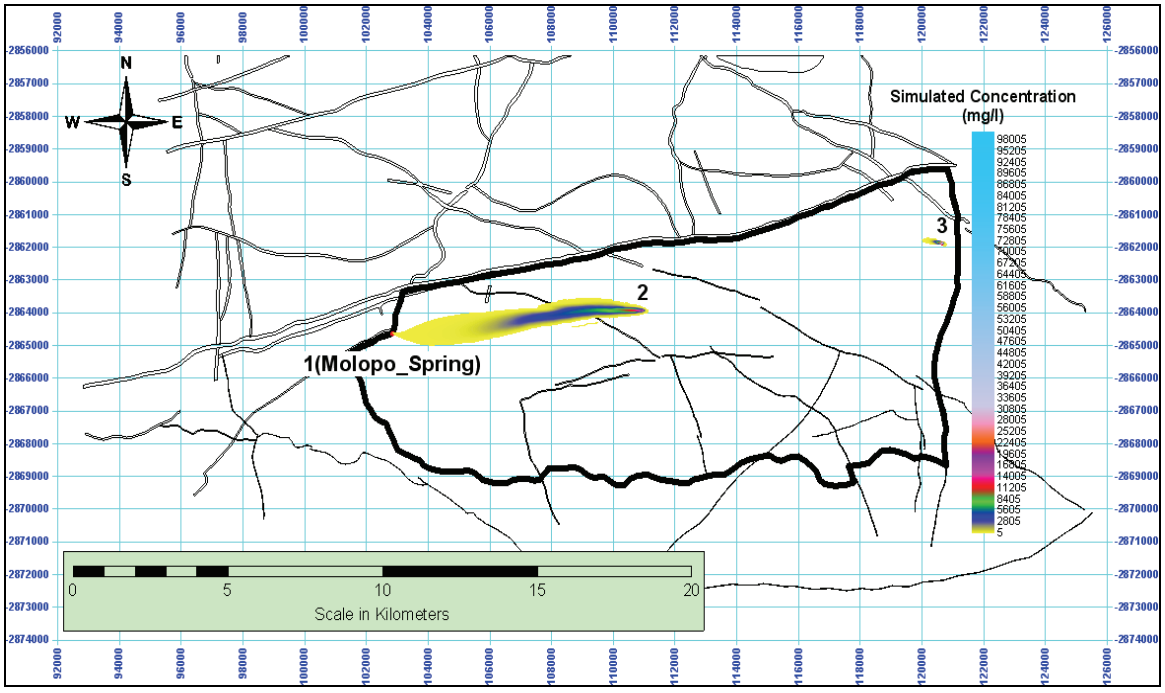

Figure 29 – The propagation of a tracer injected at point 2 and 3 in the model of the Molopo aquifer after a period of 10 years.

The same would apply to the flow-path of tracers injected at a point close to the surface that

would show a narrow plume developing with depth until it reaches the spring. In the case of an injection at point 3 it would take more than 100 years before the tracer will reach the spring (see Figure 26).

The approximate travel time from any point in the aquifer to the spring outlet, could be visualized superimposing

Figure 26 to fit onto the aquifer image (Figure 28),

To obtain a better understanding of the propagation of the flows and admixing times of water being recharged, another simulation was carried out by which tracers have been injected at the points marked in Figure 30 under a sustained long-term average recharge.

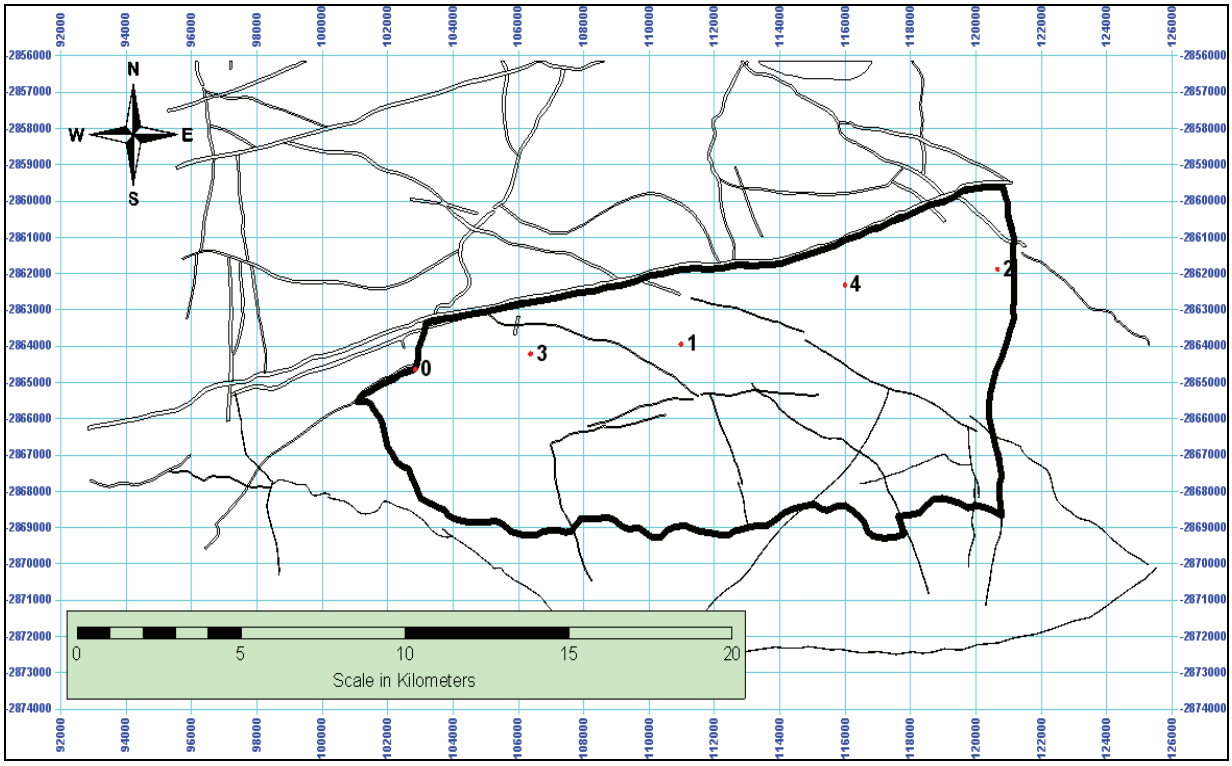

Figure 30 – Positions of the injection points of an artificial tracer to determine the arrival times of water at the spring outlet (see Figure 31).

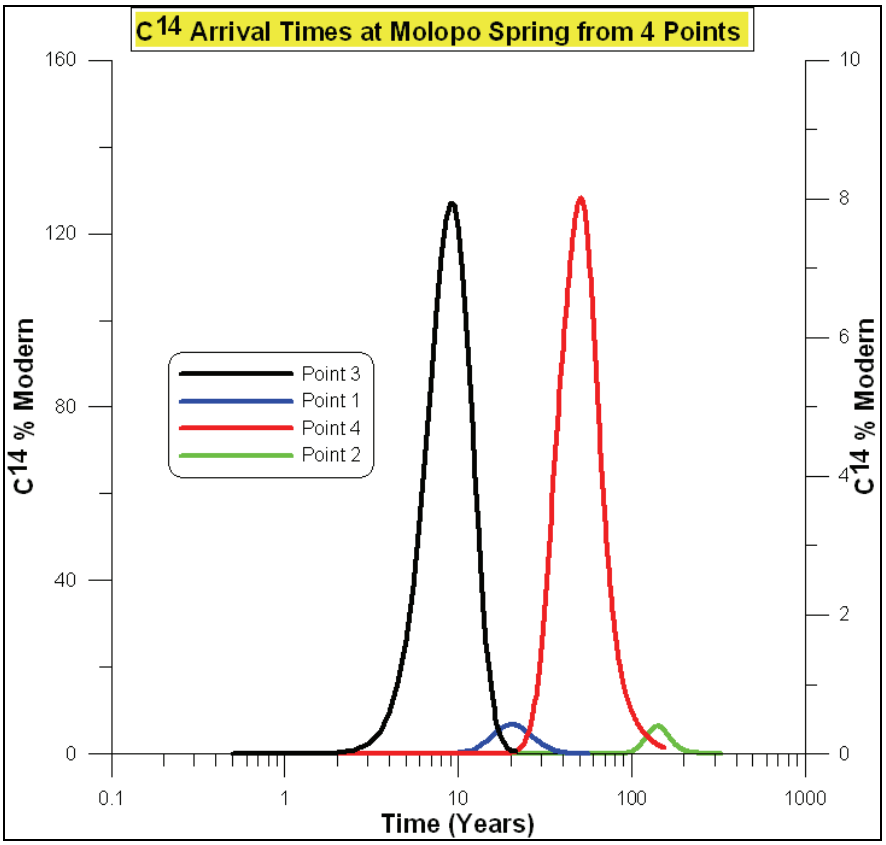

Figure 31 – The arrival times at the spring of tracers injected at points 1, 2. 3 and 4 at about equal distances from the spring outlet (see also Figure 30).

The difference in the concentrations arriving at the spring from points 3 and 4, to those injected at points 1 and 2, is attributed to the differences in the mass injected into the aquifer. The different travel time from the various injection points are listed in Table 6.

Table 6 – Deriving the travel times of tracers injected at different distances from Molopo eye

Point	Ref Figure	Dis-tance to to spring (km)	first arrival (years)	Arrival Peak (years)	Average age 1 st arrival (years)	Average age Peak (years)	Average age of 1st and peak arrival
2	Figure 11	8	10	40	5	20	12.5
3	Figure 11	18.6	95	140	47.5	70	58.75
3	Figure 30	3.2	2.4	9	1.2	4.5	2.85
1	Figure 30	8	12	20	6	10	8
4	Figure 30	13.4	23	45	11.5	22.5	17
2	Figure 30	20	100	150	50	75	62.5
		Average age of 1 st arrival =			37.7		
		Average age of peak arrival =			73.7		55.7
		Average age at 10 km from eye =			24.5		
		Average age at 20 km from eye =			125.5		
		Average age at 1km from eye =			2.39		
		Average of the last 3 =			50.79		

The first arrival times for the various injections of a tracer at the different distances are shown in Figure 32 and that of the peak concentrations in Figure 33, whereas Figure 34 illustrates the average of the peak and first arrival times. From Figure 32 and Figure 33 it is evident that the average travel time of water arriving at the spring is 4 years, and 1.5 years for the first arrival of tracer at the spring. This is in close range to the 24 to 36 month period that is used in the Excel model to represent the admixing of the recently recharged water contributed in close proximity to the spring. The rest of the mix includes all the water up to 20 km from the eye with an average travel time of about 120 years (refer Figure 33), which could be as high as 150 years for the peak arrival time of water from the furthest end of the aquifer (refer Figure 34).

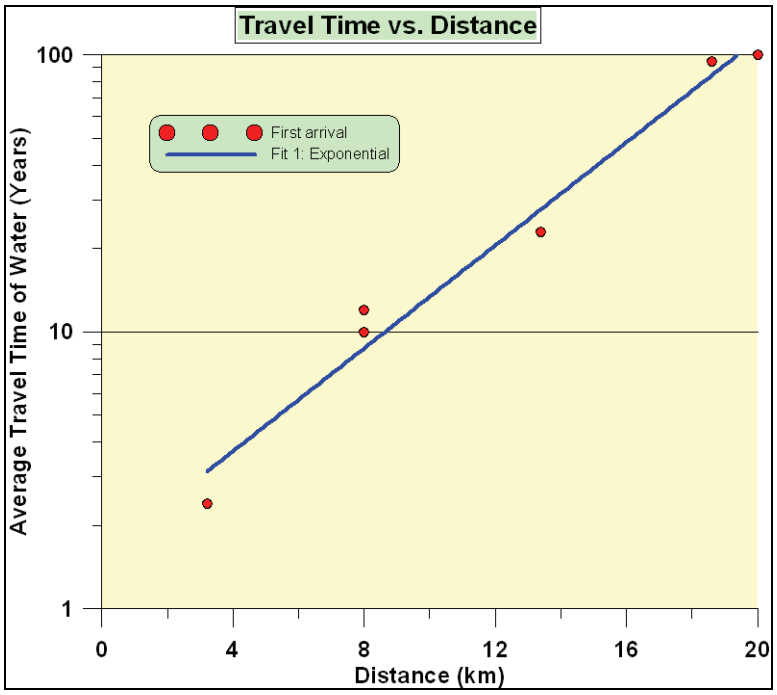

Figure 32 – Exponential increase in age for the first arrival times of tracers injected at the different distances from Molopo eye.

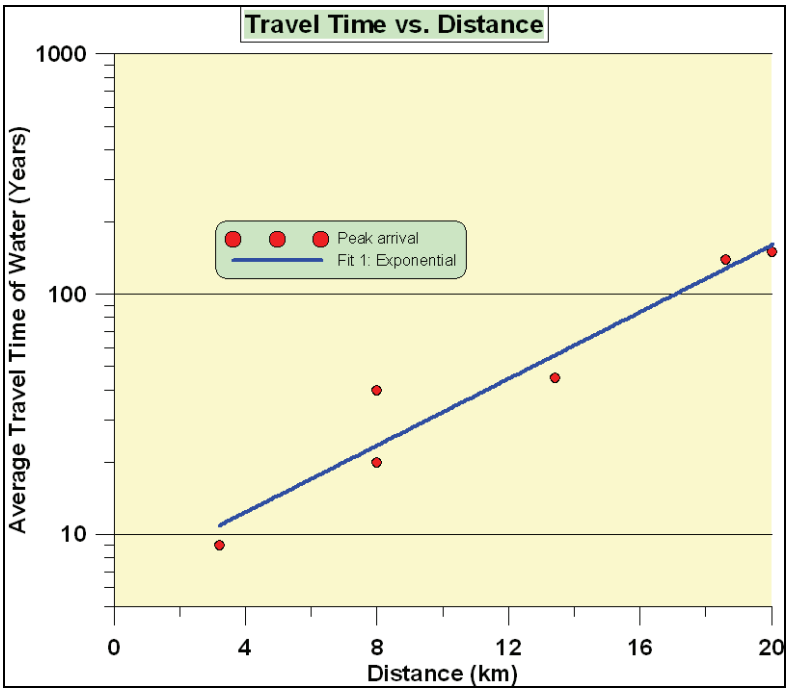

Figure 33 – Exponential increase in age for the arrival of the peak concentrations injected at the different distances from Molopo eye.

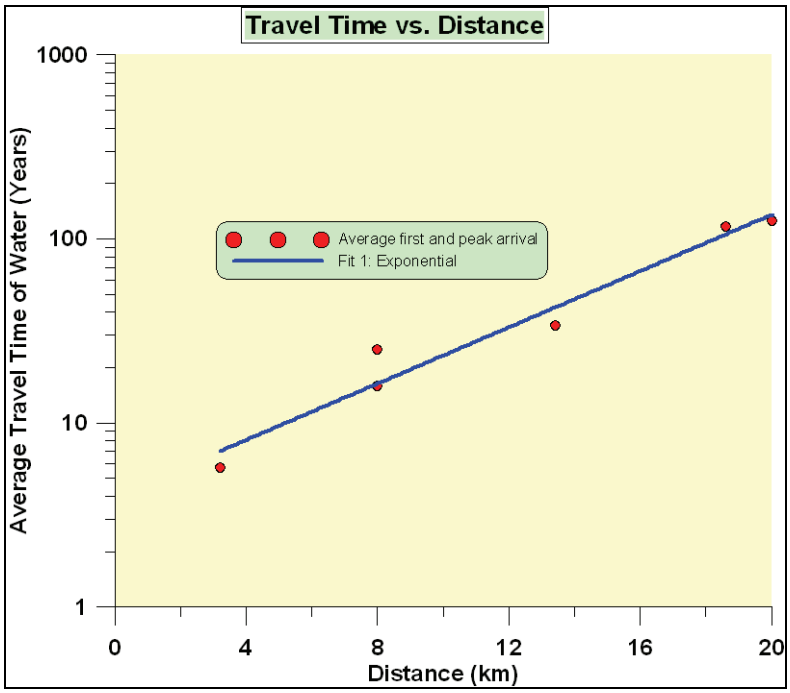

Figure 34 – Exponential increase in age of the average time of the first and peak arrival of the tracers injected at the different distances from Molopo eye.

5.1.3.8 Comparisons to the Analytical model results

The average **turnover time** of water the Molopo aquifer represents the ratio of water stored in the aquifer to the average recharge. According to the FEM model, the average recharge is 14% of the average rainfall, i.e. 78 mm per year, whilst the equivalent of the water stored in the aquifer to a depth of 70 m for an average S of 0.075, is 5.25 m. This yields a ratio of 5250/ 78 = 67 for the average turnover time. However from the chloride of the spring the CMB estimate of the average recharge is 0.119 of the average rainfall, i.e. 67.9 mm, which is 12% less than that used in the FEM.

For this value to correspond to the FEM model the recharge area would have to be increased by 12%. This is acceptable insofar that for the FEM it was assumed that all the recharge is derived only from the Eccles Formation, which is 130 km^2 compared to an area of 184 km^2 including the Lyttelton dolomite formation.

Molopo Spring		
Factors	Minimum=	28.38
Lower threshold	NA	
Higher threshold	**28.7**	
Recharge factor (L)	0.001	
Recharge factor (H)	**0.186**	
^{14}C factor (L)	0.907	
^{14}C factor (H)	**0.734**	
Relative mixing factor	1	
Final multiple factor	2.37	
Calculating Historic ^{14}C		
Lag months period 1	36	
Lag period 2	451	
Further lag Sim ^{14}C	28	
Sim HCO3 of spring =	**195.8**	
Measured HCO3 =	**199**	
Area spring (sq km) =	184	
Cl recharge =	**0.11966**	
^{14}C rech =	**0.11956**	

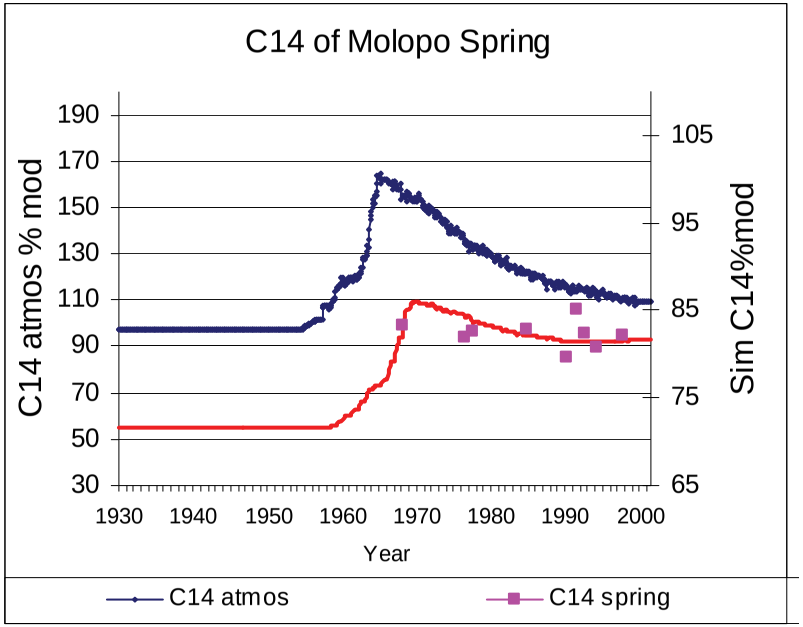

Figure 35 – Results from Excel simulation assuming that all the recharge is contributed from rainfall in excess of a threshold of 28.7 and using a multiple of 2.37 for the incorporation of the deep flow component. (The highlighted values are applicable).

According to the FEM model applying the artificial tracer, it is logical that part of the water emanating at the spring is contributed from the recharge derived from the first 36 month of rainfall preceding a specific month. This is the rainfall period that best corresponds to the flow variations of the spring, which explains why the simulated ^{14}C content of the spring shows some correspondence to the spring flow (see Figure 8 and Figure 9). The ^{14}C values derived from the deeper flow incorporates the ^{14}C values over a period of (451-36) = 415 months prior to the respective month. This period has to be multiplied by the factor that is required to extend the effective incorporation of recharge over a period of (2.37* (415+36)/2/12 = 42.5 years. This period compares well with that obtained from the arrival times of the first tracer from the most western border of the Molopo compartment (see Figure 26). However it would require about 82 years for the water in the aquifer to travel a distance of 20 km, which corresponds to an average turnover time of 41 years, which compares well to the average value of 50.1 years obtained from the tracer injections (see Table 6).

A rough estimate of the storage capacity of the Molopo aquifer based on the dimensions of the recharge area and its average porosity of 7.5% is calculated at:

Volume stored in aquifer = 20000*6500*0.075*70

$$= 682 \times 10^6 \, m^3$$

5.2 FEM model of Buffelshoek compartment

5.2.1 Recharge in relation to the catchment area of the spring

From the recharge area bounded by the dykes shown in **Figure 1** the recharge area of the spring comprises of two compartments. However from the particle trace of the flow the real drainage area of the spring is shown in **Figure 2**, but Figure 36 indicates that only about half of the recharge area falls in the Eccles dolomite and the other half in the Frisco Formation. The latter is a non-dolomitic formation and is a transitional dolomite aquifer, which represents the bottom layer of the Transvaal System, overlying the Eccles Formation of the dolomite series.

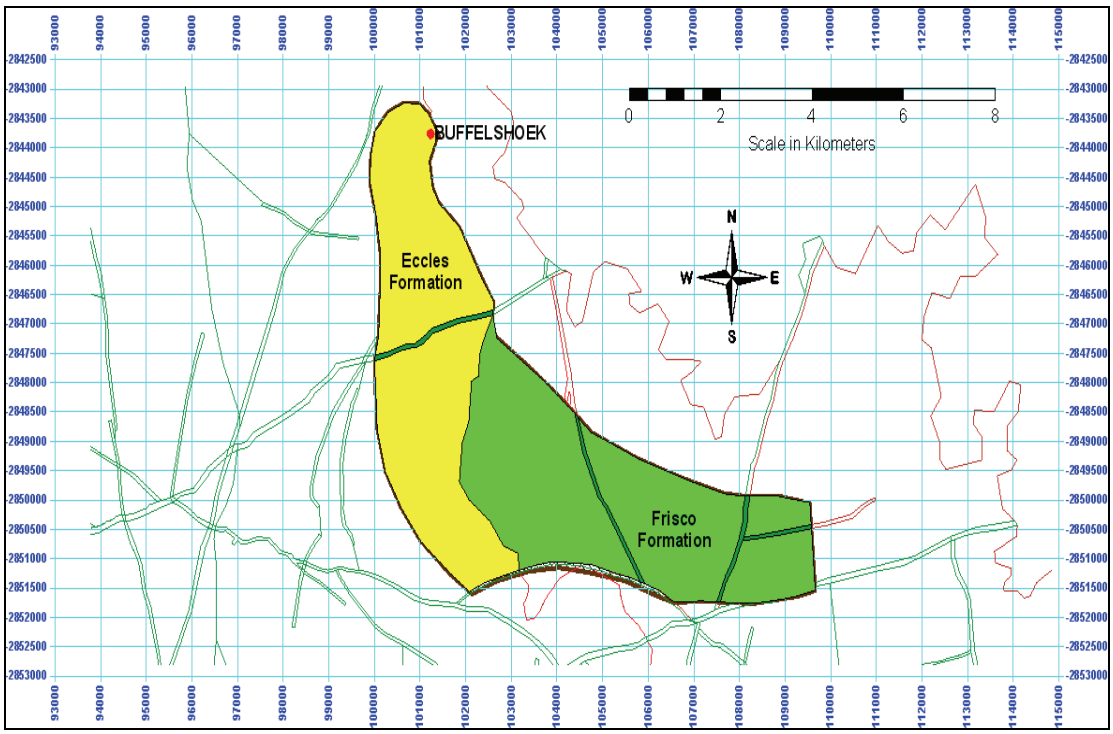

Figure 36 – The boundaries of the recharge area feeding Buffelshoek eye.

The Eccles Formation is an excellent dolomitic aquifer with an average recharge of 19% of MAP in comparison to the Frisco Formation, which has an average recharge of 3% of the MAP. This yields an average recharge of 11.1%.

According to the CMB method the average recharge of Buffelshoek eye is 11.05% of the average annual rainfall (see Figure 5 and Table 1.).

The monthly variation of the spring flow has been derived from an exponential rainfall-recharge relationship (PMA Consortium, 2002). This shows excellent correspondence to the measured flows and to the fluctuations (see Figure 37).

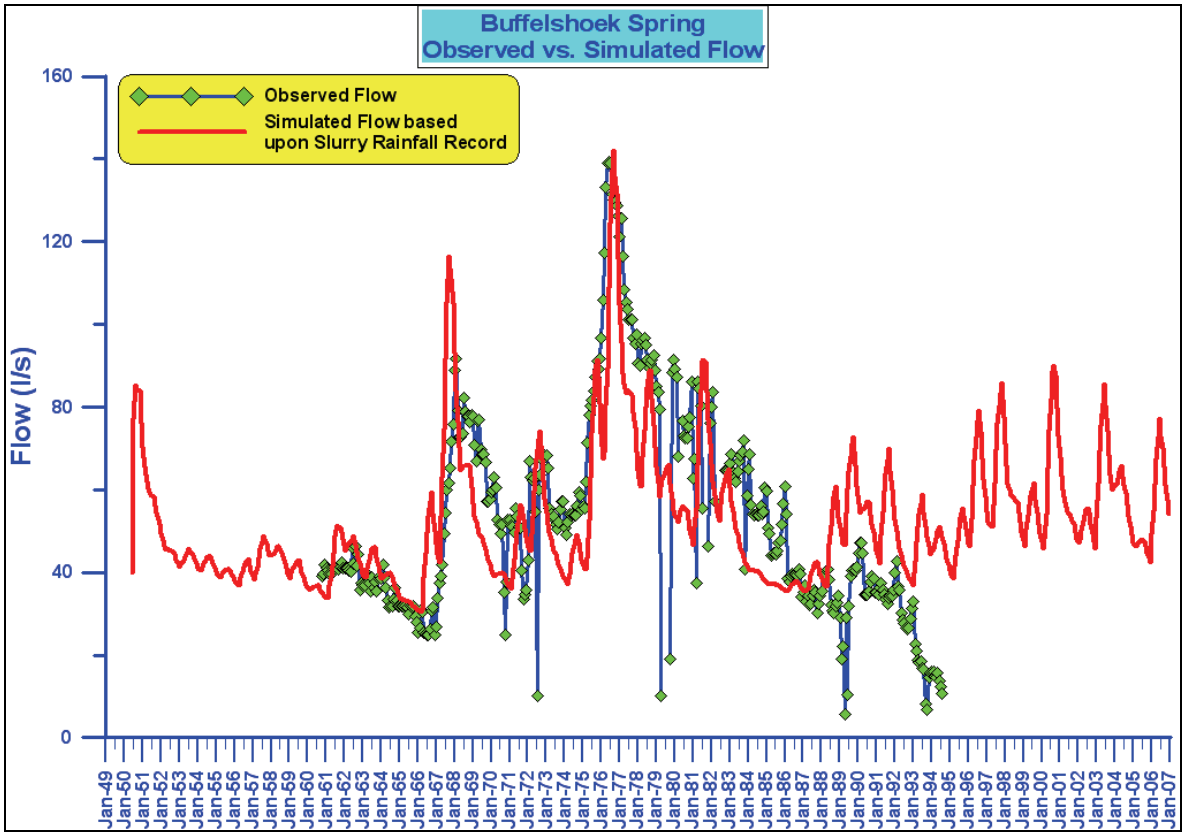

Figure 37 – Correspondence between the measured and simulated flows of Buffelshoek eye that was derived from an exponential rainfall-recharge relationship.

The simulation of the ^{14}C values of Buffelshoek eye was conducted similar to that of Molopo eye. The finite mesh that has been compiled for the FEM model is shown in Figure 38 and it comprise of 9605 elements and 9970 nodes.

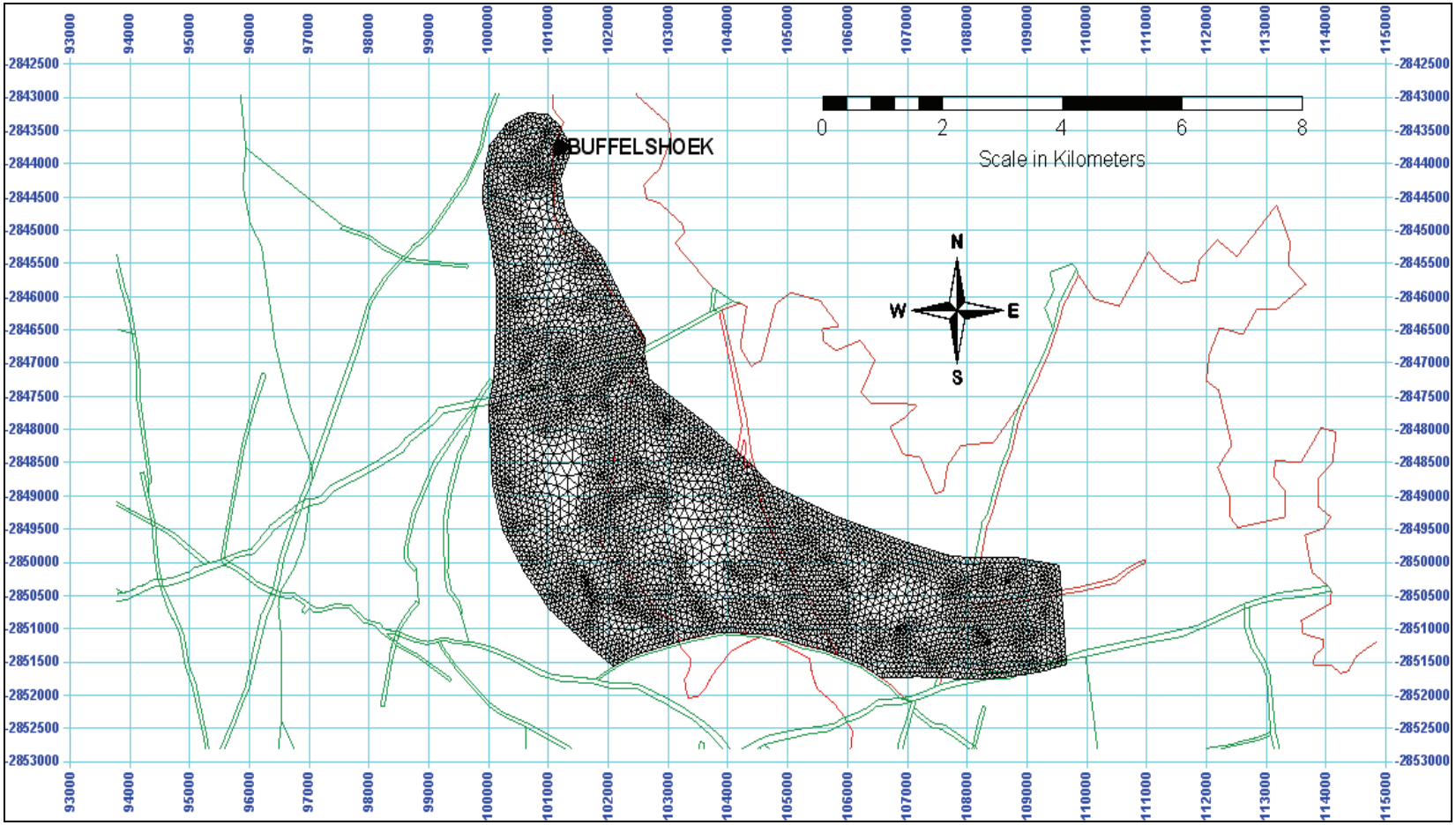

Figure 38 – Finite Element Mesh Constructed for the Simulation of the Buffelshoek Compartment.

The 70 m depth of the aquifer was represented as a single layer with a uniform S-value. The transmissivity of the aquifer was adjusted so that the flow response of the spring was similar to that shown in Figure 37.

The different aquifer parameter values are listed in Table 7.

Table 7 – Hydraulic Parameter Values Used in the Simulation of ^{14}C for the Buffelshoek Spring Catchment

Parameter	Units	Eccles Formation	Frisco Formation
Hydraulic Conductivity	m/d	240	0.31
Specific Storage	1/m	$5x10^{-4}$	$6.25x10^{-5}$
Kinematic Porosity	Dimensionless	0.035	0.0044
Recharge	% of MAP	19	3

The depth of the aquifer, as for the Molopo eye compartment, was assumed to be 80 m with a uniform average porosity of 0.035 for the Eccles Formation and 0.0044 for the Frisco Formation. Reducing the aquifer to a uniform layer without further subdivision into different layers, has been validated by the FEM model for Molopo eye. That has shown that the same simulation is obtained irrespective of a variable configuration of S with depth, provided that the average S value is 0.035 in obtaining the best simulation of the ^{14}C values. If an exponential decline of S with depth is assumed over the 70 m thickness of the aquifer, this is close to the configuration shown in Figure 21, which yields an average S of 0.027.

The excellent fit that has been obtained for the FEM simulation is shown in Figure 39 in relation to the highly variable monthly ^{14}C input from the rainfall. Figure 39 also indicates the higher ^{14}C input affected in the Eccles Formation in comparison to that of the Frisco.

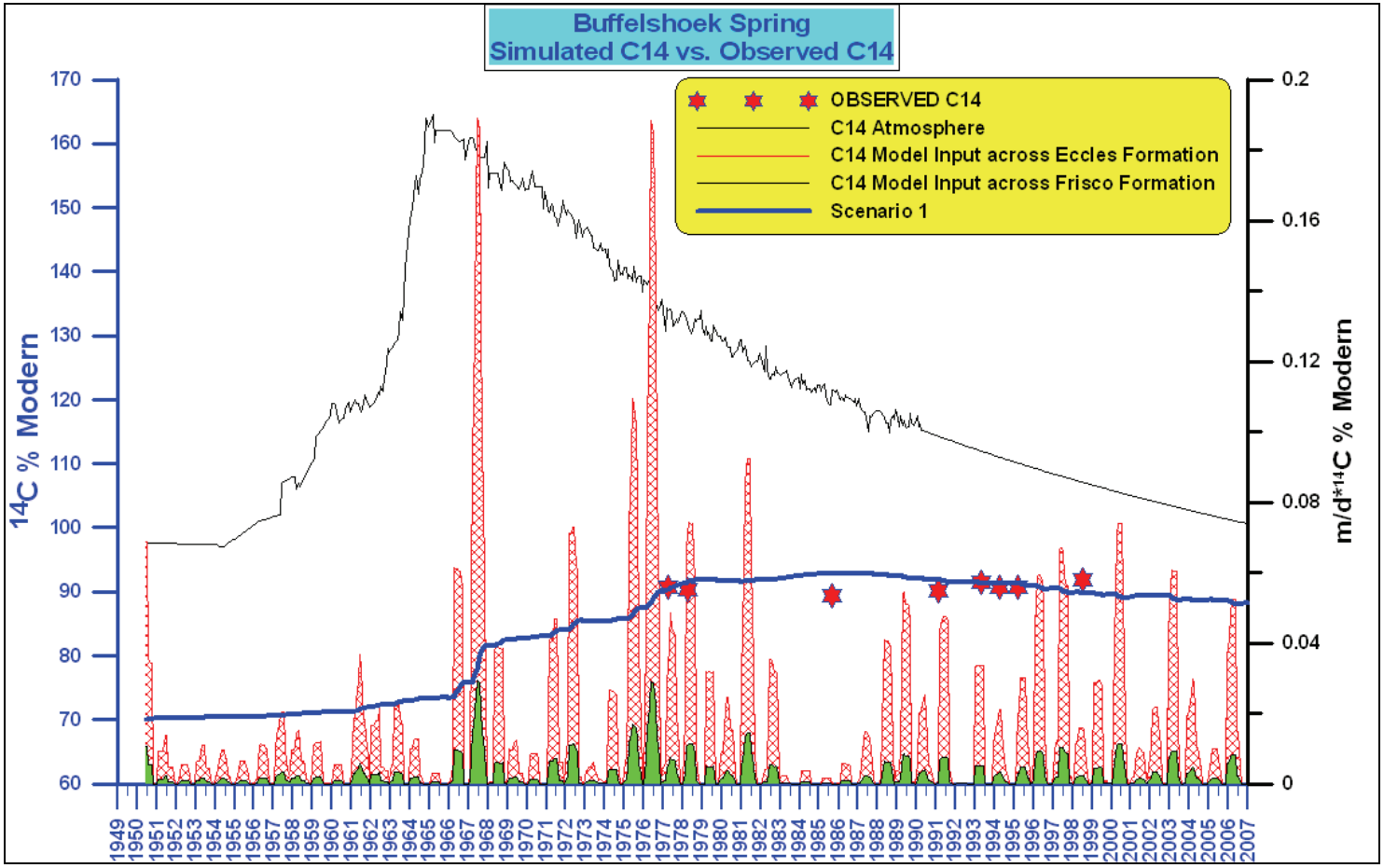

Figure 39 – Correspondence of the simulated ^{14}C values in comparison to the measured ones.

The excellent simulation that was obtained for the flow of the Buffelshoek eye and of the ^{14}C values has confirmed the reliability of FEM model and has instilled confidence in the results that was derived from Excel model, in spite of its analytical, though good conceptual approach. As have been indicated all the relevant hydrological data pertaining to Buffelshoek eye, are the most reliable data series of the Upper-Molopo dolomite area.

5.2.2 Turn-over time of water in the Buffelshoek aquifer

The turnover time of water in the aquifer has been calculated similar to that of Molopo eye recharge area. Figure 40 shows four points at which artificial injections of a tracer were made (one after the other) to determine their breakthrough at Buffelshoek eye.

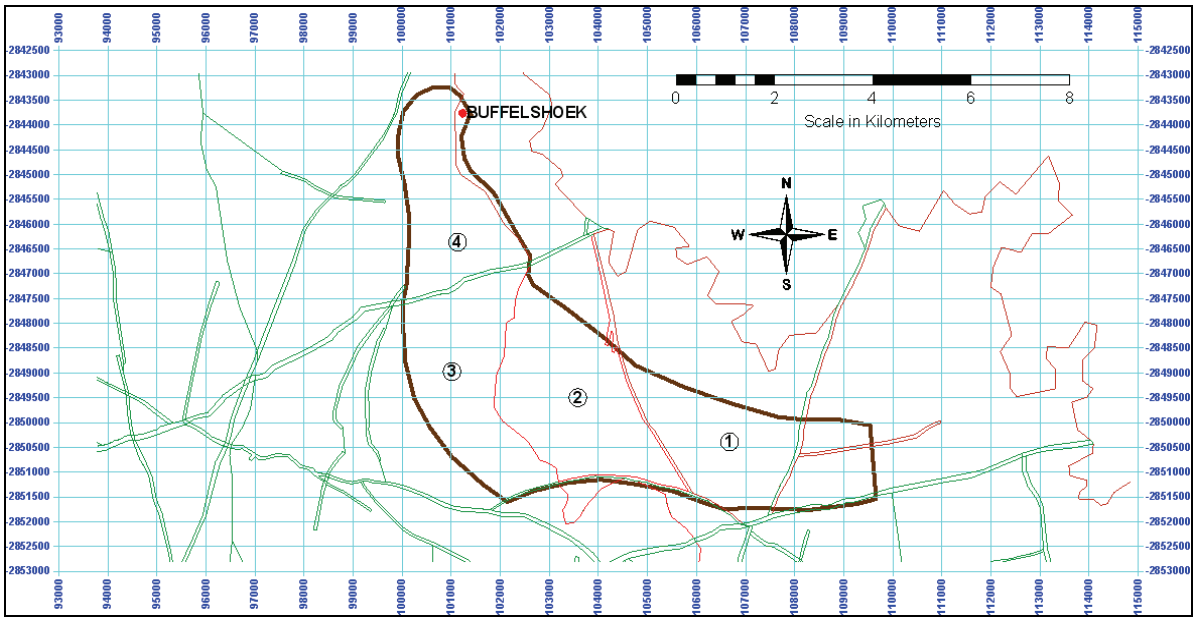

Figure 40 – Points that have been selected for an artificial injection of a tracer to determine the travel time to the spring (see Figure 41).Points 1 and 2 fall in the Frisco Formation and the other two in the Eccles dolomite.

The breakthrough of the tracers that was injected at the selected points is shown in Figure 41.

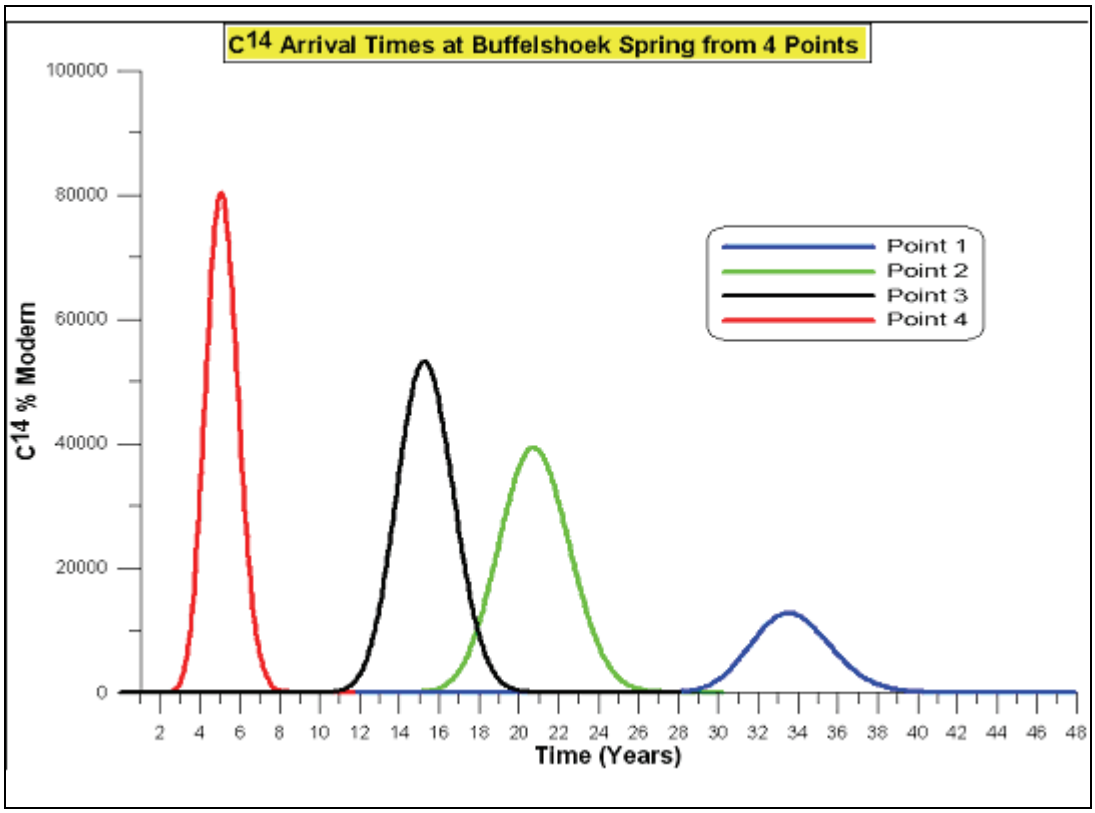

Figure 41 – The breakthrough curves of tracers injected at the four points shown in Fig. 40 to derive the travel time of water to reappear at Buffelshoek eye (See Table 8).

Table 8 – Estimation of the travel time of tracers injected at different distances from Buffelshoek eye

Point of injection	Distance from eye km	1st Arrival of tracer Years	Peak arrival of tracer Years	Average 1st and peak Years
Spring	1	1.8	2.5	2.15
4	2.9	3	5	4
3	5.5	12	15.5	13.75
2	7.2	16.2	21.4	18.8
1	10.6	30	33.5	31.75

Figure 42 shows a graphical plot of the travel times against the travel distances.

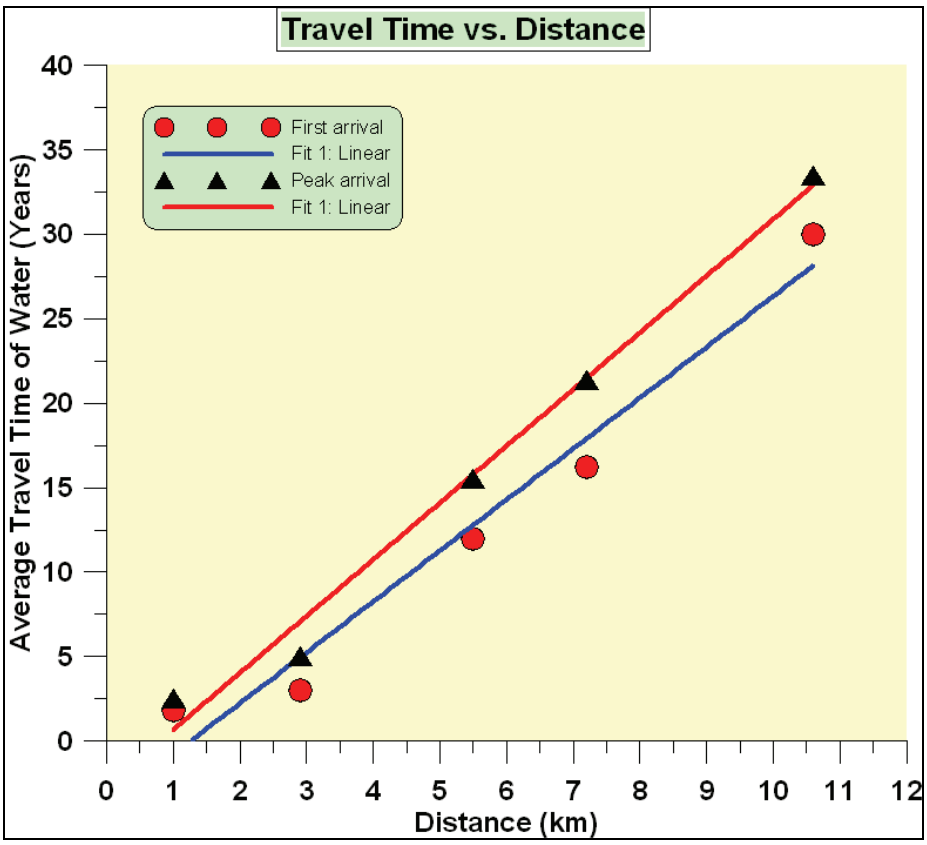

Figure 42 – The travel times of tracers from the points of injection to the spring. This shows a linear increase in accordance with the distances.

There appears to be a contradiction to Figure 32, Figure 33 and Figure 34, which show an exponential increase in age. However up to 12 km a linear change in age effectively applies.

At a distance of 2 km from Buffelshoek eye the average age of the water would be close to zero. This period corresponds to the average age of the water that has been recharged in close proximity to the spring over a period of about 24 months, which also represent the short mixing period that was derived from the Excel model. The long averaging period is (350-24) = 326 months and the multiple factor is 1.78. This yields an average turn-over time of (24 + 1.78*326)/2/12) = 25.2 years. According to Figure 42 the average age of the water oozing from the spring is 16.6 years, which is close to the 18 years derived from the Excel model.

According to the depth and S value of the total Buffelshoek aquifer the ratio of water stored in the aquifer relative to the average recharge is as follows, assuming that the recharge areas of the Eccles and Frisco formations are the same.

Water storage ratio = (70*0.035+ 70*0.0044)/(0.11*560/1000)/2 = 22.3, which corresponds well to the value of 25.2 derived from the Excel method and that obtained from the Excel results. This is a further confirmation that reliable results are obtained from the application of both methods to Molopo and Buffelshoek eyes.

6 CONCLUSIONS

The aims of the project have all been achieved satisfactorily, e.g. –

a successful simulation of the ^{14}C values of the Molopo and Buffelshoek eyes has been obtained from the 3D finite element model. It also allowed the following scenarios to be simulated: Table 9 provides a summary of the results that have been obtained.

Table 9 – Summary of parameters and results for Buffelshoek and Molopo eyes

Parameter	Buffelshoek Eccles	Buffelshoek Frisco	Molopo eye Eccles	Molopo eye Excel model
Hydraulic conductivity (K) (m/d)	240	0.31		not used
Recharge coef.	0.19	0.03	0.14	0.119
Spec storage (1/m)	5x10^-4			
Kinematic porosity (dimensionless)	0.035	0.0044	0.075	not used
Aquifer depth(m)	70	70	70	70
Turnover time(yr) tracer injection	16.6		50.2	
Turnover time	16.6		26.3	
Excel model(yr)	22.1		42.5	
Storage to Recharge ratio	25.2		50.2 [1)]	
Volume in aquifer	39.2	4.928	682	
million cub m	44.8	(total)		
^{14}C input factor	0.775		0.7	

50.2 [1)] Adjusted to smaller real recharge area of 130 km^2

The re-appearance of tracers injected at different distances from the spring has revealed the propagation of the recharged water from different points to the spring. The travel times for Molopo Compartment derived in this way were 33 years in comparison to 55 years obtained from the Excel simulations. These values convert to a storage-to-recharge ratio of 50.1 years for the flow model and 42.5 years for the Excel model. By comparison, the volume of water stored per unit area to the average annual recharge of the aquifer is 67 for the Molopo eye but if adjusted to the full area it reduces to a storage-to-recharge ratio of 50.2 and 22.1 for the Buffelshoek compartment. By comparison, the volume of water stored per unit area to the average annual recharge of the aquifer is 22.1. This provides an independent estimate of the storage to recharge ratio.

The average S-value that yielded the best simulation for Buffelshoek eye was 0.035 and for the Molopo aquifer 0.075. This is one of the most significant results obtained from the project insofar that it proved that the configuration of S-values with depth does not affect the goodness of fit obtained, as long as the average S-value is 0.075. Because of the Lyttelton part of the aquifer not being included in the 3D FEM model the effective porosity of the Molopo aquifer would be 0.075*130/180 = 0.054 but this would convert to the same volume of water stored in the aquifer.

The transmissivity of the different layers of the aquifer was chosen to conform to those that have been used in the 2D FEM model; however it was allocated in accordance with the variation of the S assigned to the different layers. Therefore both T and S could as well conform to an exponential decline with depth in accordance with Enslin and Kriel (1967) and Bredenkamp (2004).

Although the monthly recharge and therefore the ^{14}C input, proved to be highly variable the mixing has ensured that the variability is evened out. This was demonstrated by the rapid mixing that occurred in the 8 layers of the aquifer with the depth.

The mixing patterns conformed to the averaging periods that have been derived and applied in the Excel model. It showed that the water emanating from the spring conforms to an effective two-layered aquifer system. The first period of 36 months represents the contribution from within a distance of about 3 to 5 km from the eye, which admixes with the deeper flow in aquifer that is being recharge between 6 and 20 km from the spring. The deeper component obviously represents recharge that is contributed from an earlier period with recharge occurring close to the spring. The short mixing period explains why the measured ^{14}C of the springs shows correspondence to the discharge of the springs.

The simulations of the long-term response of the ^{14}C from both the Excel and FEM model is

similar, thereby confirming that both models could be applied, within their limiting constraints.

The S-value of the aquifer cannot be derived directly from the Excel model, which is possible with the FEM, but S can be inferred for the Excel model once the turnover time of water in the aquifer is determined. This would still require the depth of the aquifer to be derived or assumed. From this the average S-value could be configured according to an exponential decline with depth.

The 3D model proved to be an essential tool to determine the impact of pollution in the dolomitic aquifers, once the flow of these aquifers have been calibrated according to 3D finite element simulation of the ^{14}C measurements of the springs, issuing from their catchments..

The study has shown that the 3D model is superior to the Excel simulations; however the latter is much easier to apply, especially once certain crucial parameters have been quantified, e.g. :

- The initial ^{14}C content of the recharge water, which could be derived in relation to the bicarbonate concentration of the spring water, irrespective whether a bimodal or mono recharge process is used.

- The factor by which the deep flow is multiplied in the Excel model, proved to be a simple way to incorporate recharge at great distances from a spring. This corresponds to large deep aquifers that have big turnover times.

- The Excel model provides a simple method to determine many of the parameters and to characterise the different types of dolomitic aquifers. It provides a way to obtain the initial ^{14}C of the groundwater prior to the release of the nuclear fallout into the atmosphere. The use of an incorrect initial pre-bomb ^{14}C value would result in an incorrect estimation of the S value of the aquifer.

- The Excel method has provided a viable explanation of the variable ^{14}C input, whilst it still represents recharge of a recent origin.

7 RECOMMENDATIONS:

It is essential for 3D finite element models to be compiled for all the larger dolomitic aquifers, such as Grootfontein Compartment near Mmabatho, Lichtenburg Compartment,

Schoonspruit Compartment and Malmani Compartment in the Upper-Molopo area in view of their importance as sustainable water resource supply systems, as well as their vulnerability to pollution. The same applies to the smaller springs in the Zeerust area, which could be combined into one model. This approach would incorporate the leakage between aquifers, which has not yet been addressed previously in terms of mixing. This would also be a logical extension to the 2D modelling by which the piezometry and the discharge of the springs have been calibrated successfully.

Likewise the dolomitic compartments feeding the following springs should be modelled by 3D finite element simulations:

- Maloney eye, Gerhard Minnebron , Turffontein and eyes in the West Rand mining area,
- Pretoria Grootfontein and the Upper and Lower Fountain springs of Pretoria,
- The Delmas and East Rand dolomite,
- The eyes in the Kuruman dolomite and the aquifer supplying Sishen,

This is the best way to address the constraints of the groundwater supplies and prioritizing their investigation in South Africa.

The ^{14}C measurements should be continued to confirm the declining trend of ^{14}C, but sampling should be repeated only at intervals of about 10 years for the next twenty years. It is of utmost importance that the ^{14}C analysis should be performed according to accepted standards, which does not seem to be the case with several of the most recent samples.

8 REFERENCES

BREDENKAMP DB, Vogel JC, Wiegmans FE, Xu Y, Van Rensburg HJ: (2007).Use of natural isotopes and groundwater quality for improved estimation of recharge and flow in dolomitic aquifers. WRC Report No. KV 177/07

BREDENKAMP DB, (2000). Groundwater Monitoring: A critical evaluation of groundwater monitoring in Groundwater Resources Evaluation and Management. Water Research Commission Report No. 838/1/00.

BREDENKAMP DB (2004). Situation analysis for the preparation of institutional arrangements of groundwater management. Part 3: WRC Contract 1324, Geohydrological Assessment. Water Research Commission of South Africa.

BREDENKAMP DB, VAN WYK E (2005). Simulation of thermonuclear ^{14}C in springs and its hydrological interpretation. In: Biennial Groundwater Conference 2005, March 2005, Pretoria, South Africa.

ENSLIN JF, KRIEL JP (1967). The assessment and possible future use of the dolomitic groundwater compartments of the Far West Rand, Transvaal, Republic of South Africa. Proc. Int. Conf. Water for Peace, Washington, May 1967, Vol. 2.

PMA Consortium, (2002). 2D Finite Element Model of the dolomites to the west and northwest of Zeerust. (Unpublished).

VAN RENSBURG HJ (2005). 2D FEFLOW model of a section of the Grootfontein aquifer to simulate the reappearance of the thermonuclear ^{14}C pulse that has been introduced into the aquifer by rainfall recharge (unpublished contribution to the present report)

VOGEL JC (1970). Carbon-14 dating of groundwater. In: Isotope Hydrology 1970. International Atomic Energy Agency, Vienna, pp 225-239.

Appendix A

1. Characteristics of the of ^{14}C simulations by means of the analytical model

The Excel ^{14}C model presented Bredenkamp and Van Wyk (2004) and especially the modified version (Bredenkamp et al., 2007) proved to be effective in simulating the response of the ^{14}C content of the groundwater emanating as springs from different dolomitic aquifers in South Africa. It has enabled different characteristics of the groundwater systems to be derived by means of a simple two-component mixing model. In the present study the reliability of the Excel model was verified by a finite element 3 D flow–mix model. In this study the ^{14}C content of the groundwater was assumed to be a characteristic of the recharge of the aquifer, which can be derived according to the bicarbonate concentration of the groundwater, depending on the dominant recharge process.

The input of ^{14}C is part of the rainfall that causes the infiltration recharging the aquifer either as :

a) Infiltration through a layer of alluvium overlying the aquifer, with ^{14}C content closer to 85% modern carbon and a higher bicarbonate uptake passing through the root zone of the vegetation.
b) More rapid infiltration bypassing the root zone; which would yield ^{14}C values that are closer to 50% modern carbon. Such rapid recharge could take place from the accumulation of rainfall as a result of the collection of runoff during high intensity rainfall; or as direct infiltration in areas with a thin soil or limestone cover. This the recharge water with a ^{14}C content closer to 50 % modern carbon, which represent recent recharge and not water of which the ^{14}C has decayed over time.
c) The bicarbonate of the groundwater was derived from the regression between the partial pressure of CO_2 required for bicarbonate to remain in solution. (See Fig. 1). The factor is closer to 0.5 for more direct recharge bypassing the root zone of the vegetation; and is closer to 0.9 if the recharge slowly infiltrates through the soil zone overlying the aquifer.

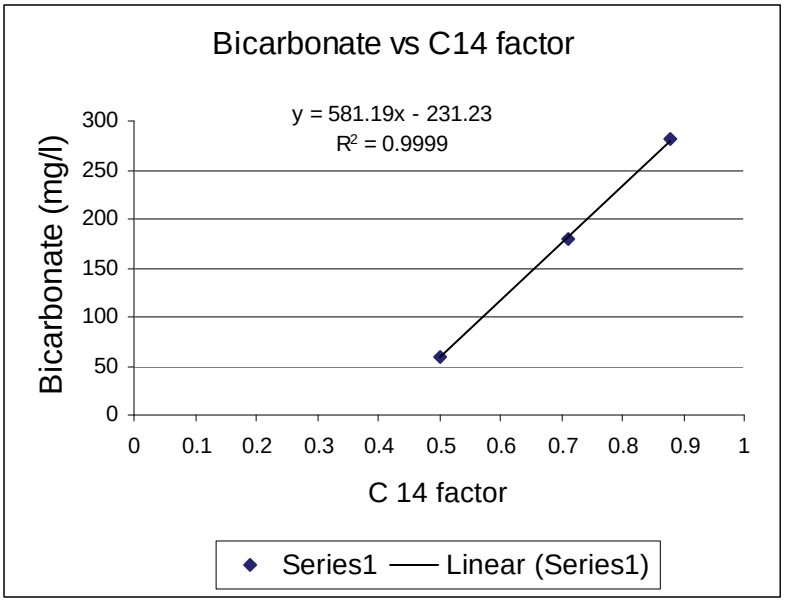

Fig. 1 – Relationship between the bicarbonate concentrations and the ^{14}C factor to derive the characteristic ^{14}C of the groundwater.

The recharge emanating at the spring is derived according to a conceptual mixing model (see Fig. 2) of which:

i) The first component represent the average ^{14}C content over a shorter period of 24 to 36 month, whilst

ii) The second deeper-flow is contributed by the average ^{14}C content over a period of about 450 months that precede the short period.

iii) In view of the rainfall record being too short, especially in the case of the larger aquifers, several multiples of the deep flow components have to be incorporated to effect a good simulation (see Fig. 2). For small shallow aquifers the mixing is derived from the average ^{14}C of the rainfall over 36 months with no deep flow component. The 24 to 36 month average rainfall proved to correspond very well to the flow of most springs, irrespective whether they emanate from a small or big/recharge area. This is because the 24 to36 month average rainfall determines the hydraulic head to which the spring flows responds. If deeper flow is present the contribution of recharge farther from the spring is incorporated as a multiple >1 of the average ^{14}C content over a period prior to this month period. The storativity (S value) of the aquifer was not included in the Excel model, arguing that on average it would be a constant and therefore is not a variable to incorporate in the calculation of the concentrations of the mix of the two components.

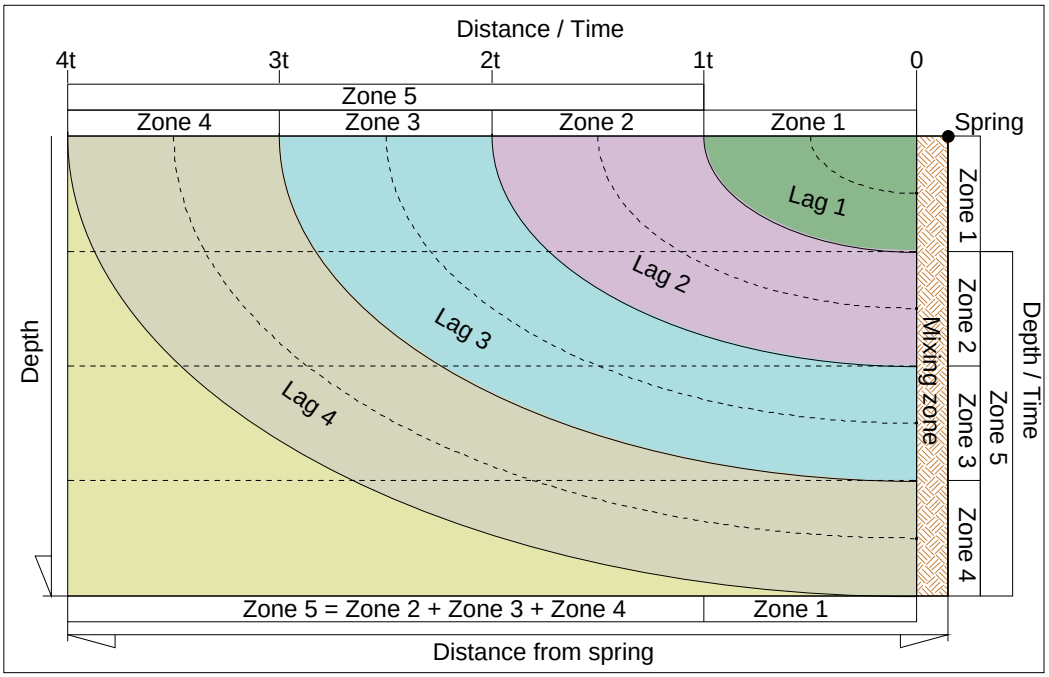

Fig. 2 – A conceptual presentation of the flow and mixing that occurs at a dolomitic spring. The deeper the aquifer, the more equivalents of the recharge of zone 1 have to be incorporated. This is included in the mixing model as a multiple factor, in comparison to that of zone 1.

According to the conceptual flow model shown in Fig. 2, the 24 to 36 month average recharge is that derived from recharge zone 1, which represents the shallow mix that is contributed from the area closest to the spring. The contributions from zones 2, 3 and 4, of which the average is combined as zone 5, represent the deep flow contribution, which admixes with zone 1 at the spring. In the Excel model the contribution from zone 5 would be incorporated as a multiple factor of 3 in relation to that of zone 1. The value of the multiple is determined by the ratio of the large mixing period (period 2 in Fig. 2) to that of the full period over which water is contributed to the final mix at the spring (i.e. periods 3 , 4, 5) . It was shown by Vogel (1970) that in an aquifer of which the S values decline exponentially with depth as is typical of the dolomite aquifers, the age of the water would increase linearly with depth. However the age would be the same at equal depths from the surface as it is determined by the travel time along the flow lines in relation to their points of recharge, which for a uniform aquifer would be similar. This obviously would not fully apply to an aquifer with an irregular variation of S with depth. However from Fig. 3 it is evident that the S values of the dolomite corresponds to an exponential decline with depth. In view of the dispersion occurring from the point of recharge along a specific flow line, there would be some dilution of the ^{14}C in addition to the admixing of water from the different layers. This however is regarded to be small.

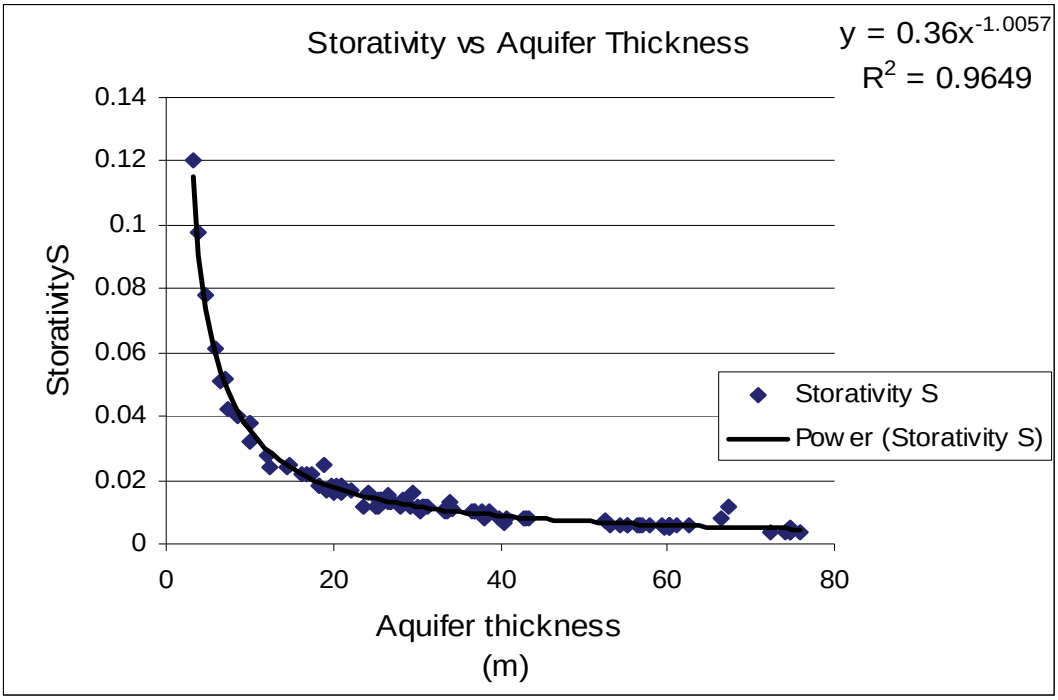

Fig. 3 – Decline of S with depth in dolomitic aquifers in the Bo Molopo area indicating an effective aquifer thickness of 80 m, compared to a thickness of 70 m used in the 3D model. (Stephens et al., 2005).

With the Excel model the ^{14}C concentration reappearing at the spring only depends on the mixed concentrations of the 36 month and the long period preceding it. The mixing of all the layers is complete after about 24 to 36 months (according to the tracer inserted in the 3D model) it is therefore incorporated the average S of the aquifer with depth of the deep flow, which represents the recharge from the furthest end of the aquifer. Thus S could be assumed to be constant for the two components so that the contributions of the ^{14}C load (^{14}C *recharge) reverts to the ^{14}C concentrations of the input recharge when divided by S.

The simulation by the 3D finite element model was different and incorporated the dilution by the kinematic porosity (S value) in the transmission of flow through the aquifer. For this reason the artificial injection of a tracer at different distances from the spring outlet was included to derive the travel times of the recharged water. In this way the results of the 3D simulation and the Excel model could be compared.

In both models the ^{14}C content of the final mix effectively conforms to a two-component recharge in the case of the deeper aquifer. In the case of a shallow aquifer the ^{14}C content of the average recharge is predominantly controlled by the mixing over 24 to 36 months. In this case the contribution of the deeper flow component would be zero.

It has also been noticed from Fig. 4, plotting the measured ^{14}C values against the flow of Buffelshoek and Molopo eyes that the ^{14}C content corresponds to the variable flow of the spring. This is a confirmation of the reliability of the Excel model in that the average recharge over 24 to 36 months is contributed close to the spring and therefore the ^{14}C contribution from the ^{14}C pulse would be higher, than that of the mixed

concentration contributed by the long-term average recharge from the most distant regions of the aquifer. The impact of the short period of mixing is evident from the synchronous response of the ^{14}C to the variable flow of the spring (see Fig. 4.)

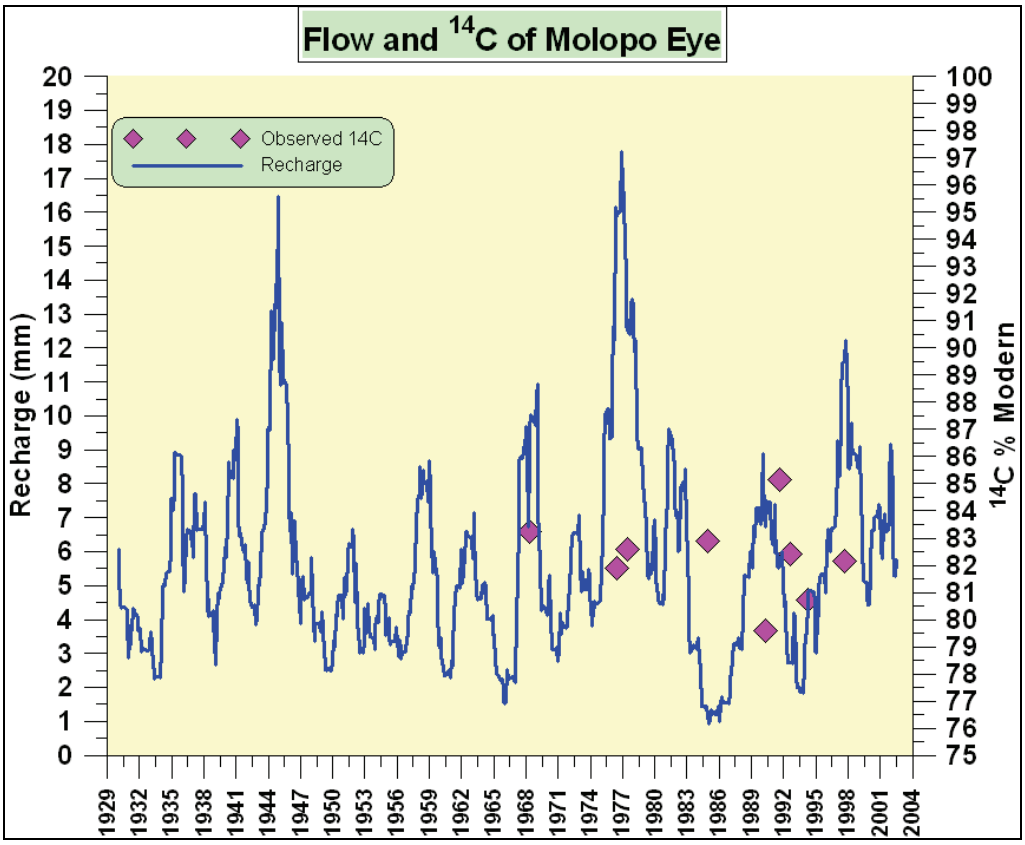

Fig. 4. – ^{14}C measurement of Molopo eye (up to 2007) in relation to the recharge.

2. Sources of errors in the ^{14}C determinations

The goodness of the fit of the ^{14}C modelling directly depends on the reliability of the sampling, the processing and measurement of a ^{14}C sample e.g.

In the case of Molopo eye, the first sample of water was obtained at the weir; thereafter it was sampled in the pool from a boat, at a point where the highest upwelling of water from the bottom of the large pool occurred, as several oozing points were available.

In the case of Buffelshoek the ^{14}C sample had been collected at the weir, which represents a reliable point source with no interference from pumping. . However the spring flow had been affected by the drought at one stage and the weir was breached to affect a lower outflow height. Both in respect of the flows, the recharge derived and ^{14}C sampling of Buffelshoek eye, it represents a reliable series of hydrological data. The spring is also in close proximity to the Wondergat sinkhole for which the most complete series of water level fluctuations over many years are available. The Wondergat levels showed a high correlation with the measured flows of Buffelshoek.

A similar correlation to the flows of other springs has been confirmed, which allowed the monthly flows of all the springs to be simulated from the water levels of the Wondergat. The latter represents the regional response of water level fluctuations because of the similarity of the rainfall in the area. This has revealed that the water levels of the Wondergat and of all the springs in the area correspond to the 36 month average rainfall, using a quadratic response of recharge relative to the average rainfall over 36 months (Bredenkamp et al., 2007).

Great care has been taken in obtaining reliable ^{14}C measurement of the spring water up to 2000. The consistency of ^{14}C interpretations from the dolomitic aquifers in different regions, has confirmed the reliability of the ^{14}C measurements up to 2004. However the most recent samples i.e. that of 2007 show inexplicable deviations from those simulated by means of the Excel model and 3D model, which indicates that the reliability is doubtful.

Appendix B

1. Sensitivity of the Excel model to the incorporation of a single or bi-modal recharge.

The sensitivity of the simulations to the following changes to the Excel model was assessed.

a) Instead of using a bimodal recharge process (Bredenkamp et al., 2007) to account for the variable ^{14}C content of the groundwater, the ^{14}C of the recharging groundwater was *assumed to be a characteristic of the aquifer* to be obtained from the model. This reduced the number of parameters of the model without incorporating the dependency of the ^{14}C bicarbonate concentration on the mode of infiltration as a check on the reliability of the bimodal recharge. However the average recharge of the different springs could still be related to the average bicarbonate of the springs, which is then used as another method to derive the recharge coefficient of the dolomitic aquifers.

b) Assessing the sensitivity of the Excel model if the historical rainfall record was extended.
This was necessary because of an insufficient length of rainfall record preceding the existing record to ensure a more reliable incorporation of the deep flow component of recharge in the simulation of the ^{14}C of the first months. For this reason the rainfall record has been extended by inserting 10 year of monthly rainfall prior to that previously used.

c) Extending the rainfall record to simulate the trend of the ^{14}C response for many years in the future, as well as to check the reliability of the latest ^{14}C measurements against the predicted values. For this the existing rainfall record has been added as it presented similar monthly variations and a similar long-term variability of rainfall to that of the monitored series.

d) An exponential rainfall-recharge relationship was employed and compared to a binomial /quadratic function. This allowed comparison of the outcome of the spring flow simulations with those derived by Van Rensburg (PMA consortium 2005) using an exponential recharge response to the rainfall (see the main report).

The exponential relationship has been incorporated in the 3D simulation models to compare the long-term responses.

2. Outcome of the ^{14}C simulations for the different scenarios listed above.

a) The parameter values of Buffelshoek eye –Exponential recharge (Van Rensburg PSA consortium 2005).

The following results have been obtained using an exponential recharge relationship for rainfall– similar to the earlier recharge equations used by Van Rensburg (PSA consortium 2005).

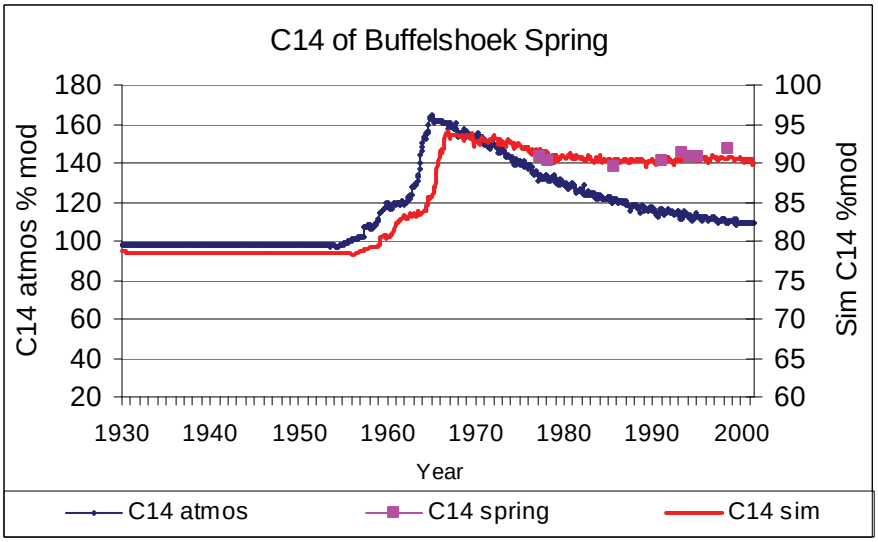

Fig.5 – Match between the simulated and measured ^{14}C values derived from an exponential rainfall-recharge response. This yielded an equal good fit to the simulated values derived by the binomial recharge relationship (see Fig.6)

b) Rainfall recharge functions

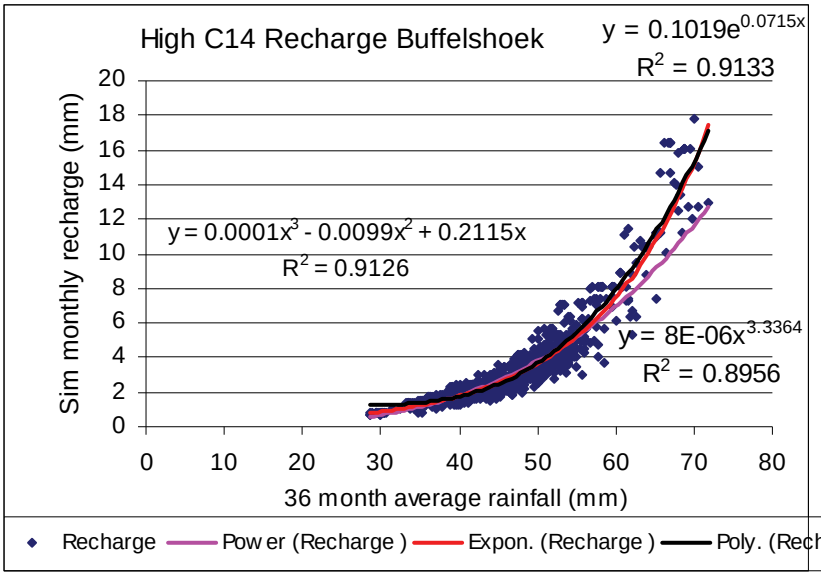

Fig.6 – Comparison between different regression fits to the exponential recharge relationship that have been applied.

This figure shows virtually identical responses for an exponential and binomial recharge rainfall relationship, but a slightly poorer fit for a power relationship. It has nevertheless increased the confidence in the previous ^{14}C models which have incorporated a binomial recharge function. It has also validated the use of the exponential relationship which has been used by Van Rensbug (PMA consortium 2005) in the simulations derived from the 2D model.

Further testing of the impact of the rainfall-recharge relationship and extending of the rainfall series was carried out.

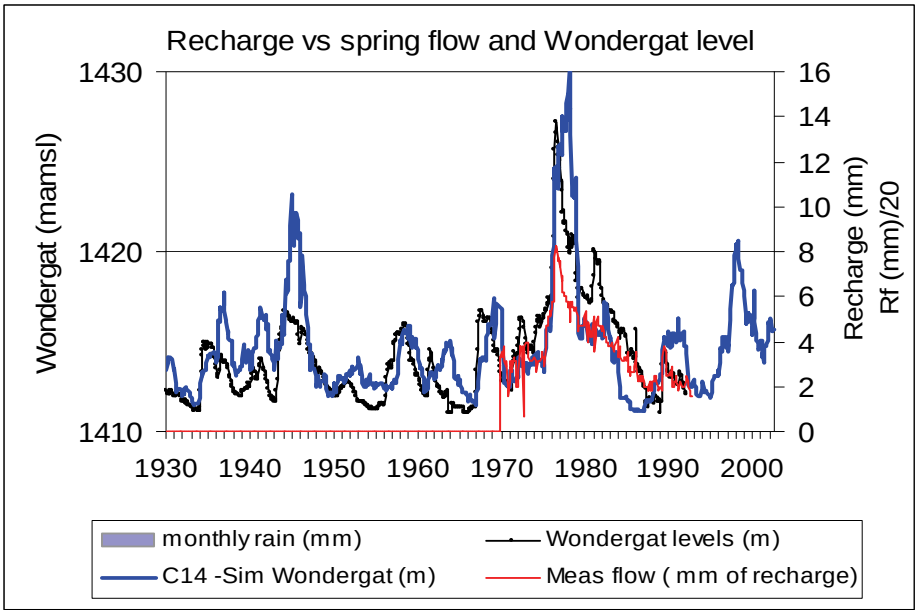

Fig.7 – Good correspondence between the measured and simulated flows of Buffelshoek eye in comparison to the water levels of the Wondergat, employing the exponential recharge relationship derived from Fig.6.

Table 1 – Results of ^{14}C simulations for different recharge formulas applied to Buffelshoek eye

Buffelshoek eye	Exponential	Exponential	Binomial	Simulating the long-term response of the ^{14}C model
Error minimized	4.80	2.79	recharge	(Extended rainfall record)
Lower threshold	12.5	12.5	9.8	9.8
Higher threshold	60.3	NA	62.1	62.1
Recharge factor (L)	none	0.124	0.072	0.072
Recharge factor (H)	0.34		0.037	0.037
^{14}C factor (L)	0.817	0.817	NA	NA
^{14}C factor (H)	NA	NA	0.83	0.83
Final multiple factor	2.51	3.22	2.9	2.9
Turnover time (yrs)	39.9	50.7	43.2	43.2
Lag months period 1	36	36	36	36
Lag period 2	367	367	345	345
Start year	1922	1922	10 yr Rf Added in front	Added 10 yrs rainfall Add in front and 80 yrs at end
Start month	1	1		
Months for Lt average	944	944		
Rainfall weighting (months)	36	36		
Further lag Sim ^{14}C				
^{14}C	23	32		
Measured HCO3	228.8	228.8	228.6	228.8
Area spring (sq km)	45	32		
Cl rech =	0.077	0.077	0.077	0.077
Model rech =	0.078	0.078	0.076	0.076

Fig.8. indicates that the simulated ^{14}C response clearly depends on the period over which the ^{14}C of the deeper flow component is averaged. In this case the long period representing 36 months; in comparison to a period of about 345 months represented by the graph in blue. It is evident that the simulated ^{14}C pulse for the shorter averaging period is significantly poorer than that derived from the longer averaging period.

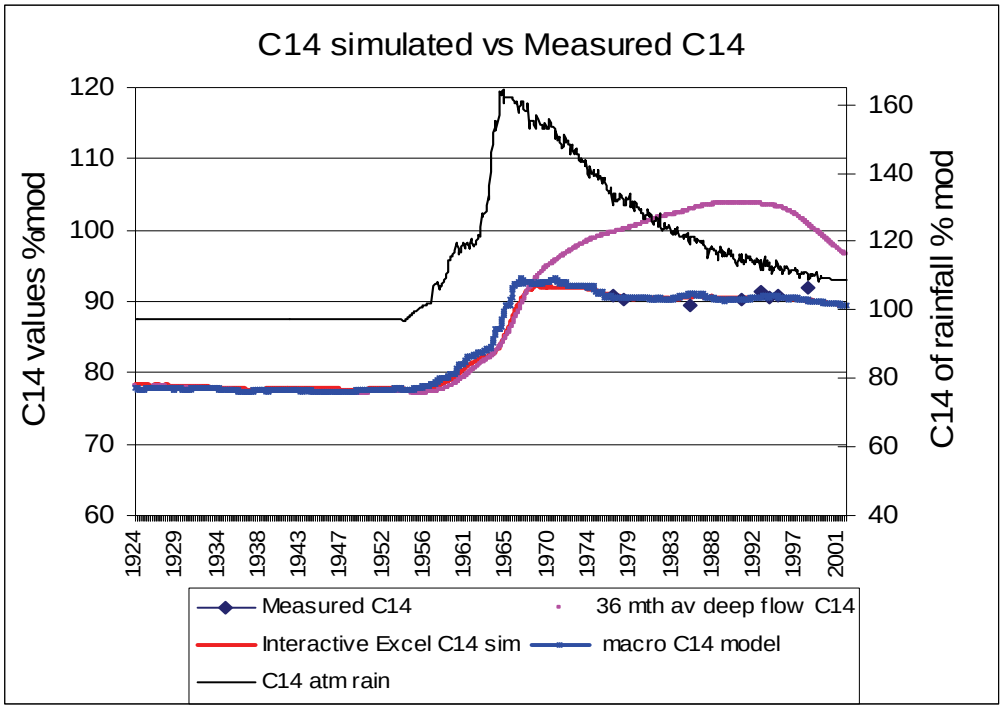

Fig. 8 – The purple graph represents the deep flow averaged over 36 months and not over 345 months, which is indicated by the graph in blue The same multiple of 2.9 of the deep flow has been incorporated – see Table.1.

The figure below shows the response of the macro-driven excel model to that obtained from the more cumbersome model. In the latter case the parameter values are changed interactively by the modeler. This has indicated that both models are reliable.

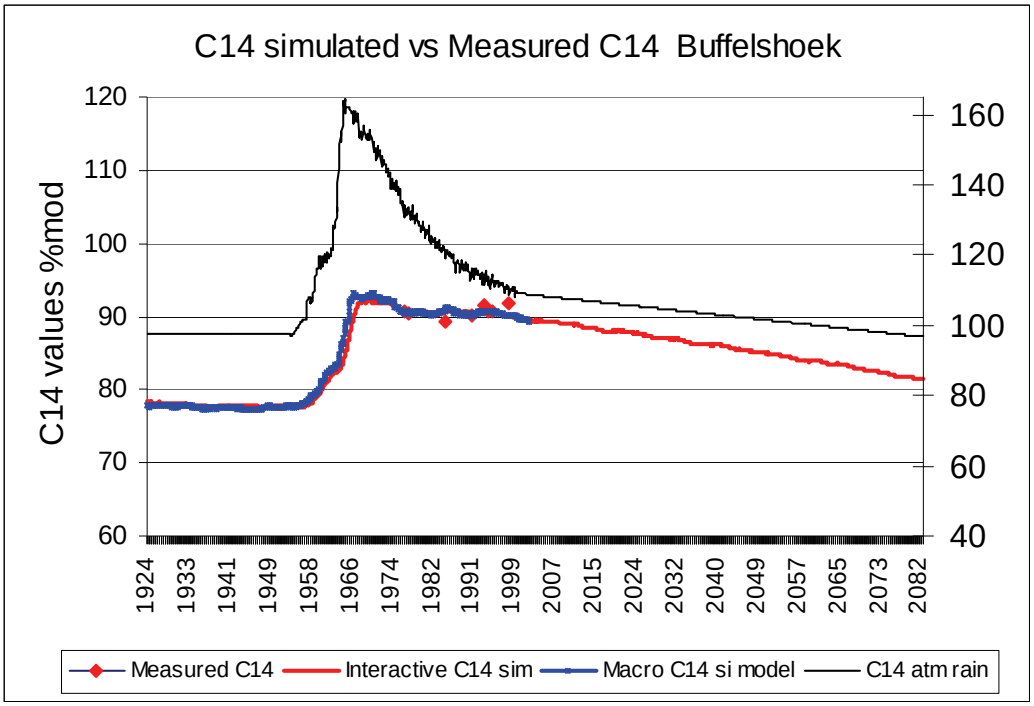

Fig. 9 – Simulated response with10 years of additional rainfall data inserted in the beginning (1912 to 1922) as well as an additional 80 years of rainfall by duplicating the existing rainfall record.

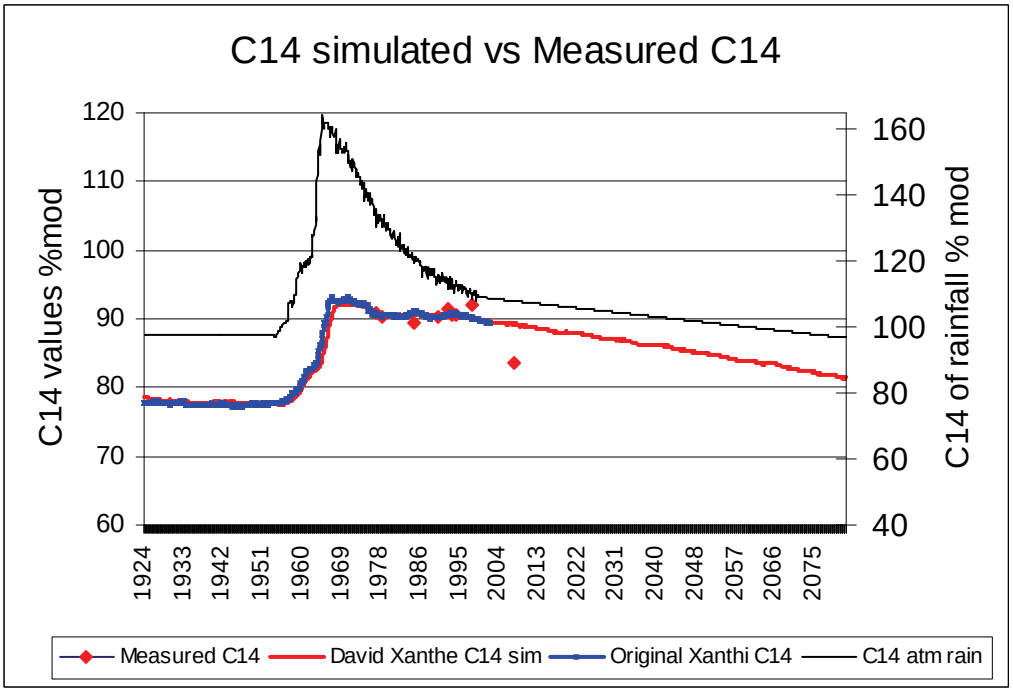

Fig. 10 – Similar result as shown in Fig. 9, which clearly indicates the deviation of the last ^{14}C measurement from the predicted values. This indicates that the last ^{14}C value is unreliable.

c) Conclusions

The following has been concluded from the different variations listed in Table 1:

i) The rainfall-recharge functions have no effect on the outcome of the model provided that the recharge increases exponentially with rainfall.

ii) The average rainfall over 36 months provides an integrated rainfall variable that corresponds to the fluctuations of the spring flows. This is because it controls the variable head which determine the hydraulic pressure driving the springs discharge. This period also corresponds to the shallow water contribution in determining the ^{14}C of the spring, with the deeper component being contributed over the longer period of about 350 months.

iii) The multiple of the deep flow component that is required to obtain the best simulation of ^{14}C concentrations, is similar to the incorporation of the S value of the aquifer in the 3D FEM model.

iv) The S value could only be derived from the FEM model and is a critical parameter to effect the dilution during the flow of groundwater until it reappears at the spring. In the case of the Excel model the admixing is obtained from the recharge that is calculated from the two-box mixing model, which incorporates the concentrations of recharge that had occurred over a long period preceding a specific month.

3. Additional examples of simulation by means of the Excel method

Figures 11 to 18 show that a good simulation of the ^{14}C values of the springs can be obtained, assuming that the recharge process either conforms to the slow infiltrating water via the root zone of the vegetation, or bypasses it.

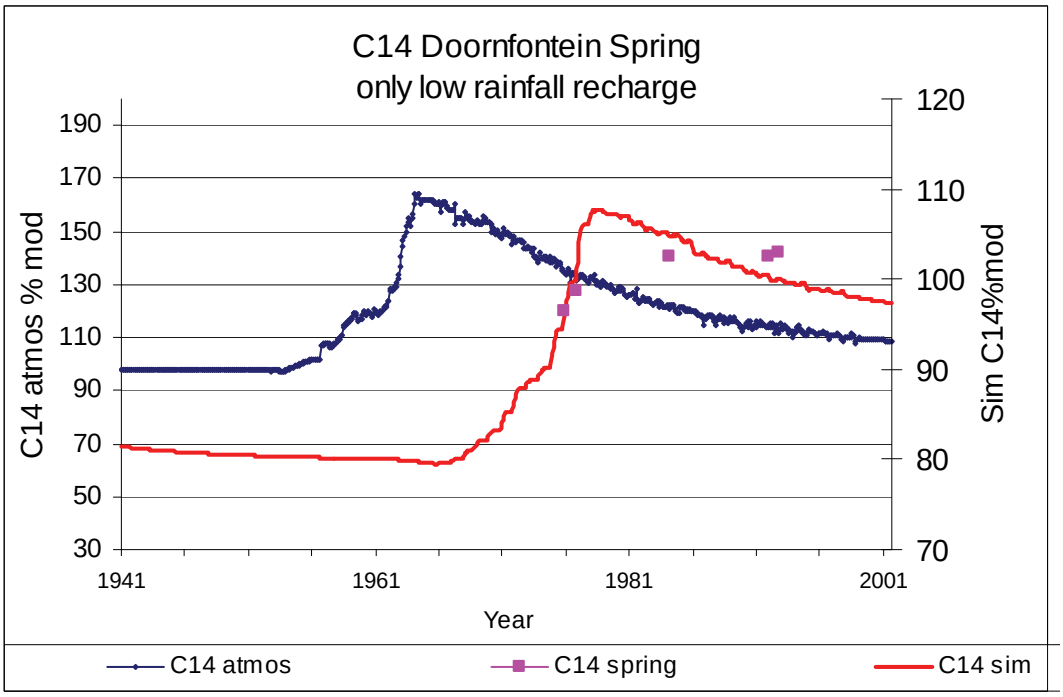

Fig. 11 – Simulated ^{14}C assuming all the recharge to occur from infiltration passing through the root zone of the vegetation- using only recharge in excess of a low threshold rainfall.

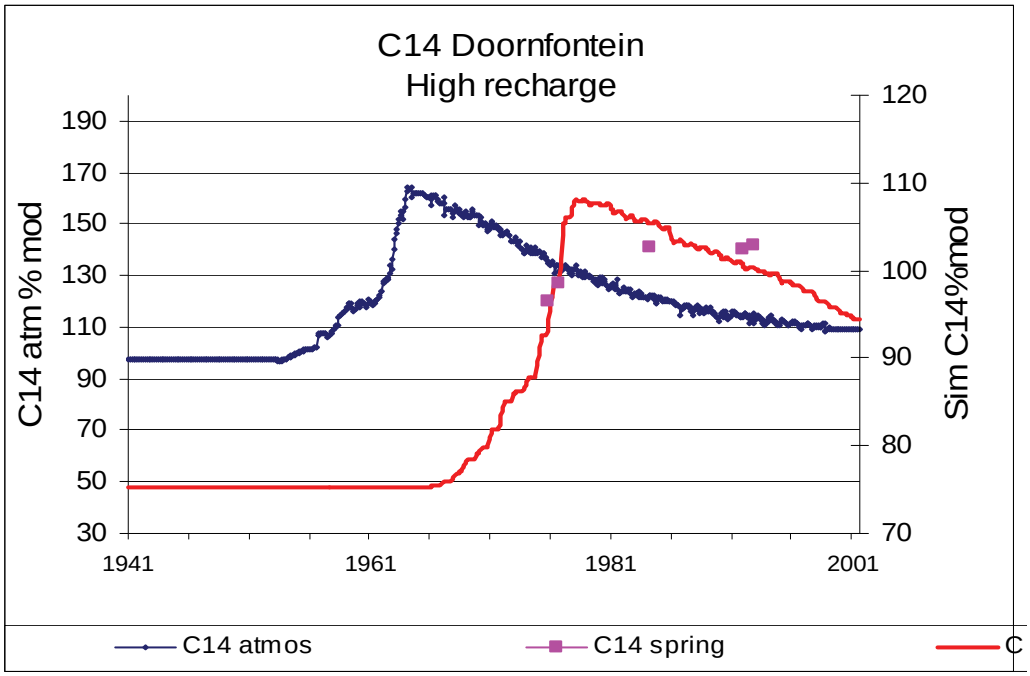

Fig. 12 – Simulated ^{14}C assuming the recharge bypasses the root zone of the vegetation – using only recharge in excess of a high threshold rainfall.

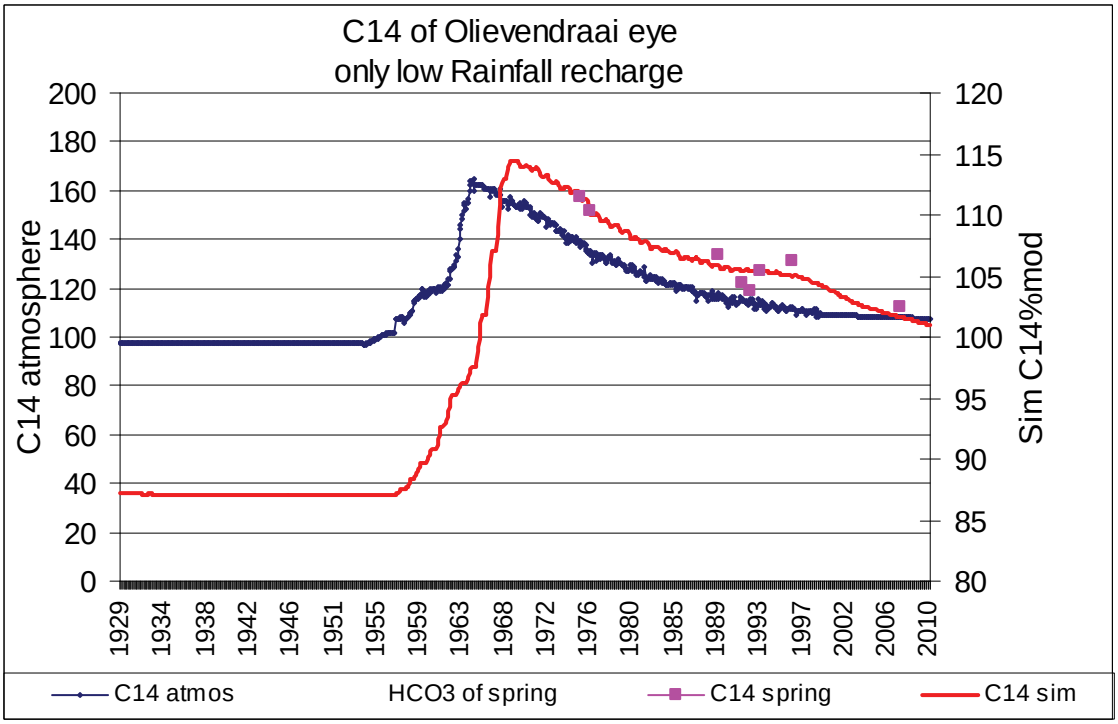

Fig. 13 – Simulated ^{14}C assuming all the recharge to occur from infiltration passing through the root zone of the vegetation – using only recharge in excess of a low threshold rainfall.

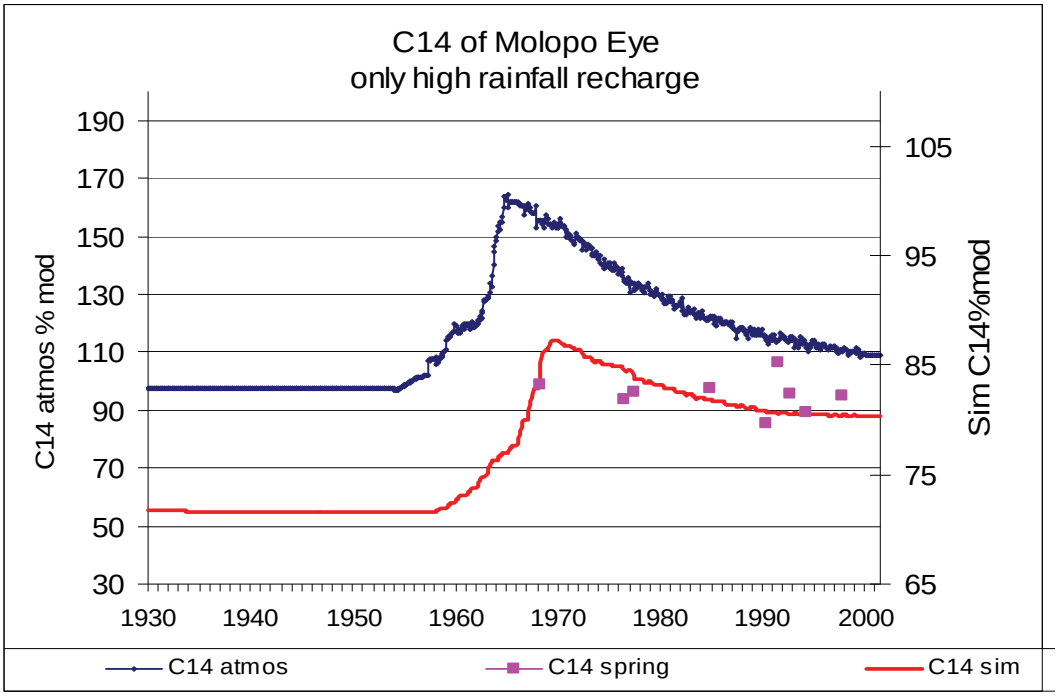

Fig. 14 – Simulated ^{14}C for Molopo eye assuming that all the recharge occur from infiltration bypassing the root zone of the vegetation – using only recharge in excess of high threshold rainfall.

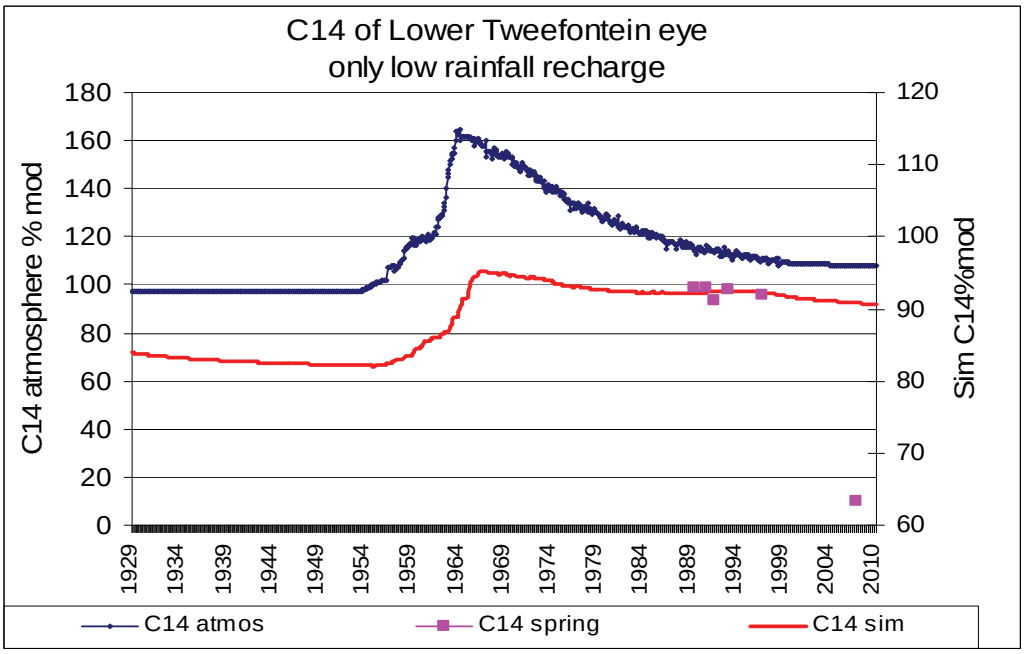

Fig. 15 – Simulated ^{14}C assuming all the recharge to occur from infiltration passing through the root zone of the vegetation – incorporating only low rainfall threshold applying.

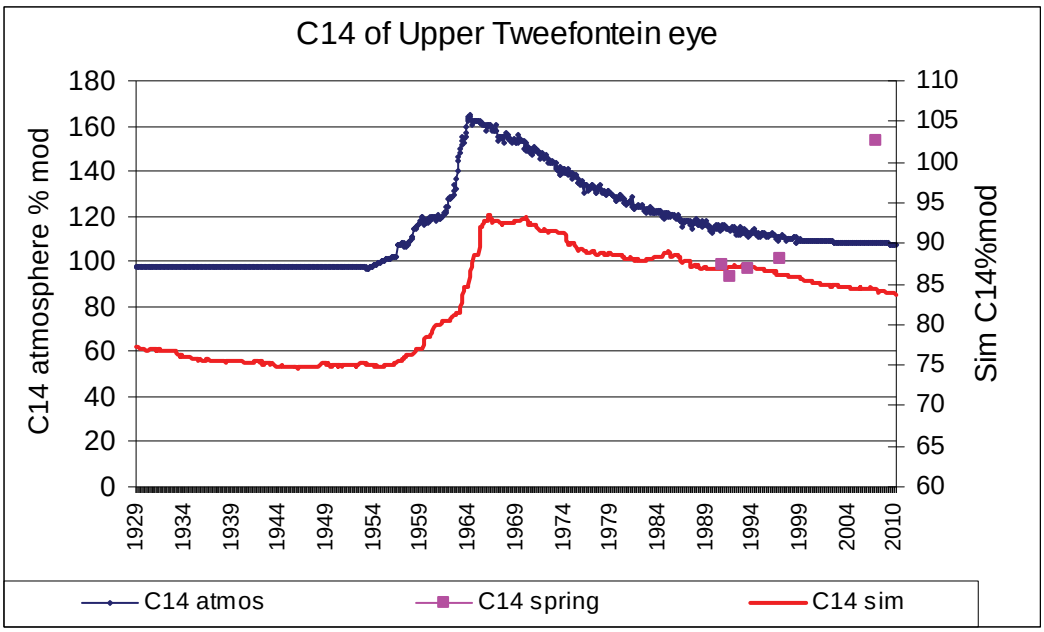

Fig. 16 – Simulated ^{14}C assuming all the recharge to occur from infiltration bypassing the root zone of the vegetation – i.e. in excess of only a high rainfall threshold.. The latest ^{14}C measurement is clearly an outlier and therefore unreliable.

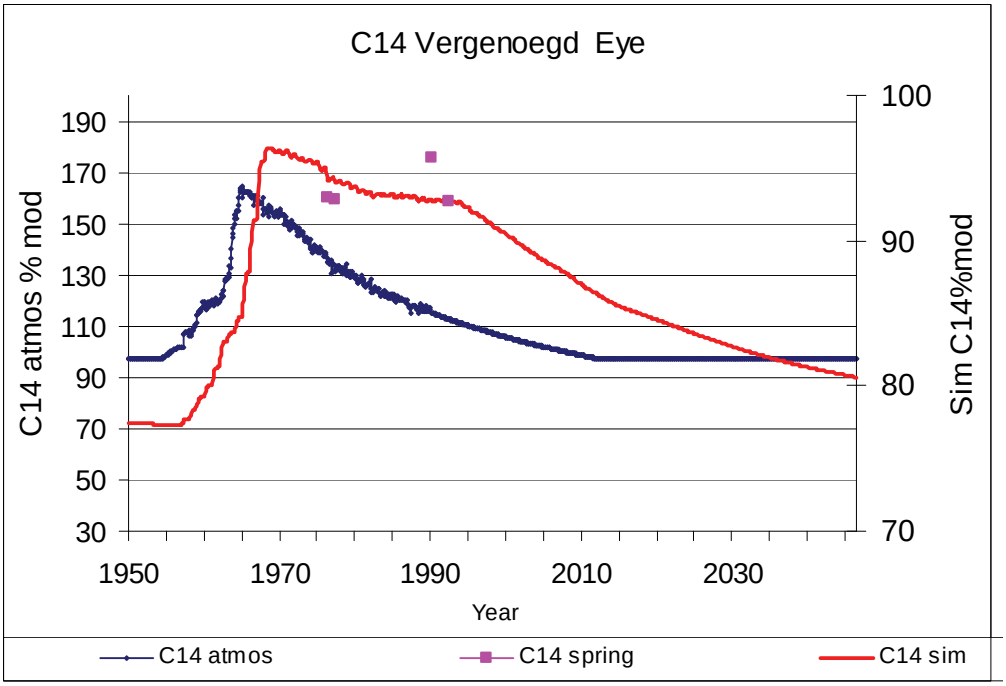

Fig. 17 – Simulated ^{14}C of Vergenoegd eye assuming all the recharge to occur from infiltration bypassing the root zone of the vegetation i.e. only recharge in excess of a high threshold rainfall. (No measured value for 2007)

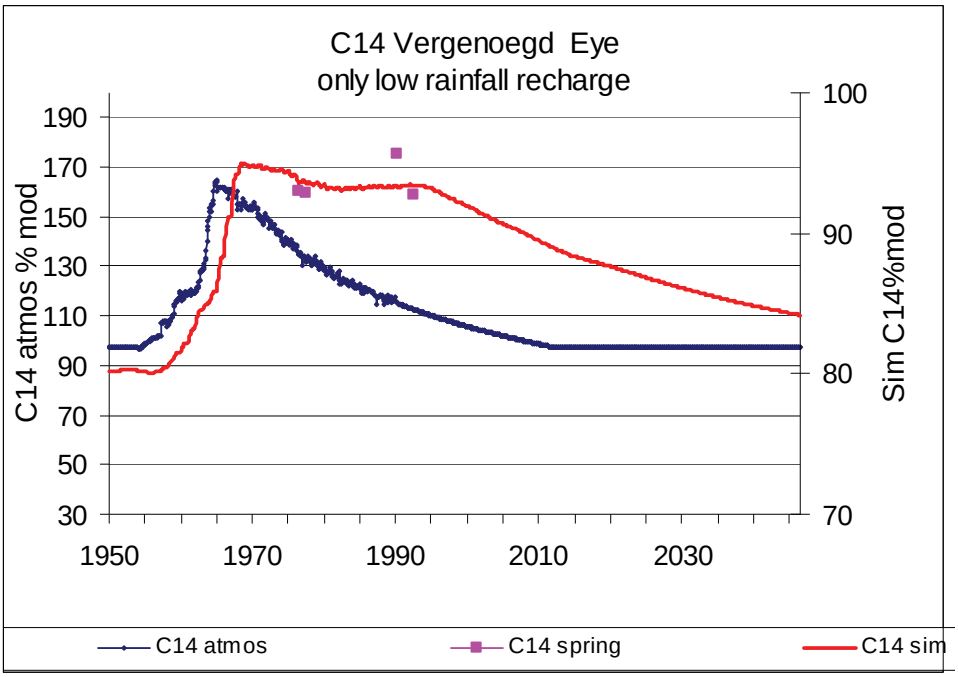

Fig. 18 – Simulated ^{14}C assuming all the recharge to occur from infiltration passing through the root zone of the vegetation – i.e. rainfall in excess of a low threshold.
(No measurement for 2007)

The next result represents that of Buffelshoek using a short mixing period of 24 months with only a high recharge (low ^{14}C factor). As is shown in the main report the most recent ^{14}C measurement is clearly unreliable.

Buffelshoek eye

Factors Minimum	25.98
Lower threshold	NA
Higher threshold	18
Recharge factor (L)	0.001
Recharge factor (H)	0.142
^{14}C factor (L)	NA
^{14}C factor (H)	0.775
Relative mixing factor	1
Final multiple factor	1.84
Turn-over time (yrs)	27.7
Lag months period 1	24
Lag period 2	348
Rainfall weighting	24
Further lag Sim ^{14}C	1
HCO3 of spring water	219.29
Measured HCO3	228
Area spring (sq km)	28
Cl of spring	5.07
Cl ratio recharge	0.1105
^{14}C sim recharge	0.1102

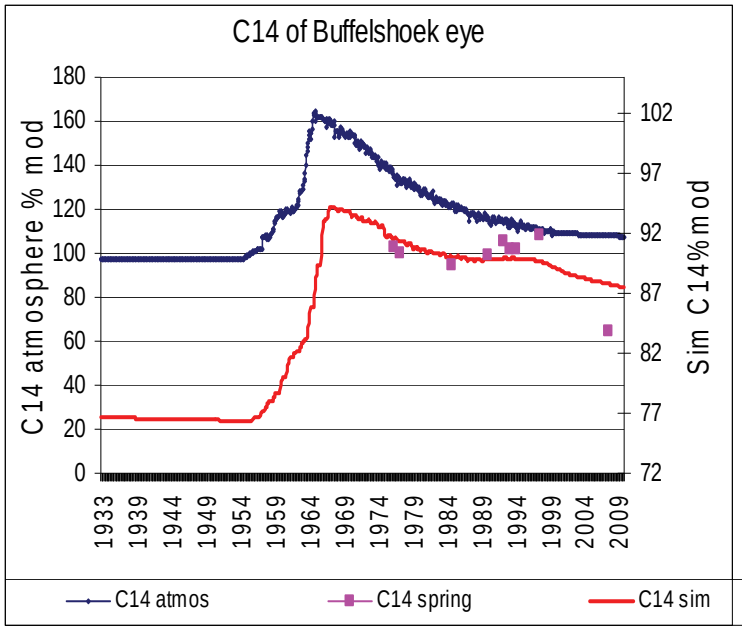

References

Vogel JC. (1970): Carbon-14 dating of groundwater. In: Isotope Hydrology 1970. IAEA Atomic Energy Agency, Vienna 1970.